

W-AM-Sym1-1**cAMP-DEPENDENT PROTEIN KINASE PROVIDES A STRUCTURAL FRAMEWORK FOR THE PROTEIN KINASE FAMILY.**

((Susan Taylor, Jianhua Zheng, Janusz Sowadski, Wei Wen, Friedrich Herberg, Dominic Fantozzi, and Wes Yonemoto)) Dept. of Chemistry, Univ. of California, San Diego, 9500 Gilman Drive, La Jolla, CA 92093-0654.

cAMP-dependent protein kinase (cAPK) is one of the simplest members of a family of enzymes that play critical regulatory roles in the eukaryotic cell. cAPK, being one of the smallest protein kinases, has served as a prototype for the entire family of over 200 enzymes. The catalytic (C) subunit of cAPK is itself also subject to posttranslational modifications, both phosphorylation and myristylation. The crystal structure of a ternary complex containing the C-subunit, an inhibitor peptide, and MgATP shows how key conserved residues converge at the active site. It also describes the sites of posttranslational modification. Two stable phosphorylation sites exist and replacing these phosphates leads to a destabilized or inactive enzyme that, in some cases, is unable to recognize the regulatory (R) subunit. Phosphorylation at Thr197 is particularly critical and a homologous residue, critical for activation, is found in other protein kinases such as the cell division cycle kinases, cdc2. Myristylation stabilizes the enzyme by folding into a hydrophobic pocket. The inhibition of the C subunit by either the type I R-subunit or a heat stable protein kinase inhibitor (PKI) depends on the synergistic high affinity binding of MgATP. Mutant C-subunits that are catalytically intact but unable to be regulated by either PKI or R, we can demonstrate that different regions of the enzyme surface are important for the high affinity binding of these two physiological inhibitors. The dissociated C-subunit is free to migrate between the cytoplasm and the nucleus while association with either R or PKI prevents access to the nucleus. Microinjecting directly into the nucleus shows that free C-subunit can move in both directions while R and the holoenzyme cannot escape from the nucleus.

W-AM-Sym1-3**DECODING Ca²⁺ SIGNALS BY MULTIFUNCTIONAL Ca²⁺/CALMODULIN-DEPENDENT PROTEIN KINASE? Howard Schulman, Phyllis Hanson, Tobias Meyer, Melanie MacNicol and Lubert Strayer. Stanford University School of Medicine, Stanford, CA 94305-5332.**

Multifunctional Ca²⁺/calmodulin-dependent protein kinase (CaM kinase) is one of the major protein kinases coordinating cellular responses to hormones and neurotransmitters. CaM kinase has structural/functional properties that may facilitate its response to changes in Ca²⁺ that are transient or pulsatile. Substrate phosphorylation and autophosphorylation are stimulated when calmodulin binds and disrupts the autoinhibitory/calmodulin-binding domain. After calmodulin dissociates from an autophosphorylated subunit, the kinase no longer deactivates because its autoinhibitory domain is disrupted by the anionic phosphate moiety. The effects of transient rises in Ca²⁺ are potentiated by the conversion of CaM kinase to this Ca²⁺-independent form. The frequency of Ca²⁺ oscillations or spikes may be decoded by CaM kinase. The affinity of CaM kinase for calmodulin increases more than 100-fold by autophosphorylation which traps calmodulin by increasing its off-rate from less than a second to several seconds. Trapping is a cooperative process that is inefficient at low occupancy of calmodulin on the multimeric kinase. Cooperativity results from the mechanism of autophosphorylation which involves a subunit phosphorylating its neighbor in the holoenzyme, each with bound calmodulin. Simulations of kinase activation at limiting calmodulin show that repetitive Ca²⁺ pulses lead to recruitment of calmodulin to the holoenzyme, which further stimulates autophosphorylation and trapping. This cooperative positive feedback loop potentiates the response of the kinase to sequential calcium spikes and establishes a threshold frequency at which the enzyme becomes highly active. The biochemical properties of CaM kinase provide for molecular potentiation of calcium signals and frequency detection.

W-AM-Sym1-2**MOLECULAR PROPERTIES OF MYOSIN LIGHT CHAIN KINASES. ((Stull, J.T., Herring, B.P., Gallagher, P.J., Gao, Z.-H. and Zhi, G.)) Department of Physiology, UT Southwestern, Dallas, TX 75235.**

Ca²⁺/calmodulin (CaM)-dependent myosin light chain kinases (MLCK) are dedicated protein kinases that phosphorylate a Ser near the N-terminus of regulatory light chains (RLC) of vertebrate myosins. RLC phosphorylation plays an important role in cytokinesis, receptor capping, initiation of smooth muscle contraction, and potentiation of striated muscle contraction. MLCK in smooth and non-muscle cells has catalytic and physicochemical properties that distinguish it from the enzyme found in striated muscles. However the structures and relative organization of functional domains are similar, including a catalytic core, an autoinhibitory region, and a calmodulin-binding domain. The structural basis for intrasteric activation by CaM and catalysis has been examined by site-directed mutagenesis and chemical cross-linking procedures. Basic residues in the autoinhibitory region bind to specific acidic residues on the surface of the larger lobe of the catalytic core, thereby preventing RLC binding. Upon activation by CaM, RLC binds to the larger lobe of the catalytic core and is phosphorylated in the active site. Residues on both sides of the phosphorylatable Ser in the RLC are important for catalysis. Studies demonstrate similarities, but also important differences in the molecular properties of these 2 types of MLCKs.

W-AM-Sym1-4**STRUCTURE: FUNCTIONAL ANALYSIS OF THE EPIDERMAL GROWTH FACTOR RECEPTOR. ((G.N.Gill)) UCSD, La Jolla, CA92093-0650.**

The EGFR consists of 4 major subdomains: an amino terminal ligand binding ectodomain, a membrane spanning domain, a cytoplasmic tyrosine kinase catalytic core and a regulatory carboxyl terminal domain. Signal transduction depends on the intrinsic protein tyrosine kinase (PTK) activity of the receptor. To identify structural features that distinguish tyrosine from serine protein kinase (PSK), a molecular model of the kinase domain of EGFR was constructed by substituting its amino acid sequence for that of the catalytic subunit of cyclic AMP-dependent protein kinase (cAPK) in a 2.7 Å refined crystallographic model containing bound ATP and a peptide inhibitor. General folding and the configuration of invariant residues at the active site were conserved. The unique kinase nucleotide binding site was conserved with most contact provided by the small lobe. Two sequence motifs that distinguish PTK and PSK correspond to loops that converge at the active site. An arginine in the catalytic loop is proposed to interact with the 7 phosphate of ATP. The second loop provides a binding surface that positions the tyrosine of the substrate. A positively charged surface provides additional sites for substrate recognition. The regulatory C' terminus contains 5 identified sites of tyrosine self-phosphorylation. Self-phosphorylation activates the enzyme, provides sites for assembly of SH2 domain proteins and exposes multiple endocytic codes which act combinatorially to attenuate signal transduction.

POTASSIUM CHANNELS III**W-PM-A1****VOLTAGE-DEPENDENT K⁺ CHANNELS REGULATE ARTERIAL SMOOTH MUSCLE MEMBRANE POTENTIAL AND TONE.**

((Harry J. Knot, Blair E. Robertson, Joseph E. Brayden and Mark T. Nelson)) University of Vermont, Dept. of Pharmacology, Colchester Medical Research Facility, Colchester, VT 05446-2500. (Spon. by J.M. Quayle) BER is an International Research Fellow of the AHA. Supported by the NSF and NIH.

Voltage-dependent K⁺ channels have been identified in many different tissues and have been traditionally thought to be involved in the repolarization of the action potential. In contrast, the role of these K⁺ channels in the control of steady-state membrane potential, particularly in arterial smooth muscle, is unclear. We tested the hypothesis that steady-state K⁺ efflux through voltage-dependent K⁺ channels is involved in the regulation of arterial smooth muscle membrane potential. Both 4-aminopyridine (4-AP) and 3,4-diaminopyridine (3,4-DAP) inhibited whole-cell, voltage-dependent K⁺ currents in smooth muscle cells isolated from rabbit cerebral arteries. 4-AP and 3,4-DAP produced half-maximal inhibition at concentrations of 1 mM and 0.5 mM, respectively. To minimize the contribution of the Ca²⁺-activated K⁺ channel, intracellular Ca²⁺ was buffered to 20 nM, and TEA⁺ or ibertoxin and nimodipine were included in the bath solution. Elevation of intravascular pressure constricts and depolarizes smooth muscle cells in small cerebral arteries from about -65 mV to -40 mV resulting in myogenic tone. We used isolated mid-cerebral arteries (110 ± 24 μm) that depolarize and develop myogenic tone in response to pressure. Blockers of voltage-dependent K⁺ channels, 3,4-DAP (300 μM) and 4-AP (1 mM) depolarized the arteries by about 19 mV. The compounds constricted these arteries by 27 and 55 μm when subjected to a transmural pressure of 30 and 50 mm Hg respectively. The depolarization to 4-AP and 3,4-DAP was unaltered by blocking calcium channels (which dilated the arteries and closed K_{Ca} channels) and by the K_{ATP} channel inhibitor, glibenclamide. We, therefore, propose that steady-state K⁺ efflux through 4-aminopyridine-sensitive, voltage-dependent K⁺ channels plays an important role in the regulation of membrane potential of arterial smooth muscle and consequently myogenic tone.

W-PM-A2**RESCUE OF LETHAL SUBUNITS INTO FUNCTIONAL HETEROMULTIMERIC VOLTAGE-DEPENDENT K⁺ CHANNELS.**

((M. Tagliatela, J.P. Payne*, J.A. Drewe, H. Hartmann and A.M. Brown)) Depts. Molecular Physiology and Biophysics and *Internal Medicine, Baylor College of Medicine, One Baylor Plaza, 77030 Houston, TX.

We have shown that injections of cRNAs of a chimeric K⁺ channel (CHM) (Hartmann et al., *Science* 251:942, 1991) having mutations at positions 369 and 374 expressed currents in *Xenopus* oocytes with altered channel conductance, ion selectivity and TEA block. Further mutagenesis of these sites has shown that not all cRNAs expressed macroscopic or single channel currents. The function of one nonexpressing mutation, CHM V369L, was recovered by coinjection with the cRNA of a potent expressor, CHM L374V. Coinjection produced a new heteromeric phenotype in addition to the parent CHM L374V homomer. The single channel outward K⁺ conductance of CHM L374V was significantly different from the heteromultimer in asymmetric conditions (4.5±0.2 pS, n=16 vs. 14.8±0.7 pS, n=16). Gating also differed substantially (mean open time for CHM L374V was 5.4±0.3 ms vs. 13.3±1.8 ms for the heteromultimer and mean closed time for CHM L374V was 32.4±8 ms vs. 5.1±1.6 ms for the heteromultimer). The single channel outward Rb⁺ conductance, however, was nearly identical for the two phenotypes (13.9±1.5 pS for L374V vs. 13.1±1.1 pS for the heteromultimer). The stoichiometry of the heteromultimer was determined by coinjection of different ratios of the cRNAs of CHM L374V and CHM V369L. Binomial analysis suggested that the heteromultimer comprised of three CHM L374V subunits and one CHM V369L subunit was an active form of the channel. (Supported by the NS23877 grant to AMB and by the CNR 215.24 grant to MT).

W-PM-A3

A SITE NEAR THE TRANSMEMBRANE SEGMENT S6 OF POTASSIUM CHANNELS INTERACTS WITH BARIUM IONS. ((E. Y. Isacoff, G. A. Lopez, Y. N. Jan and L. Y. Jan)) Howard Hughes Medical Institute and Departments of Physiology and Biochemistry, University of California San Francisco, San Francisco, CA 94143-0724.

Voltage and calcium-gated potassium channels are very sensitive to blockade by internal Ba^{++} . The similarity in dehydrated ionic radius of Ba^{++} and K^+ suggests that Ba^{++} binds to at least one of the sites where K^+ binds as it moves through the pore. In order to identify the part of the pore which interacts with Ba^{++} , we have made a chimeric channel in which parts of the NGK2 (Kv3.1) channel were transplanted into a non-inactivating N-terminal deletion mutant of *Shaker B*, since the two channels were found to exhibit different conductances to K^+ and sensitivities to block by internal Ba^{++} . A chimera, in which most of the S6 and several amino acids on its carboxyl end were transplanted, displayed a sensitivity to Ba^{++} different from *Shaker B*. Multiple point mutations have been made to identify the responsible residue(s). We are examining the voltage-dependence of the Ba^{++} block in order to estimate the location along the length of the pore where the relevant residue(s) exert their effect. We are also examining Ba^{++} on and off rates in order to gauge whether the effect of Ba^{++} affinity can be ascribed to changes in the Ba^{++} binding site directly or in Ba^{++} access to the site.

W-PM-A5

TETRAMERIC CONSTRUCTS OF RCK1 K-CHANNELS MIGHT ELUCIDATE THE ROLE OF HYDROPHOBIC RESIDUES IN VOLTAGE-DEPENDENT GATING. ((Adrian Gross and Peter Hess)) Department of Cellular and Molecular Physiology, Harvard Medical School, Boston, MA 02115.

A leucine zipper motif, five leucines spaced seven residues apart, is closely associated with the S4 domain of most known K-channels. The S4 domain is the putative voltage sensor of the molecule. We found that in RCK1 K-channels, mutation of leucines 2 and 4 into valines (V2, V4) causes a shift in the activation curve of +70 mV and -45 mV, respectively. In these experiments, the shift was measured at an open probability of 0.1. Dimeric constructs containing one wild-type and one mutant channel (WTV2, WTV4) in a single reading frame show intermediate phenotypes with shifts of +47 mV and -20 mV. However, data from monomeric and dimeric constructs alone do not allow us to postulate a model which describes the role of these residues in gating. Using a sequential model which assumes four voltage sensors per channel and cooperative subunit interactions, the data can be fitted by adjusting the amount of gating charge (and/or introducing charge separation), the midpoint of activation, the degree of cooperativity, or a combination of the three. We are currently engineering and measuring various tetrameric constructs containing one, two, or three mutant channels in a single reading frame. This should enable us to determine more accurately what role the hydrophobic residues play in the process of voltage-dependent gating.

W-PM-A7

DELAYED RECTIFIER CURRENTS IN SKELETAL MUSCLE OF CONTROL AND MDX MICE. ((S. D. Hoehnerman and F. Bezanilla)) UCLA School of Medicine, Los Angeles, CA 90024.

Delayed rectifier currents were measured in the extensor digitorum longus muscle (EDL) of control (C57BL/10SnJ) and *mdx* mice (an animal model of muscular dystrophy) using the cell-attached patch clamp technique (see Mathes et al., 1991, Am. J. Physiol., 30:C718) with physiological K^+ concentrations (bath 150 mM, pipette 2-3 mM). Macroscopic currents were measured from macro patches (up to 5 μ m diameter pipettes). Outward currents could be detected at potentials positive to -60 mV, with a $V_{1/2}$ of -37 mV in control muscle. In *mdx* both the probability of opening ($V_{1/2}$ = -32 mV) and the τ of activation as function of V seemed to be shifted to the right. Tail currents (I_T) were linear in the range of -60 mV to 20 mV. Below -60 mV, a rectification was apparent. I_T reversed around -100 mV. Mean-variance analysis estimates of single channel current at V=0 yielded a normalized conductance of 20 pS for the linear portion of the I_T -V curve. Inactivation was discernible at potentials positive to -10 mV with pulses as short as 18 msec in duration. Prepulses of 500 msec yielded incomplete inactivation, with $V_{1/2}$ = -55 mV. At V=0, inactivation displays two τ 's, of 70 msec and 600 msec. Although single channel data confirmed the results obtained with the macroscopic data, a smaller amplitude channel was also observed with less frequency. Upon excision, the delayed rectifier tended to run down with a time constant of tens of minutes. ATP in the bath solution only marginally increased the probability of opening of the channels after rundown, and protein kinase A with ATP did not seem better than ATP alone. These findings indicate that the delayed rectifier is under complex intracellular control, and may be difficult to characterize in excised patches.

* Supported by the MDA

W-PM-A4

MODULATION OF 4-AMINOPYRIDINE BLOCK BY MUTATION OF DEEP PORE RESIDUES IN DELAYED RECTIFIER K^+ CHANNELS. ((G.E. Kirsch, D.F. Vener, J.A. Drewe and A.M. Brown)) Departments of Anesthesiology, and Molecular Physiology and Biophysics, Baylor College of Medicine, Houston, TX 77030.

The characteristics of 4-aminopyridine (4-AP) block of voltage-gated K^+ channels vary widely among channel subtypes and the 4-AP site in the channels is not known. We examined 4-AP's mechanism and blocking site in Kv2.1 and Kv3.1 K^+ channels cloned from rat brain and expressed in *Xenopus* oocytes. Patch clamp analysis of Kv3.1 showed that 4-AP ON and OFF rates were at least 100 times faster in open channels than in closed channels. An intracellular route to the blocking site is likely because the bath-applied, tertiary amine readily blocks channels in cell-attached patches while its quaternary derivative selectively blocks when applied to the intracellular surface of excised patches. Whole cell analysis showed that 4-AP blocked Kv3.1 with IC_{50} more than 300-fold lower than Kv2.1. But unlike external tetraethylammonium block that shows a qualitatively similar difference in potency between the two channels, high affinity 4-AP block was not transferred when 21 pore residues in the S5-S6 linker of Kv2.1 were replaced with those of Kv3.1. In fact the resulting chimeric channel was at least 40 times less sensitive to 4-AP than Kv2.1. 4-AP insensitivity was produced in Kv2.1 by the double mutation of I369V and V374L. Moreover, I \rightarrow V and L \rightarrow V mutations at the analogous positions in Kv3.1 increased 4-AP sensitivity 10-fold over wild type. We conclude that although deep pore residues strongly influence 4-AP block, the critical residues for high-affinity binding lie outside the S5-S6 pore region. (Supported by NIH grants NS29473 and NS23877).

W-PM-A6

COOPERATIVE AND NON-COOPERATIVE SUBUNIT INTERACTIONS DETERMINE VOLTAGE-DEPENDENT K^+ CHANNEL GATING. ((J. Tytgat, K. Nakazawa and P. Hess)) Dept. of Cellular and Molecular Physiology, Harvard Medical School, Boston, MA 02115.

Neutralization of the 3rd to 6th of the 7 positive charges in the S4 region of RCK1 K^+ channels abolishes functional expression in *Xenopus* oocytes. Tetrameric cDNA containing 3 wildtype (WT) and 1 mutant RCK1 subunits (R3I, R4I, K5I, R6N), however, expresses K^+ currents with unique gating properties: the activation is shifted negatively for R4I and positively for R3I, K5I and R6N. Currents expressed from tetrameric cDNA composed of 1 mutant subunit (R3I, K5I, R6N) plus either 3 WT or 3 R2N (2nd Arg in S4 neutralized) subunits were then used to investigate more in detail the gating mechanism. When activation curves were fitted by a sequential model that includes 4 voltage sensors per channel, phenotypes could be predicted correctly if cooperative subunit interactions were assumed for WT, R2N and R3I subunits, in contrast to non-cooperative behaviour for K5I and R6N subunits. Gating valences for K5I and R6N subunits were not different from WT, suggesting that K5 and R6 are not part of the voltage sensor.

Phenotypes for K^+ currents expressed from tetramers with different combinations of WT and R1Q (1st Arg in S4 neutralized) subunits could be explained if R1Q subunits were gating in a non-cooperative way. In conclusion, the tetrameric cDNA approach has enabled us to investigate the contribution of all charged amino acid residues in S4 to the total gating valence of RCK1 K^+ channels. A mechanism of cooperative and non-cooperative interactions between WT and mutant subunits helps to explain the voltage-dependence of the activation process.

W-PM-A8

THE 4-AMINOPYRIDINE-SENSITIVE TRANSIENT OUTWARD CURRENT IN COLONIC MYOCYTES IS MODULATED BY β -AGONISTS. ((F. Vogalis, R.J. Lang, R.A. Bywater and G.S. Taylor)) Department of Physiology, Monash University, Victoria 3168, Australia.

We have identified a rapidly inactivating voltage-gated K^+ current (I_{Kw}) in smooth muscle cells of the guinea-pig proximal colon. Smooth muscle cells were bathed in a Ca^{2+} -containing HEPES-buffered solution which also contained tetraethylammonium (TEA; 5-12 mM) and either Cd^{2+} (0.1 mM) or nifedipine (2 μ M) to block calcium channels. Cells were internally perfused with a HEPES-buffered KCl solution containing 3 mM EGTA. At room temperature (22°C), activation of I_{Kw} by a test depolarization to +40 mV from a holding potential of -80 mV, was complete within 2-5 ms, and the current inactivated with two time constants: 19 \pm 1.8 ms and 86 \pm 12 ms (n=6). Noradrenaline (NA; 50 μ M) reduced I_{Kw} slowly over 10-15 min: at a test depolarization of +40 mV, I_{Kw} was reduced significantly (p<0.05, paired t-test) from 563 \pm 17 pA to 453 \pm 13 pA (n=4). Isoprenaline (ISO; 50 μ M) also significantly decreased (p<0.05, paired t-test) I_{Kw} from 468 \pm 96 pA to 391 \pm 81 pA (n=10), an action that was blocked by propranolol (10 μ M). Replacement of Ca^{2+} with Mg^{2+} decreased the latency of ISO-mediated reduction in I_{Kw} . The voltage of half availability ($V_{1/2}$) was little affected by ISO (-81 \pm 3 mV to -84 \pm 4 mV, n=6). Substitution of Na^+ with Li^+ abolished the ISO-mediated reduction in I_{Kw} . Forskolin (100 μ M) significantly decreased (p< 0.05, paired t-test) I_{Kw} from 383 \pm 91 pA to 267 \pm 51 pA (n=4) by shifting $V_{1/2}$ negative from -81.8 \pm 5 mV to -89 \pm 6 mV. These data suggest that the β -adrenoreceptor activation of adenylate cyclase in colonic myocytes causes inhibition of I_{Kw} .

W-PM-A9

REDOX REGULATION OF K⁺ CHANNELS AND ITS RELATIONSHIP TO HYPOXIC PULMONARY VASOCONSTRICTION (Joseph M. Post, E. Kenneth Weir, Stephen L. Archer, Joseph R. Hume) University of Nevada, Reno NV 89557 and V.A. Medical Center and University of Minnesota, Minneapolis, MN 55417

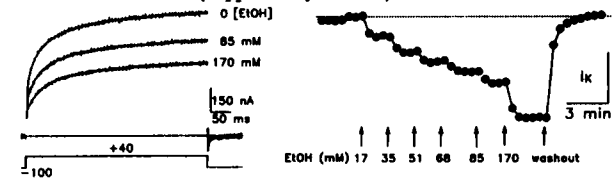
Hypoxia inhibits K⁺ currents in pulmonary artery smooth muscle cells causing membrane depolarization (AJP 262:C882, 1992), Ca²⁺ influx and contraction of pulmonary arteries. The mechanism by which a reduction in pO₂ inhibits K⁺ channel activity is not known. We have suggested that alteration of cellular redox status by oxygen may modulate pulmonary artery tone (Herz 11:127, 1986). We examined the effects of hypoxia, reduced glutathione (GSH), N-acetyl-L-cysteine (NAC; a membrane permeable analog of GSH) and diamide (a thiol oxidant) on K⁺ currents in patch-clamp experiments using canine pulmonary artery smooth muscle cells. Two K⁺ channels with conductances of 250 ± 10 and 82 ± 11 pS (symmetrical K⁺) were present in inside-out patches. Ca²⁺ (10⁻⁶-10⁻⁸ M) increased N⁺p(open) of the large conductance K⁺ channel in a concentration dependent manner. Hypoxia (pO₂ = 40 mmHg) reduced the open probability of the large conductance K⁺ channel (inside-out patches). NAC (5 mM) decreased whole-cell K⁺ current 36 ± 5 % at 60 mV (HP = -70 mV). GSH (5mM) similarly decreased N⁺p(open) of the large conductance K⁺ channel from 0.969 to 0.360 (inside-out patch). In contrast, the oxidant diamide (10 μM) increased whole-cell K⁺ currents by 40 ± 6% at 0 mV (HP = -70 mV) and increased N⁺p(open) of the large conductance K⁺ channel from 0.19 ± 0.05 to 1.36 ± 0.56. We conclude that oxygen tension modulates K⁺ channel activity such that a cytosolic environment which favors a reduced redox state inhibits K⁺ channels and/or an environment which favors oxidation of intracellular substrates enhances K⁺ channel activity. Studies are currently underway to investigate the effects of hypoxia and agents which alter the redox status on a smaller conductance K⁺ channel (= 80 pS) also present in these cells.

POTASSIUM CHANNELS IV

W-PM-B1

ETHANOL SELECTIVELY BLOCKS A NON-INACTIVATING K⁺ CURRENT ENCODED BY DROSOPHILA SHAW2. ((M. Covarrubias)) Jefferson Medical College, Alcohol Research Center, Philadelphia, PA 19107.

Using *Xenopus* oocytes and the two-electrode voltage-clamp technique, we investigated the action of ethanol on five structurally homologous cloned K⁺ channels (*Drosophila Shaw2*, *Drosophila ShakerH37*, mouse *mShal1*, rat *Kvl1* and human *HKSh3C*). We found that only the *Drosophila Shaw2*, which does not inactivate upon prolonged depolarization, is rapidly and reversibly blocked by ethanol in a concentration-dependent manner (17 - 170 mM). The concentration dependence of the blockade can be explained by assuming a bimolecular interaction between ethanol and the channel (*K_{app}* = 192 mM). In addition, we also found that *Shaw2* K⁺ channels are selectively blocked by halothane (1 mM). These results support the "protein hypothesis" of ethanol and anesthetic action and open new ways to elucidate directly the molecular mechanism of interaction between ethanol and a voltage-sensitive K⁺ channel. (Supported by NIAAA).

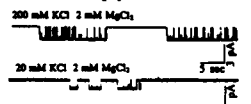


W-PM-B3

INTERACTIONS OF MAGNESIUM AND POTASSIUM IONS WITH INWARDLY-RECTIFYING POTASSIUM CHANNELS DURING CURRENT INACTIVATION.

((Teryl R. Elam & Jeffrey B. Lansman)) Depts. of Physiology and Pharmacology, University of California, San Francisco, CA 94143.

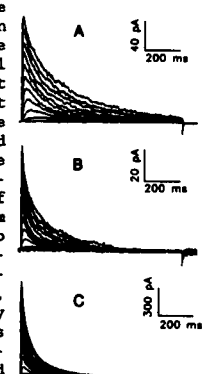
Inwardly rectifying K⁺ channels in cultured bovine aortic endothelial cells were studied using cell-attached patch clamp techniques. Inward currents through these channels displayed a voltage-dependent inactivation which was abolished when Mg²⁺ was removed from the external solution. Examination of single channel currents at negative membrane potentials revealed that bursts of channel current were separated by a long-lived non-conducting state (~10s) which, like the inactivation of inward current, was not observed when Mg²⁺ was removed from the external solution. Reducing the external [K⁺] while holding the external [Mg²⁺] constant had no effect on the duration of the non-conducting state, but markedly decreased the burst duration of inward currents as shown in the figure below. The results suggest that inactivation of inward current is the result of external Mg²⁺ binding to a site on the channel which induces a long-lived non-conducting state. The effects of varying external [K⁺] on single channel currents imply that K⁺ is also capable of binding to either the same or a nearby site on the channel; when this site is occupied by K⁺, it is more difficult for Mg²⁺ to bind to the channel and induce a period of zero conductance.



W-PM-B2

LOW MOLECULAR WEIGHT POLY(A)⁺ mRNA ENCODES FACTORS THAT MODULATE NON-SHAKER A-TYPE K⁺ CURRENTS. L.D. Chabala¹ and M. Covarrubias², Depts. of Medicine¹ and Pathology & Cell Biology², Jefferson Medical College, Phila., PA 19107.

It is an open question as to whether there are cellular mechanisms that regulate inactivation of A⁺-type K⁺ channels in their native environment. To investigate this, we co-expressed an A-type K⁺ channel encoded by *mShal1* and low molecular weight (LMW) poly(A)⁺ mRNA (both from rodent brain) in *Xenopus* oocytes. Under these conditions, time constants of rapid and slow inactivation of *mShal* currents are significantly reduced, and the rapid component dominates the time evolution of inactivation. Moreover, K⁺ currents from co-expression experiments are similar to those in mouse fibroblast (NIH3T3) transfected with *mShal*. Thus, a mammalian post-translational modification or co-factor, normally absent in *Xenopus* oocytes, may regulate the kinetics of A-type K⁺ channels in their native environment. Oocyte macro-patch data are shown for *mShal* (A) and *mShal*+LMW poly(A)⁺ mRNA (B), while whole-cell recordings are shown from an NIH3T3 cell transfected with *mShal* (C).



W-PM-B4

ION CHANNEL INACTIVATION: IS IT REALLY A BALL TETHERED ON A CHAIN?

((Larry S. Liebovitch, Lev Y. Selector, and Richard P. Kline)) Departments of Ophthalmology and Pharmacology Columbia University, NY 10032

We calculated the distribution of times it takes for a tethered ball to reach its binding site when its motion is a random walk in 1, 2, and 3 dimensions, and when it is also influenced by directed forces.

At long times, this distribution is a single exponential with a rate constant *k* that depends on the length *L* of the chain. For motion in 1 dimension we found that *k* ∝ *L*⁻². The data from Hoshi et al. (Science 1990 250:533) imply that *k* ∝ *L*⁻⁵. Our simple calculations produce such a steep dependence on *L* only if there is a repulsive force on the ball, and only if it is long range. This suggests that the ball is attached by sticks and springs, rather than freely tethered.

If more was known about the structure of the chain, then more accurate quantitative experimental measurements of the distribution of inactivation times could be used to determine the starting position and the forces acting on the ball.

Supported by Amer. Heart Assoc., RPB Inc., and NIH EY6234.

W-PM-B5

MOLECULAR DYNAMICS SIMULATIONS OF ION PERMEATION FOR GUY-DURRELL ATOMIC SCALE STRUCTURES OF V-GATED K-CHANNELS. ((O. Alvarez, G. Appleby, and G. Eisenman)) Biol. Dept. Fac. of Sci. U. of Chile, Santiago, Chile, and Physiol. Dept. UCLA Med. School, L.A., CA Supp. by USPHS GM24749; FONDECYT (CHILE) #1134-1992.

We have used Free Energy Perturbation / Molecular Dynamics (FEP/MD) simulations with the Gromos force field at 298 K in the presence of water, to explore the ion permeability of the Guy-Durrell "short beta barrel" and "random coil" structures for the P(pore) segment of the Shaker K channel. The "short beta barrel" is a tetramer of hairpins beginning from the extracellular side at VAL437, turning at VAL443, and ending at THR449. The tetramer of "random coils" begins at ASP439, turns at THR442, and ends at TYR449. In both cases, the relevant part of the structure used for simulation encompasses residues VAL345 to PHE404 and SER424 to HIS486. For simplicity in the initial exploration, no residues were ionized. To make up for the missing structure we examined a variety of ways of constraining the relevant atoms. We describe here the expectations for two increasingly unconstrained situations: Case 1: most of the protein is constrained at the Guy-Durrell coordinates (harmonic restraint of 50 KCal/A²), and only the side chains lining the channel are allowed to move (THR441, TYR445, THR439, ASP447, VAL437 for the "short beta barrel"; TRP434, VAL438, THR441, TYR445, ASP447, TYR449 for the "random coil"). Case 2: besides allowing the side chains to move freely, the constraints on all other atoms of the P segment are reduced to 0.2 KCal/A². The free energy the Na ion was computed at 2 Å intervals along the channel axis and in solution. This was done by creating the ion at each location and filling all available space within 10 Å of it with SPC water molecules. After 9 ps of MD dynamics equilibration, the ion was discharged in 37 appropriately spaced 1-ps steps (and also recharged to verify reversibility). This procedure yields the free energy of charging as a function of position. Plotting these energies with reference to the free energy simulated in water at a large distance from the channel (verified to be identical to experimental hydration free energy) yields the free energy profile (see figure in following abstract). For the beta barrel, owing to the rigidity of the backbone of the hairpin for Case 1, so high a barrier is formed by the TYR445's that the channel would be ion-impermeable. However, in Case 2 the increased mobility of the hairpin reduces this barrier and yields a functionally plausible profile (see following abstract). For these structures ion conduction requires some molecular flexibility.

W-PM-B7

POTASSIUM CHANNELS FROM SQUID AXOPLASMIC ORGANELLES. BLOCK BY QUATERNARY AMMONIUM (QA) IONS. ((R.J. French and W.F. Wonderlin)) Medical Physiology, University of Calgary, Calgary, AB, Canada T2N 4N1; Pharmacology and Toxicology, West Virginia University, Morgantown, WV 26506.

One type of potassium channel, incorporated into planar lipid bilayers from transport organelles isolated from the axoplasm of squid giant axons, shows voltage-dependent gating and kinetics reminiscent of the delayed rectifier conductance of the axolemma (Wonderlin & French, 1991, *P.N.A.S.* 88:4391). We have studied block of these channels by tetraethylammonium (TEA), C₅-triethylammonium (C₅), and tetrapentylammonium (TPeA) ions applied to the axoplasmic ends of the channels. Single channels were studied in neutral, planar bilayers (POPE:POPC, 80:20), bathed by 500 mM K acetate, 10 mM HEPES, pH 7.0, between E = -60 and +80 mV, using both voltage-step protocols and steady state recordings. For positive voltages, at room temperature and a bandwidth of 2 kHz, TEA (1-9 mM) produced poorly resolved, flickery interruptions in single channel current. Longer, discrete blocking events were induced by C₅ (100-300 μM), and the longest by TPeA (30-100 μM). The single channel observations that we have made so far are consistent with the 'open-pore block' model of QA action on the macroscopic delayed rectifier current developed by Armstrong (*J. Gen. Physiol.*, 1971, 58:413): 1) Potency of block increases with increasing hydrophobicity; 2) Depolarization enhances block; 3) Block increases when Na replaces K in the external solution (C₅ & TPeA); 4) Duration of bursts of single channel openings increases in the presence of blockers (TEA & C₅).

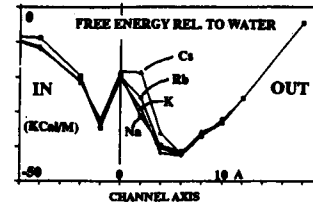
W-PM-B9

COMPARATIVE STUDY OF CALCIUM-ACTIVATED POTASSIUM CHANNEL VARIANTS EXPRESSED IN *XENOPUS* OOCYTES. ((A. Lagrutta, K.-Z. Shen, R.A. North, J.P. Adelman)) Vollum Institute and Dept. of Cell Biology and Anatomy, OHSU, Portland, OR. 97201.

The *Slo* locus in *Drosophila* encodes a family of alternatively spliced variants that direct expression of calcium-activated potassium channels in *Xenopus* oocytes (Atkinson, N.S. et al., *Science* 253, 551, 1991; Adelman, J.P. et al., *Neuron* 9, 209, 1992). The central third of the amino acid sequence has five variable regions (boxes A1-3, C1 or 2, E1 or 2, G1-6, and I in or out). Single channel recordings from inside-out patches of *Xenopus* oocyte membranes expressing *Slo* C2lo variants (having C2 and lacking I) showed functional differences among these variants. Channels with G2, G3 and G4 have longer openings than channels with G5; the longer of the two open time constants (τ_{o2}) at 60 mV/3 μM [Ca]_i is 44.1 ± 7.1 ms (n = 10) in A1C2E1G3lo and 7.1 ± 1.2 ms in A1C2E1G5lo (n = 10). Channels with E1 have greater sensitivity to [Ca]_i than those with E2; the apparent equilibrium constant at 80 mV was 1.9 μM in A3E1G5 and 85 μM for A3E2G5. Channels with G5 also activate more rapidly on depolarization than channels with G3; τ_{act} at 80 mV/10 mM [Ca]_i is 3.0 ± 0.16 ms (n = 10) in A1E1G5 and 41.7 ± 7.0 ms (n = 18) in A1E1G3. These results provide a functional basis for the observed diversity of *Slo* transcripts and map structural domains underlying specific *Slo* channel characteristics.

W-PM-B6

FREE ENERGY PERTURBATION STUDIES OF ION-SELECTIVE PERMEATION IN GUY-DURRELL "SHORT BETA BARREL" AND "RANDOM COIL" STRUCTURES FOR THE SHAKER K CHANNEL PORE. ((G. Eisenman, G. Appleby, and O. Alvarez)) Physiol. Dept. UCLA Med. School, L.A., CA and Biol. Dept. Fac. of Sci. U. of Chile, Santiago, Chile.



Using the FEP/MD simulation strategy of Case 2 of the preceding abstract to "mutate" the Lennard-Jones 6-12 parameters for Na⁺ to those for K⁺, Rb⁺, Cs⁺, and Cl⁻, we have examined the energy profiles for Guy-Durrell "short beta barrel" and "random coil" structures of the P-segment of the Shaker K channel. For the "short beta barrel" (see figure) the profile consists of a wide energy minimum split into two regions by an asymmetric barrier. For the "random coil" (not shown) we find a somewhat narrower, and unsplit, minimum of comparable depth. For the "short beta barrel" the different peak heights of the barrier for Na, K, Rb, and Cs indicate that the this structure would exhibit a K selective permeability at low concentration (K > Rb > Na, Cs) compatible with experiment. The calculated deep and wide minima imply multiple ion occupancy, as observed. Multiple occupancy should enable ions to traverse the structure at observed rates. Simulations show the channel to be Cl⁻ impermeable. Selectivity varies within the channel encompassing a variety of non-hydrophobic, therefore, non-trivial, sequences. The inner site is made by a ring of four THR441-OH's and binds ions in Eisenman sequence VII: Na > K > Rb > Cs. The outer multiple site regions are lined by rings of four TYR445-OH's, THR439-OH's, and ASP447-COO's which exhibit sequences VII: K > Na > Rb > Cs; VI: K > Rb > Na > Cs; IV: K > Rb > Cs > Na at various loci. In the present modelling, which does not yet include bond polarizability or aromatic pi electrons, the main parameter determining K vs Na selectivity is the extent to which the channel can swell or shrink to accommodate different sized ions.

Supp. by USPHS GM24749 and FONDECYT (CHILE) #1134-1992.

W-PM-B8

MODELS OF THE SLOWPOKE CALCIUM-ACTIVATED POTASSIUM CHANNEL. H. Robert Guy & Stewart Durell, LMMB, MCI, NIH, Bethesda, Md 20892

Atomic scale computer models of transmembrane and extracellular portions of the Slowpoke channel were generated and minimized. The general folding pattern of the Slowpoke S1-S6 segments is postulated to be similar to that proposed previously for the Shaker channel (Durell and Guy, *Biophys. J.*, 62:238-250); however, other segments differ. Slowpoke residues 1-39 are postulated to form an extracellular helical hairpin; residues 41-63 are postulated to form an additional transmembrane α helix, S0, that is in contact with lipid, and residues 74-103 are postulated to form an amphipathic α helix that lies in the intracellular water-lipid-protein interface. The ion selective P segment between S5 and S6 was modeled two ways: (1) residues 273-283 form an α helix that spans the outer half of the transmembrane region and residues 287-294 form a series of β turns, and (2) residues 273-293 form a β hairpin that is part of a β barrel formed by four subunits. In both models the narrowest portions of the pore are formed by tyrosine side chains; Tyr277 in the outer portion and Tyr288 in the inner portion. All cysteines of the putative extracellular domains are postulated to form disulfide bridges; Cys5-Cys35, Cys27-Cys140, and Cys275-Cys293. The latter links the beginning of the P segment in one subunit to the end of the P segment in an adjacent subunit. Cys61 and Cys62 at the end of S0 are positioned at the intracellular lipid-water interface where they may bind covalently to lipid head groups. We are developing models with similar conformations for S1-S6 and P segments for voltage-gated K⁺, plant K⁺, and cyclic nucleotide-gated channels.

W-PM-C1

PERFORATED PATCH RECORDINGS OF Ca^{2+} CURRENTS FROM NEUROHYPOPHYSIAL TERMINALS USING AMPHOTERICIN B ((José R. Lemos and Gang Wang)) Worcester Foundation for Experimental Biology, 222 Maple Avenue, MA 01545

The neurohypophysial nerve terminals of the rat are so small (approximately 5-7 μm in diameter) that 'rundown' of Ca^{2+} currents recorded using conventional tight-seal 'whole-cell' patch-clamp technique is usually very fast (less than 5 min). Efforts have been made in this study to prevent dialysis of the cytoplasm of the terminal by utilizing amphotericin B to perforate nerve terminals through the patch in the pipette. Neither nystatin nor α -toxin had any permeabilizing effect on the terminal membrane, but amphotericin B strongly reduced the access resistance. Both the current-voltage relationships and average amplitudes of the terminal Ca^{2+} currents were very similar to those recorded with the conventional 'whole-cell' patch-clamp technique (Wang et al., 1992 *J. Physiol.* 445:181), but Ca^{2+} currents were stable for 40 to 120 min. This technical improvement has enabled us to perform pharmacological studies on the Ca^{2+} channels in the nerve terminals, including dihydropyridine effects on the long-lasting Ca^{2+} current. (Supported by NIH & NSF grants to JRL)

W-PM-C3

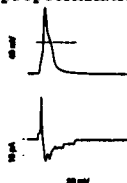
EFFECTS OF DILTIAZEM ON THE Ca CHANNEL CURRENT IN HUMAN MESENTERIC ARTERIAL CELLS. ((Sergey V. Smirnov and Philip I. Aaronson)) Department of Pharmacology, St. Thomas's Hospital, London SE1 7EH, UK. (Spon. by J. R. Hume)

The effect of diltiazem (DILT) was studied on Ca channel currents in human mesenteric arterial (HMA) cells, using 10 mM Ba as the charge carrier with the whole-cell patch clamp technique. 20 μM Dilt (EC_{50} was 23 μM at a holding potential (HP) of -60 mV, pH=7.2) suppressed peak I_{Ba} with a significant acceleration of current decay. The same concentration of DILT caused a 24 mV negative shift in the steady-state availability for I_{Ba} . We found that DILT blocked I_{Ba} in HMA cells in both a potential- and a use-dependent manner. Tonic block was greater at a HP of -60 than at -90 mV (32 vs 12%). The use-dependent block, which was observed at stimulus frequencies of 0.1 and 1 Hz, was also more pronounced at a HP of -60 than at -90 mV. A comparison of block at pH 6.2 (where DILT is largely charged) and pH 8.2 (where DILT is largely neutral) indicated that tonic block was reduced, but use-dependent block increased at pH 6.2. These observations are consistent with channel state-dependent interactions of the charged and uncharged forms of DILT with the Ca channel in HMA. (Supported by the British Heart Foundation).

W-PM-C5

LONG OPENING OF HIGH-THRESHOLD Ca CHANNELS TRIGGERED BY ACTION POTENTIAL IN NEURONAL CELLS. ((A. Galli, L. Bertolini, A. Ferroni, and M. Mazzanti)) Dipartimento di Fisiologia e Biochimica Generale, Università Statale di Milano, Via Celoria 26, I-20133, Milano, Italy.

Dihydropyridine sensitive Ca channels show two distinct gating mechanisms. The function of L-type Ca channels long openings remain unclear, e.g., their contribution to the action potential and their role in the increase of intracellular calcium during excitation. In the present study we investigate the occurrence of different "modes" of openings during nerve action potentials. Using the two-electrode technique on dorsal root ganglion neurons from adult rat, we explore the behavior of single Ca channels conducting 20 mM Ba during action potentials and activation occurs between ± 20 mV. Fast repolarization at lower potentials maintain the channel in the open state and with long open kinetics. The prepotentiation voltage protocol used to increase the probability of long openings mimics the action potential shape. Mode 2 openings not only increase at -20/-30 mV, but also at -50/-60 mV (see figure) during action potentials. Our results suggest that high-threshold Ca channels help to maintain the cell depolarized during action potential bursts or in high frequency voltage oscillation.

**W-PM-C2**

ANALYSIS OF HIT CELL CALCIUM CURRENTS USING A BURST-WAVEFORM VOLTAGE CLAMP COMMAND.

((L. S. SATIN, S.J. TAVALIN AND P.D. SMOLEN*)), Dept. of Pharm./Tox., Med. Coll. of Virginia and *Biomath. Res. Branch, NIDDK, NIH, Bethesda, MD. 20892 (Coll. R. Pittman)

The mechanism by which pancreatic islet B-cells burst in elevated glucose is still not understood, but recent experimental (Hopkins et al. *J. Mem. Biol.*, 119:229-239, 1991) and theoretical studies (Keizer and Smolen, PNAS, 88:3897-3901, 1991) support the hypothesis that slow inactivation of Ca current may be important. To test this more fully, we used a computed burstwave that mimicked B-cell bursting as a voltage clamp command. Insulin-secreting HIT cells were patch-clamped using standard techniques to isolate whole-cell Ca currents (Satin and Cook, Pflugers Archiv. 411:385-7, 1988). Burst commands were applied to cells in control solutions (3 mM Ca) and re-applied after Ca channel blockade by Cd (Satin and Cook, 1988). Control and Cd burst currents were subtracted to eliminate capacity and leak current. In response to bursts from -65 mV, Ca current activated with each computed spike but then declined during the train, as predicted from models based on slow inactivation (Keizer and Smolen, 1991). To further probe Ca inactivation during bursting, repetitive test pulses to +10 mV were added to the burst command. The Ca current was constant prior to the onset of the burst, but then slowly and reversibly decreased to 0.804 ± 0.206 of control (mean \pm s.e.m.; n=5) during the plateau phase. Inactivation was potentiated by changing holding from -65 mV to -55 mV but only partially reduced by replacing Ca with Ba. These results suggest that Ca and depolarization contribute to the inactivation produced by the burstwave commands, and are consistent with models based on Ca channel inactivation.

W-PM-C4

A SINGLE POOL INOSITOL 1,4,5-TRIPHOSPHATE RECEPTOR BASED MODEL FOR AGONIST STIMULATED CALCIUM OSCILLATIONS. ((G. De Young and J. Keizer)) Institute of Theoretical Dynamics, UC Davis, Davis, CA 95616

Relying on quantitative measurements (1,2) of calcium activation and inhibition of the inositol 1,4,5-triphosphate (IP_3) receptor/calcium channel in the endoplasmic reticulum (ER), we have constructed a simplified kinetic model to describe the properties of this channel (3). Selecting rate constants to fit key kinetic and equilibrium data, we find that the model reproduces a variety of *in vivo* and *in vitro* experiments. In combination with calcium ATPase activity for calcium uptake into the ER, the model leads to cytoplasmic calcium oscillations at fixed IP_3 concentration and only a single pool of releasable calcium, the ER. Incorporation of a positive feedback mechanism of calcium on IP_3 production via phospholipase C enriches the properties of the oscillations and leads to calcium oscillations accompanied by oscillations in IP_3 . We discuss the possible significance of these results for the interpretation of experiments.

- 1) Bezprozvanny, I., Watras, J., and Ehrlich, B. E. (1991) *Nature*, 351:63.
- 2) Watras, J., Bezprozvanny, I., and Ehrlich, B. E. (1991) *J. Neurosci.*, 11:3239.
- 3) G. De Young and J. Keizer, *Proc. Natl. Acad. Sci. USA* (1992), in press.

W-PM-C6

LARGE DEPOLARIZATION RELIEVES PURINERGIC P_{2Y} RECEPTOR-INDUCED SUPPRESSION OF VOLTAGE-GATED CALCIUM CURRENTS IN ADRENAL CHROMAFFIN CELLS. ((Craig A. Doppnik and Ray Y.K. Fan)) Dept. Physiol. & Biophys., Univ. of Cincinnati, Cincinnati, OH.

The effect of extracellular ATP, a secretory product co-released with catecholamines, was examined on Ca^{2+} channel currents (I_{Ba}) recorded from bovine chromaffin cells under whole-cell voltage clamp. Local perfusion of cells with ATP rapidly (within 1 s) suppressed I_{Ba} (30 μM ATP, $37 \pm 2\%$, n=19) in a dose-dependent manner ($EC_{50} = 0.7 \mu M$, n=58). The selective P_{2Y} receptor agonist 2-methylthio-ATP similarly suppressed I_{Ba} (100 nM, $39 \pm 3\%$, n=11), but was more potent ($EC_{50} = 2$ nM, n=34). The P_1 receptor agonist 2-chloro-adenosine (100 μM) had no effect on I_{Ba} (n=6). Inhibition of I_{Ba} by ATP was completely abolished by either pertussis toxin pretreatment (300 ng/ml for -20 hr, n=4) or substitution of intrapipet GTP (200 μM) with GDP- βS (200 μM , n=6). Facilitation of I_{Ba} by large depolarizing prepulses was not observed during local control solution perfusion, but was prominent during ATP-induced I_{Ba} inhibition. The I_{Ba} facilitation was voltage dependent ($V_{1/2}$ at +16 mV), with prepulses to +100 mV completely "relieving" the ATP-induced suppression. Interestingly, I_{Ba} inhibition and facilitation was also observed after cessation of control solution perfusion, or during perfusion with control solution pre-exposed to cells for 10 min. Our findings demonstrate that voltage-gated Ca^{2+} channels in chromaffin cells are suppressed by P_{2Y} receptors via a pertussis toxin G-protein pathway that can be relieved by large depolarization. Furthermore, chromaffin cell secretory products similarly suppress I_{Ba} , and together implicate a direct G-protein block in chromaffin cell Ca^{2+} channel facilitation. Supported by AHA SW-91-18 and PHS HL07571-08.

W-PM-C7

KINETIC PROPERTIES OF STIMULUS-COUPLED EXOCYTOSIS OF LARGE DENSE-CORED VESICLES FROM MAMMALIAN PEPTIDERGIC NERVE TERMINALS. ((E.P. Seward, N. Chernevskaya, M.C. Nowycky)) Dept. Anatomy & Neurobiology, Med. Coll. Penn., Philadelphia, PA 19129.

Ca-secretion coupling in isolated neurohypophysial (NHP) terminals was studied with the 'whole-terminal' membrane capacitance (C_m) detection technique (Lim et al. 1990). Ca entry through voltage-dependent Ca channels and jumps in C_m were elicited with trains of depolarizing pulses delivered every 1-2 min. Secretion was exquisitely sensitive to Ca buffering provided by exogenous buffers in the recording pipette. Increasing EGTA from 0.1 to 0.5mM produced ~7-fold increase in the number of Ca ions required to initiate C_m jumps, indicating that the Ca receptor(s) for exocytosis is not responding to the very high [Ca] predicted for the immediate vicinity of Ca channels (Simon and Llinas, 1985). When using short duration pulses to mimic action potentials (20 pulses, 10ms duration, 5Hz), C_m jumps were observed only late in the train. Increasing the total amount of Ca entry by prolonging pulse duration or changing the current amplitude by varying test potential were equally effective in initiating secretion earlier in the train. The ability of brief pulses to elicit C_m jumps was lost as the frequency was lowered to 1Hz.

These results can be explained in terms of a "bound receptor" hypothesis. We propose that the Ca receptor for secretion has a forward rate constant (k_{on}) comparable to that of EGTA and that the pool of receptors effectively integrates Ca influx during a pulse. A relatively slow backward rate constant (k_{off}) causes the receptor to 'remember' prior Ca entry and can explain the ability of bursts of action potentials to stimulate peptide secretion, while single impulses are ineffective.

W-PM-C9

NOVEL CONOPEPTIDE REVERSIBLY BLOCKS IMR-32 HVA CALCIUM CHANNELS by James A. Fox, NEUREX CORP. 3760 Haven Ave., Menlo Park CA 94025.

Whole-cell patch-clamp studies were performed on differentiated IMR-32 human neuroblastoma cells. HVA currents were activated by pulses to +10 mV from a V_h of -80 mV every 10 seconds.

Novel conopeptide SNX-260 (iodinated MVIIC, Neuron 9:69-77 (1992)) reversibly blocked HVA calcium channel currents with an apparent IC_{50} of 50 nM. Blockade was complete at high concentration in some cells (a nifedipine-sensitive component of the current was found in some cells). Block onset time constant was concentration dependent (53 ± 5 sec/ μ M (n=25)). The time constant for removal of block was 104 ± 65 sec (n=20). This current was also blocked at comparable concentrations by another conopeptide, SNX-111 (MVIIA). SNX-111 blockade was nearly complete at high concentrations. Blockade by SNX-111 or conotoxin GVIA was not reversible. These results show both reversible and irreversible blockade of an HVA current in human neuroblastoma cells. The irreversible effects of SNX-111 on IMR-32 cell calcium channel currents differ from its reversible effects on rat neurons (e.g., hippocampal slice field potentials, Soc. Neurosci. Abs. 17(2):1161#462.10).

W-PM-C8

ETHANOL INHIBITS SINGLE L-TYPE Ca^{2+} CHANNELS OF ISOLATED NEUROHYPOPHYSIAL TERMINALS. ((X. Wang, J.R. Lemos*, and S.N. Treistman)) Univ. Mass. Medical School, Worcester, MA 01655 and *Worcester Found. Experimental Biology, Shrewsbury, MA 01545

Ingestion of ethanol (EtOH) results in decreased levels of plasma vasopressin, which may be caused by inhibition of release from the neurohypophysis. Activation of voltage-gated Ca^{2+} channels plays an important role in hormone release. Single channel recordings demonstrate that EtOH, at concentrations constituting legal intoxication, blocks dihydropyridine (DHP)-sensitive 'L-type' Ca^{2+} channels in isolated nerve terminals of rat neurohypophysis. EtOH reduced open probability in a concentration-dependent manner. To better characterize the mechanism of EtOH action, Bay K 8644 was used to prolong the openings of L-type Ca^{2+} channels. In the presence of this DHP, EtOH still reduced the channel open probability, and this could be seen to be due primarily to a shortening of the open duration. Channel conductance was not affected by EtOH, even at high concentrations. These results are consistent with previous macroscopic data indicating that calcium channels in the peptidergic nerve terminals are targets for EtOH action, and indicate that EtOH acts primarily by altering the gating characteristics of the L-type Ca^{2+} channel. (Supported by NIH grants to SNT & JRL)

ACTOMYOSIN INTERACTIONS**W-PM-D1**

THE DUTY CYCLES OF SMOOTH AND SKELETAL MUSCLE MYOSIN ARE INDISTINGUISHABLE AT ZERO LOAD IN THE *IN VITRO* MOTILITY ASSAY. ((D.Harris, K.Trybus & D.Warshaw.)), Physiol. & Biophys., U. of Vermont, Burlington, VT, *Rosenstiel Sci. Ctr., Brandeis U., Waltham MA. (Intro. by E.Blanchard)

Smooth muscle's stress equals that of skeletal muscle with less myosin suggesting a higher average force per smooth muscle cross-bridge. Thus, under isometric conditions, smooth muscle myosin may spend a higher fraction of each cross-bridge cycle attached to actin in the high force state (i.e. higher duty cycle). To determine if smooth muscle myosin has a greater duty cycle under unloaded conditions as well, we used an *in vitro* motility assay in which fluorescently labeled actin filaments move freely over a sparsely (5-20 μ g/ml) coated myosin surface. Over low myosin densities, actin filament velocity (V) is a function of the number of cross bridges capable of interacting with the actin filament (N) and the duty cycle (f), $V = A * [1 - (1-f)^N]$, as proposed by Uyeda et al. (1990) and Harada et al. (1990). "N" was estimated from the myosin density on the motility surface (determined by myosin NH_4^+ -EDTA ATPase activity) and the actin filament length. Data for "V" vs. "N" were fit to the above equation to predict "f". The duty cycle of smooth muscle myosin ($4.0 \pm 0.7\%$) was not significantly different from that of skeletal muscle myosin ($3.8 \pm 0.5\%$) in agreement with values estimated by Uyeda et al. (1990) for skeletal muscle myosin. Although the duty cycles for smooth and skeletal muscle myosin are similar under unloaded conditions, they may differ under isometric conditions, explaining the apparent increased average force per smooth muscle cross-bridge. (support:NIH AR34872 & HL45161)

W-PM-D2

CROSS-BRIDGE FORCE AND VELOCITY OF SMOOTH AND SKELETAL MUSCLE MYOSIN IN THE *IN VITRO* MOTILITY ASSAY. ((P. VanBuren, S. Work, B. Wright and D. Warshaw)), Physiol & Biophys, U. of Vermont, Burlington, VT 05405

In isolated muscle preparations, smooth muscle generates as much stress as fast skeletal muscle with 1/5 the myosin content. Smooth muscle also has a substantially slower maximum shortening velocity. To compare the force:velocity relations generated by thiophosphorylated smooth (turkey gizzard) and skeletal (chicken pectoralis) myosin, we employ an assay which uses monomeric myosin (250 μ g/ml) adhered to a nitrocellulose coated surface at 30°C and low ionic strength (25mM KCl). A fluorescently labeled actin filament, attached to an ultracompliant (50-200nm/pN) microneedle, is brought into contact with the myosin surface. The actin filament velocity and force are measured, based on the rate and extent of microneedle deflection. The maximum average force per cross-bridge for smooth and skeletal myosin appears to be in the range of 0.3-1.4 pN, as determined from the myosin head density on the surface and the actin length in contact with the surface. Surface head density is estimated from myosin binding and ATPase measurements. The maximum smooth muscle myosin velocity under these conditions is approximately 5 times slower than that of skeletal. The auxotonic force:velocity relation, obtained by this technique, approximates that previously described for whole muscle and *in vitro* preparations (Chaen et al., 1989), being concave down. (Support: NIH to PVB HL07647, DW HL45161)

W-PM-D3

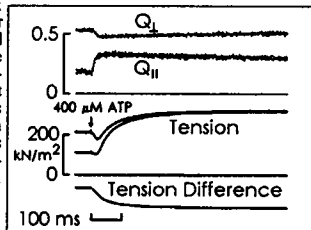
CHARACTERISTICS OF THE V_3 MYOCARDIAL MYOSIN CROSS-BRIDGE CYCLE. (N.R. Alpert, S. Nakajima, E. Seppet, J.N. Peterson) Univ of Vermont, Physiology and Biophysics, Burlington, Vermont 05405.

When mixtures of V_3 and V_1 myosin are used in an in vitro motility assay, the V_3 predominates (Warshaw et al *Biophys J* 59(2): 186a, 1991). This is interpreted in terms of the V_3 myosin exerting compressive forces in resisting the movement generated by the V_1 myosin on the actin filament. Based on these findings, we hypothesized that heart muscle, containing pure V_3 myosin, would exhibit a translocation distance, per cross-bridge cycle, many multiples of the expected 12 nm and negative force during part of the cycle. Using mechanical, myothermal and biochemical measurements and the ratio of active to rigor stiffness, we calculated the translocation distance, the cross-bridge force and the cross-bridge work per cross-bridge cycle as a function of external load. Enthalpy available is 60 pJ per molecule of ATP. Per cross-bridge cycle, maximum work was about 20 pJ while the force varied from 0.5 pN at P_0 to 0.1 pN at $0.2 P_0$. Translocation distance increased from 0.0 at P_0 to 68 nm at $0.2 P_0$. This data will be discussed in terms of cross-bridge compression (negative force) during part of the cross-bridge cycle.

W-PM-D5

KINETICS OF ORIENTATION CHANGES OF RHODAMINE PROBES ON MYOSIN REGULATORY LIGHT CHAINS IN SKINNED MUSCLE FIBERS FOLLOWING PHOTOLYSIS OF CAGED ATP. (T. S.C. Allen, N. Ling*, Y.E. Goldman, and M. Irving*) U. of Penn., Phila., PA 19104, *King's College London, London, UK, and *U. of Waikato, Hamilton, N. Z.

To examine the relationship between mechanics and angular motions of cross-bridges, we exchanged rhodamine labelled regulatory light chains (RLC) from chicken gizzard muscle for native RLC in glycerinated, single fibers from rabbit psoas muscle and measured tension, stiffness and fluorescence polarization following photolysis of ATP in fibers in rigor at $\sim 30 \mu\text{M}$ free Ca^{2+} , 20°C (Allen et al *Bioophys. J.* 61:A286, 1992). Fluorescence polarization ratios Q_{\parallel} and Q_{\perp} were measured with 3 kHz bandwidth (Tanner et al *J. Mol. Biol.* 223:185-203, 1992). On release of ATP, Q_{\parallel} increased and Q_{\perp} decreased, indicating disordering of probes. These events were faster than convergence of tension transients in paired isometric and pre-stretch ($\sim 0.5\%$ 1 s before photolysis) trials (Fig.). Q_{\parallel} and Q_{\perp} were unaffected by the pre-stretch. Assuming ATP is released at 118 s^{-1} , we obtain apparent second-order rate constants $5-10 \times 10^3 \text{ M}^{-1} \text{ s}^{-1}$ for Q_{\parallel} , $2-5 \times 10^3 \text{ M}^{-1} \text{ s}^{-1}$ for Q_{\perp} , and $1-2 \times 10^3 \text{ M}^{-1} \text{ s}^{-1}$ for tension convergence in RLC exchanged fibers. The results suggest that, after the liberation of ATP, either 1) the cross-bridges promptly become disordered, but detach more slowly, or 2) cross-bridges detach promptly, but the increment in force resulting from the pre-stretch is maintained after detachment and subsequent reattachment. Supported by MDA, NIH, and Wellcome Trust, U.K.

**W-PM-D7**

THE EFFECT OF S1 ON THE DISSOCIATION RATES OF NUCLEOTIDE AND CALCIUM FROM NATIVE AND PROTEOLYTICALLY MODIFIED G-ACTIN. (Andrzej A. Kasprzak) CRBM, CNRS-INSERM U.249, Univ. Montpellier I, Montpellier, France

The dissociation rates of the nucleotide eATP and Ca^{2+} from G-actin and from its binary complex with S1A₂ were measured by recording a large decrease of the fluorescence intensity of eATP upon transferring the ethenobase from the protein environment to the solution. The released nucleotide was hydrolyzed by either alkaline phosphatase or pyrophosphatase to trap the released Ca^{2+} . EDTA was used. The dissociation rate (k_{off}) of eATP in the G-acto-S1A₂ complex decreased from $\sim 6 \times 10^4 \text{ s}^{-1}$ (free actin) to $1 \times 10^4 \text{ s}^{-1}$ (complex); $k_{\text{off}}(\text{Ca}^{2+})$ was also reduced from $\sim 3 \times 10^2$ to $4 \times 10^3 \text{ s}^{-1}$, respectively. The effects of two proteolytic modifications of actin on the k_{off} were also examined. Specific subtilisin cleavage at Met-47/Gly-48 resulted in an increase, as compared to the unmodified protein, of the value of $k_{\text{off}}(\text{eATP})$ for free subtilisin-cleaved actin to $\sim 1.1 \times 10^3 \text{ s}^{-1}$. In the presence of S1 this value was reduced to $1.6 \times 10^4 \text{ s}^{-1}$. The corresponding data for $k_{\text{off}}(\text{Ca}^{2+})$ were $\sim 3.3 \times 10^2$ and $7 \times 10^3 \text{ s}^{-1}$, respectively. In the truncated actin (actin with the last 3 amino acid residues proteolytically removed), the inhibitory effects of S1 on k_{off} were also seen. The accessibility of the nucleotide base in all the above complexes was assessed from acrylamide quenching and in all cases it was found negligible. The importance of these results for the ideas of actomyosin-based motility that emphasize a more active role of actin, is discussed.

W-PM-D4

MUSCLE CONTRACTION STUDIED WITH AN INDANE DIONE SPIN LABEL PROBING MYOSIN HEAVY AND LIGHT CHAINS

((Osba Roopnarine, Kálmán Hideg[†], Andrew G. Szant-Györgyi^{*}, and David D. Thomas)) University of Minnesota Medical School, Minneapolis, MN 55455, [†]University of Pécs, Hungary, ^{*}Brandeis University, Massachusetts.

We have used an indane dione spin label, designated InVSL, to label cysteines in myosin for studying the rotational and orientational dynamics of myosin heads during muscle contraction. InVSL has a rigid structure that makes it immobilized and well-oriented on myosin, when attached selectively to SH groups either on myosin heavy chains or on light chains. EPR spectra of labeled myosin indicate that the label is rigidly immobilized, so that it reports the global rotation of myosin heads, which undergo μs segmental rotation. The EPR spectra of glycerinated muscle fibers show that the principal axis of the heavy-chain spin label is aligned almost perfectly with the muscle fiber axis, making it the first spin label capable of providing unambiguous information about axial rotations of myosin heads. Our results are consistent with previous EPR results with other spin labels, but they show much more clearly that (a) MgADP causes only a small axial rotation ($\sim 8^\circ$) of the heads, (b) relaxation with MgATP only partially broadens the angular distribution of the heads, and (c) no new angles are observed in contraction. The EPR spectra of *Placoepecten magellanicus* scallop fibers with InVSL-labeled rabbit or *Mercenaria* regulatory light chains show that the spin labels are much more disordered than heavy chain labels, even in rigor, suggesting that the neck region of the myosin heads is not as ordered as the region containing the SH1 site.

W-PM-D6

A NEW METHOD TO MEASURE ATP TURNOVER RATE IN FULLY RELAXED MYOFIBRILS USING A FLUORESCENT NUCLEOTIDE ((K.H. Myburgh and R. Cooke)). CVRI and Department of Biochemistry & Biophysics, University of California, San Francisco, CA 94143-0524

Direct measurements of ATP turnover rate in fully relaxed skinned muscle are complicated by the presence of a few active cross bridges. To surmount this problem we developed a technique to measure ATP turnover rate using the analogue methylantraniloyl ATP (mant-ATP), which increases fluorescence emission on binding to the myosin head. Rabbit skeletal myofibrils that were fully relaxed in the presence of 800 μM ATP, 40mM PC and 2mg/ml CPK, were mixed rapidly with an equal volume of 80uM mant-ATP. The fluorescence is enhanced as mant-ATP binds to myosin during nucleotide turnover. A rate constant was calculated by fitting the data to a single exponential. Turnover rates were 0.0121 ± 0.002 and $0.0107 \pm 0.001 \text{ s}^{-1}$ at 12 and 20°C respectively. The decrease in rate at 20°C is probably due to a stronger bond between the myosin head and the core of the thick filament at the higher temperature. The rate at 20°C is slower than that of myosin alone indicating that filament structure restricts the nucleotide turnover rate. Myosin light chain phosphorylation may also affect filament structure and thus ATP turnover rate. Phosphorylation (90%), achieved by incubating myofibrils in calcium insensitive light chain kinase, had no effect on ATP turnover rate at 12°C , but increased it slightly at 20°C .

Supported by HL32145, and an AHA postdoctoral fellowship to KHM

W-PM-D8

TRITIUM EXCHANGE STUDIES OF SKINNED MUSCLE FIBERS

((M.E. Rodgers¹, J.J. Englander², S.W. Englander² and W.F. Harrington¹)) ¹Department of Biology, The Johns Hopkins University, Baltimore, MD 21218 and ²Department of Biochemistry and Biophysics, University of Pennsylvania, Philadelphia, PA 19104

Solvent-protein tritium exchange has been used to probe structural transitions in skinned muscle fibers. Bundles of two rabbit psoas fibers were labeled with ^3H under activating conditions and placed in rigor in the presence of tritium to lock the fiber in a static state. Background ^3H was removed by washing in non-tritiated rigor solvent. Upon reactivation, a pulse of ^3H was released. The amount of ^3H released corresponds to ~ 50 amide protons per myosin molecule in the muscle. When similar experiments were carried out by labeling in rigor, no pulse of ^3H was observed upon activation. These results show that a class of amide protons undergo a transition to a rapid exchange state associated with the active state of muscle. The experiments were carried out at pH 6, 22°C . The extent of exchange of this class of activation associated protons was found to increase both with pH and temperature. When fibers labeled under activating conditions and washed as above were relaxed with MgPPi prior to reactivation, two pulses of tritium were released. Relaxation resulted in a release of $\sim 40\%$ of the total label while the remainder was released by activation. Our interpretation is that part of the ^3H is being trapped in the acto-myosin interface and part is associated with active tension generation. Further experiments on fibers stretched to non-overlap indicate that a small amount ($\sim 10\%$) of the total signal is associated with the changes in the state of myofibrillar proteins induced by binding Ca^{2+} . Supported by grants AR-04349 (WFF) and DK-11295 (SWE).

W-PM-D9

PERSISTING *IN VITRO* MOTILITY OF ACTIN FILAMENTS AT NANOMOLAR ATP CONCENTRATIONS ((M.S.Z. Kellermayer, T.R. Hinds*, and G.H. Pollack)) Bioengineering, *Pharmacology, University of Washington, Seattle, WA 98195

Actin-filament motility is abolished at 2-4 μM free ATP concentration in the continued presence of a significant ATP turnover in the *in vitro* motility assay. This is in contrast to muscle fibers and myofibrils, where unloaded rapid shortening takes place at little¹ or no² ATP turnover. We hypothesized that, by pretreating actomyosin with millimolar concentrations of ATP—resembling physiological conditions—*in vitro* actin movement would continue at the low ATP turnover characteristic of the rapidly shortening sarcomere.

In vitro motility assay was performed in the initial presence of 1 mM ATP. To reduce ATP turnover, the ATP concentration was lowered by washing the 10- μl sample chamber with 100 μl rigor solution. Interestingly, actin filaments did not stop; they continued travelling at a lower rate. In fact, filament motility persisted up to five rigor-solution washes. By the third wash, the ATP concentration—monitored by luciferin-luciferase assay—dropped to nanomolar levels (Table).

Our results imply that ATP's energy is stored during the initial ATP-treatment of actomyosin, and this energy can later be used to fuel actin filament motility.

1. Homsher, E. *Ann. Rev. Physiol.* 49, 673-90 (1987).

2. Ohno, T. & Kodama, T. *J. Physiol.* 441, 685-702 (1991).

(Supported by AHA #92-WA-120-R and NIH #s HL18676 and HL31962.)

N ^o of wash	Velocity	[ATP]
1.	1.7 $\mu\text{m/s}$	6.8 μM
2.	1.1 $\mu\text{m/s}$	0.55 μM
3.	0.61 $\mu\text{m/s}$	0.05 μM

W-PM-D10

CROSS-BRIDGE MODEL BASED ON DISCRETE ACTIN STEPS IN WEAK CROSS-BRIDGE STATE ((P. Dreizen, J. Shi, U. Ghodke, C. Shen, J. Feng)) Physiology & Biophysics, SUNY Brooklyn, Brooklyn, NY 11203.

A cross-bridge model has been proposed having no "power stroke". It is based on evidence of 2-state actin filaments: flexible (F) with rapid oscillations of actin conformation and bonds, and rigid (R) (Oosawa, Yanagida, et al). The model postulates that F-state actin oscillations support sequential movement of S1 weak cross-bridges (AM-ADP-P_i) in a rocking motion (-2.7nm) between EDC cross-linked sites of S1 20K and 50K domains and N-terminal actin monomers. Recent evidence in support of this model follows: (1) Determination of apparent equilibrium constant from A³H-C kinetics indicates K_e values of 6-10 μM at EDC sites, consistent with K_d for A-S1 in presence of ATP. This supports the hypothesis that both EDC sites are involved in weak cross-bridge state. (2) EDC cross-linking of regulated acto-S1 in presence of MgATP indicates that formation of A²20K and A²50K exhibits μM Ca²⁺-sensitivity. Thus, the putative rocking motion of S1 along actin sites is supported in Ca²⁺-on state, and absent in Ca²⁺-off state. (3) HMM in presence of Mg²⁺/Ca²⁺ shows thermally-dependent self-association. Self-association is greatest in absence of nucleotide, somewhat less with ADP, and negligible at ATP and AMP-PNP concentrations saturating catalytic site. This suggests stabilization of neighboring HMM heads with enhanced tension in strong cross-bridge states, and detachment in weak cross-bridge states. (4) The model postulates that actin F/R transition varies with applied force. We are testing this hypothesis in acto-S1 systems.

PROTEIN FOLDING

W-PM-E1

SINGLE AMINO ACID SUBSTITUTIONS CORRECTING PROTEIN FOLDING DEFECTS *IN VIVO* AND *IN VITRO* ((Jonathan King, Cammie Haase-Pettingel, and Anna Mitraki)) Dept. of Biology, MIT, Cambridge, MA 02139.

The failure of newly synthesized polypeptide chains to fold into their native structures, and accumulation as intracellular inclusion bodies is a practical problem in the laboratory and the biotechnology industry. For the thermostable trimeric P22 tailspike protein, folding intermediates in the intracellular pathway can be distinguished from both the native state and the aggregated inclusion body state. The inclusion body forms from an early single chain folding intermediate at elevated temperatures and represents a kinetically trapped form of the intermediates. Temperature sensitive folding (*tsf*) mutations at more than 30 sites in the chain further destabilize the critical intermediate, shifting the partitioning between productive and aggregation pathways at higher temperature. Global suppressor mutations in the center of the 666 residue chain - Val331>Ala and Ala334>Val - correct many of the *tsf* defects (Mitraki et al, *Science*, 253, 54-58, 1991). The stability of the native state is not altered by either class of mutation. Examination of the *in vitro* refolding of purified tailspike chains (Fuchs, Seiderer & Seckler, *Biochemistry*, 30, 6598-6604, 1991) carrying the suppressor substitutions reveals that they suppress aggregation *in vitro* in the temperature range of 15-20°C. These results argue against nonspecific models for the aggregation process. One model consistent with this result is that the suppressors alter a site in the folding intermediate needed to nucleate the aggregation pathway. Alternatively the suppressors may destabilize an intermediate along the aggregation pathway.

W-PM-E3

DISTINGUISHING FEATURES OF β -LACTOGLOBULIN COLD AND HEAT DENATURATIONS ((Yu.V. Griko, V.P. Kutysenko*, P.L. Privalov)) The Johns Hopkins University, Baltimore, MD 21218, USA., Institute of Biological Physics of the Russian Academy of Sciences, Russia*.

Changes in β -lactoglobulin upon cold and heat denaturation were studied by scanning calorimetry, CD and NMR spectroscopy. In solutions containing urea above and below 35 °C these processes are accompanied by different structural and thermodynamic changes. Structural rearrangements in the β -lactoglobulin molecule upon cold denaturation yield a stable intermediate state which is not observed with heat denaturation. The equilibrium intermediate state can be obtained also in 6 M urea solution and disrupted by either cooling or heating. Its disruption with decreasing temperature appears as cooperative changes in heat capacity, while with increasing temperature, the heat capacity changes only gradually. Considering the sigmoidal shape of the heat capacity change as an extended heat absorption peak, we propose that the intermediate state is stabilized by enthalpic interactions.

W-PM-E2

PROTEIN INTERNAL MOTIONS MEASURED BY HYDROGEN EXCHANGE ARE NOT AFFECTED BY LARGE CHANGES IN GLOBAL STABILITY ((C. Woodward, K.-S. Kim, & F. Tao)) Dept. of Biochemistry, Univ. of Minnesota, St. Paul, MN 55108.

Bovine pancreatic trypsin inhibitor (BPTI) mutants with single amino acid replacements have been constructed; highly conserved, buried aromatic or asparagine residues are replaced with alanine or glycine. The solution behavior of the mutant proteins has been characterized by hydrogen exchange and calorimetry, and their high resolution crystal structures determined. In many mutants removal of the larger side chain leaves large concave crevices on the molecular surface. The mutants are highly destabilized; differences in the free energy of N \rightarrow D reaction, $\Delta\Delta G(\text{WT-mut})$, are in the range of 5-6 kcal/mol. Hydrogen isotope exchange of buried peptide protons may occur by either of two mechanisms. One mechanism involves global unfolding, and gives values for $\Delta\Delta G(\text{WT-mut})$ which agree well with those obtained calorimetrically. The second exchange mechanism involves fluctuations of the folded state which expose buried and H-bonded protons to solvent. Rates for protons exchanging by the second mechanism are the same in WT and in the destabilized mutants, unless the exchanging proton is in the vicinity of the mutation. Implications for the internal motions exposing buried protons to solvent for exchange will be discussed.

W-PM-E4

THE SOLUTION STRUCTURE & DYNAMICS OF A PROTEIN MOLTEN GLOBULE: APOCYTOCHROME B562 ((A. J. Wand, Y. Feng and S. G. Sligar)) Department of Biochemistry, University of Illinois at Urbana-Champaign, Urbana, IL 61810

Apo cytochrome b562 displays many of the features ascribed to the molten globule state. The solution structure of protein has been determined by NMR methods. The secondary and tertiary structure of the protein is very similar to the holoprotein. All four helices are present, though some disorder of the c-terminal helix is evident. One side of the heme binding pocket is preserved and is exposed to solvent. This may indicate that the molten globule state represents a penultimate step in the folding of the protein. The internal dynamics of the protein have also been examined. NMR relaxation studies indicate that the amplitude of motion of amide N-H vectors is not much different from that found in proteins in the native state. In contrast, the effective correlation times are found to vary over a much wider range than is normally seen in proteins in the native state. In sum, these results provide the first comprehensive structural view of a protein in the molten globule state.

W-PM-E5**PROTEIN FOLDING DURING BIOSYNTHESIS PROBED WITH A CONFORMATIONAL-DEPENDENT MONOCLONAL ANTIBODY.**

((B. Friguet, A.N. Fedorov*, L. Djavadi-Ohanian, Y.B. Alakhov* and M.E. Goldberg)) Unite de Biochimie Cellulaire, Institut Pasteur, Paris, France and * Institute of Protein Research, 142292 Pushchino, Russia.

Folding on the ribosome of nascent chains of the *E. coli* Tryptophan Synthase beta subunit has been investigated using a conformation dependent monoclonal antibody (mAb 19). This antibody recognizes an antigenic determinant that appears during the *in vitro* refolding of the protein only after several folding steps have been achieved. Upon biosynthesis of beta chains in a *E. coli* cell-free system, it has been shown that ribosome-bound nascent polypeptides can react with the monoclonal antibody provided their size is above 11.5 kDa, which is smaller than that of the N-terminal domain of the protein. After construction and expression of the gene fragments coding for the 11.5 kDa N-terminal fragment either free or bound to the ribosome, it has been shown that the free fragment acquires a condensed structure. This structure resembles that of the native protein in the vicinity of the epitope for mAb 19. Indeed, the affinity of mAb 19 for the 11.5 kDa fragment, either free or bound to the ribosome, has been measured and shown to be close to that of the native protein. It is proposed that the polypeptide chain may start to fold during its biosynthesis and that a folded intermediate is formed that exhibits some structural features of the native state and of an immunoreactive intermediate previously detected during the *in vitro* refolding of denatured beta chains.

W-PM-E7**KINETICS OF FOLDING/UNFOLDING OF STAPHYLOCOCCAL NUCLEASE (SNase) BY CIRCULAR DICHROISM (CD) STOPPED-FLOW.**
(H.M. Chen¹ and T.Y. Tsong^{1,2}) ¹Dept of Biochem, Univ of Minn, St. Paul, MN 55108, and ²Hong Kong Univ of Sci & Technol, Kowloon, Hong Kong.

Previous study of the folding/unfolding kinetics has monitored Trp140 fluorescence. Trp140 is located near the flexible end of the protein, and its fluorescence may not reflect the overall structure of the protein. CD at 222 nm, which measures helical content, has now been used to study the same folding (from pH 3.0 to pH 7.0) and unfolding (from pH 7.0 to pH 3.1) reactions in the time range between 30 ms and 300 s. Similar to previous results by fluorescence detection, the folding by CD detection was triphasic and the unfolding was monophasic, although the time constants were substantially slower with the CD signal (47 s, 5.3 s and 190 ms for folding; 6.0 s for unfolding) than with the fluorescence signal (30 s, 870 ms, 51 ms for folding; 1.15 s for unfolding). With CD detection, there was an unresolved reaction for the unfolding (14% of total signal) and the refolding (14% of total signal). The dead time of the CD stopped-flow was 30 ms. CD signal also detected a very slow reaction, with time constant much greater than 300 s, for the unfolding (25% of total signal) and the refolding (19% of total signal). The time resolved CD kinetics (30 ms to 300 s) support the mechanism proposed earlier for the folding of SNase: $D_3 \rightleftharpoons D_2 \rightleftharpoons D_1 \rightleftharpoons N_0$. The three D's denote three macroscopic sub-states of the unfolded form and the N_0 denotes the native state. The three D's have similar free energies but are separated by activation barriers greater than 6.5 kcal/mol. The unresolved fast reactions could mean the presence of microscopic states, between which conversion is fast, i.e. with low activation barriers. The very slow reactions could reflect isomerization of N_0 . Two isomeric forms of SNase in the native state have been detected by NMR.

MEMBRANE FUSION**W-PM-F1**

EFFECTS OF HEXADECANE ON THE KINETICS OF $L_{II}/Q_{II}/H_{II}$ PHASE TRANSITIONS IN DOPE-Me (D. Alford¹, J. Bente², P. Yeagle², D. Siegel¹) ¹Dept. Biosci. & Biotech., Drexel Univ., Phil. PA 19104; ²Dept. Biochem., Med. Schl., SUNY, Buffalo, NY 14214; Procter & Gamble Co., P.O.B. 398707, Cincinnati, OH 45239.

We studied the effects of hexadecane (HD) on inverted phase formation in N-monomethylated dioleoyl-PE (DOPE-Me). Long-chain alkanes partition preferentially into hydrophobic interstices within H_{II} phases [1,2]. This stabilizes H_{II} (lowers T_H) because otherwise the interstices are filled by entropically-disfavored stretching of DOPE-Me chains. As in [1], we found that T_H decreases with increasing HD concentration. However, we found that T_H as determined by DSC is more scan-rate dependent in the presence of HD. This may be due to a transition rate-limiting partition of HD into nascent H_{II} phase at fast scan rates. X-ray diffraction (XRD) data collected at static temperatures for several hours are compatible with DSC values of T_H obtained at 1°/hr. A Q_{II} phase forms slowly in pure DOPE-Me [3], but less Q_{II} phase was detected by XRD as the HD concentration increased. No Q_{II} phase was detected at 4 mol % HD. Apparently, Q_{II} forms near T_H because, though not as stable in terms of curvature free energy as H_{II} , Q_{II} lacks the unfavorable chain-packing free energy of H_{II} in excess water. HD reduces the chain-packing free energy, so Q_{II} disappears with increasing HD content. This study will be extended to the effects of HD on liposome fusion kinetics in DOPE-Me.

[1] Biochem.28:5010; [2] Biochem.31:1356; [3] Biochem. 29:5975.

W-PM-E6

A CONFORMATIONAL INTERMEDIATE IN THE FOLDING OF A TROPOMYOSIN COILED COIL MODEL PEPTIDE. ((N.J. Greenfield and S.E. Hitchcock-DeGregori)) Department of Neuroscience and Cell Biology UMDNJ-Robert Wood Johnson Medical School, 675 Hoes Lane, Piscataway, NJ 08854-5635.

A 43 residue peptide was designed to serve as a model for the N-terminal domain of tropomyosin. The sequence of the peptide is MDAIKKMQMLKLDVENLLDRLEQLEADLKALEDTRYKQLEGGC. The peptide forms a coiled coil at low temperatures (<25 °C) under physiological conditions. When CD spectra are examined as a function of temperature, the folding of the peptide is non-cooperative. Different T_m 's are obtained when the folding is followed at 222, 208 and 280 nm. Deconvolution of the spectra suggests that at least 3 curves contribute to the CD in the far UV. One curve is similar to the CD spectrum of the coiled coil α -helix of native α -tropomyosin. The second resembles that of single stranded short α -helical segments found in globular proteins. The third is similar to that of polypeptides in the random coil conformation. The results suggest as the peptide is cooled, an α -helical intermediate (3.6 res./turn) forms before most of the coiled coil (3.5 res./turn) is gained. An intermediate is not detected if folding of a coiled coil is followed at a single wavelength¹ but is seen when entire spectra are examined². ¹Lau *et al* J. Biol. Chem. 259 13253 (1984). ²Engel *et al* Biochemistry 30 3161 (1991). Supported by NIH and MDA.

W-PM-F2

BICONTINUOUS AND DISCONTINUOUS CUBIC PHASES IN PHOSPHOLIPID-CHOLESTEROL-DIACYLGLYCEROL AQUEOUS SYSTEMS. IMPLICATIONS FOR MEMBRANE FUSION.

((J.L.Nieva,R.Vargas,A.Alonso,F.M.Goffi and V.Luzzati)) Departamento de Bioquímica, Universidad del País Vasco, Spain and Centre de Génétique Moléculaire,C.N.R.S.,91198 Gif-sur-Yvette, France.

The thermotropic behaviour of aqueous dispersions of phosphatidylcholine:phosphatidylethanolamine:cholesterol (2:1:1 mole ratio) containing different proportions of diacylglycerol have been studied by ³¹P-NMR and X-ray diffraction. Lamellar, hexagonal and cubic phases have been detected. Low (5-10%) levels of diacylglycerol induce formation of a bicontinuous Q_A cubic phase (No.224).With higher (230X) diacylglycerol levels, X-ray diffraction data are compatible with a structure consisting of two types of disjointed type II micelles, quasi-spherical in shape, organized in a cubic cell. Such a structure could correspond to the recently published (Luzzati *et al.*, Biochemistry 31, 279). The bicontinuous Q_A cubic phase constitutes a medium permeable to both water and oil, while the Q_{II} cubic phase corresponds to a water-impermeable medium. These data may be correlated with observations of phospholipase C-induced liposome fusion according to which low amounts of diacylglycerol induce mixing of aqueous contents between vesicles in apposition, while, above a certain level of diacylglycerol, vesicle fusion does no longer occur.

W-PM-F3

A MECHANISM OF CATION-INDUCED LIPID VESICLE MEMBRANE FUSION. S. Ohki, Department of Biophysical Sciences, SUNY at Buffalo, 224 Cary Hall, Buffalo, NY 14214-3005.

A theory of the mechanism of cation-induced lipid vesicle fusion is proposed: As fusogenic cations bind more to an acidic lipid membrane and the membrane surface becomes more hydrophobic, the electrostatic and hydration repulsive interaction forces, which exert on two interacting lipid vesicles, are reduced. Thus, the minimum distance for two interacting vesicles to be able to approach is reduced, which is expressed as a function of the cation concentration. At a sufficient concentration of the cation, two vesicles come to a close distance like a molecular distance. At the fusion point for acidic lipid vesicles induced by divalent cation, such vesicle adhesions should be attained. In such a situation, the boundary region between the adhered and non-adhered membranes of the adhered two vesicles becomes a higher energy state than the other parts of the membranes due to the stressed shape created by the closely adhered vesicles. The excess energy in the boundary region depends upon the size of vesicles: The smaller the vesicle, the higher the excess energy. Such a region, therefore, is physically and chemically unstable and may well be the site of vesicle fusion. The experimental results seem to support the above proposed fusion theory.

W-PM-F5

THE FUSION ACTIVITY AND RELATED CONFORMATIONAL CHANGES IN THE ARENAVIRUS LCMV GLYCOPROTEIN SPIKE ((Christopher Di Simone and Michael J. Buchmeier)) Scripps Research Institute, CVN-8, 10666 N. Torrey Pines Rd., La Jolla, CA 92037

The arenavirus lymphocytic choriomeningitis virus (LCMV) has served as the premier model for examining virus-host interactions and persistent infection. LCMV is a lipid enveloped virus and contains two ambisense RNA's which encode for four protein products, NP, GP, Z, and L. GP is posttranslationally cleaved into GP-1 and GP-2 glycoproteins which make up the viral spike complex. The complex is a tetramer with GP-1 as a peripheral headpiece and GP-2 as a membrane embedded stalk. We have found that chloroquine, a lysosomotropic weak base, inhibited LCMV infectivity indicating a pH dependent endosomal route of cell entry. The pH dependence of fusion was examined using the R18 fluorescence dequenching assay. Rates and extent of fusion were measured with both negatively charged multilamellar vesicles and BHK cells. Fusion with cardiolipin vesicles at acidic pH (5.0) was very rapid while no fusion was observed at neutral pH (7.2). As pH was decreased from pH 7.2 to pH 4.8 a linear increase in rate and extent of fusion was observed. Quantitation of LCMV bound to BHK cells revealed 300 virus particles bound per cell and 30 particles fused per hour. Binding was saturated at 1000 LCMV particles per BHK cell. pH induced conformational change in the protein structure was examined by looking at changes in accessibility of several monoclonal GP-1 and GP-2 specific antibodies to their respective epitopes. A marked increase in exposure of epitopes on GP-2 was observed at acidic pH (5.0). Treatment of LCMV at pH 5.0 resulted in dissociation of the GP-1 component from the GP-2 transmembrane stalk of the protein complex with a concomitant loss in viral infectivity between pH 5.45 and 5.3. A model of LCMV fusion consistent with this data will be presented. C. D. was supported by NIH training grant # GM 07437.

W-PM-F7

GRANULE-GRANULE FUSION DURING EXOCYTOSIS IN HORSE EOSINOPHILS. ((M. Lindau and S. Sceppek)) Molecular Cell Research, Max-Planck-Institut für medizinische Forschung, D-6900 Heidelberg, Germany.

The fusion of granules with the plasma membrane during exocytosis leads to a stepwise increase of plasma membrane capacitance which can be recorded by time-resolved patch-clamp capacitance measurements. When horse eosinophils were stimulated by intracellular GTPγS the size of the steps was a function of the GTPγS concentration. Between 5 and 20 μM the step size distributions were in agreement with the granule size distribution determined in resting cells by electron microscopy. At 80 and 160 μM the number of such 'normal' steps was decreased and in addition much larger steps occurred. However, the total capacitance increase remained the same. At 160 μM almost all of the capacitance increase may occur in a single step indicating fusion of a large exocytotic vacuole. These results show that at high GTPγS concentrations granule-granule fusion occurs inside the cell. This is the first demonstration of G protein-mediated granule-granule fusion.

Supported by DFG LI 443/3-1 and Sfb 312/B6

W-PM-F4

The Viral Fusion Inhibitor, ZffG, Alters Phospholipid Packing by Altering Phospholipid Headgroup Conformation. A. R. Dentino & P. L. Yeagle, Department of Biochemistry, University at Buffalo School of Medicine, Buffalo, NY 14214

The antiviral peptide, ZffG, operates by inhibiting membrane fusion¹. Inhibition of membrane fusion appears to be the result of inhibition of the formation of highly curved phospholipid surfaces in fusion intermediates¹. ¹H, ²H, ¹³C and ³¹P NMR experiments suggest that ZffG alters the headgroup conformation of phosphatidylcholine (PC) when added to the surface of PC large unilamellar vesicles (LUV). 2-D ¹H NMR experiments show changes in the internuclear interactions in the headgroup. ²H NMR data of d₄ (choline)-labeled PC show changed quadrupole splittings indicative of an alteration in the choline orientation. ³¹P NMR data show a changed powder pattern consistent with an altered headgroup conformation. ¹³C NMR data of PC labeled with ¹³C in the carbonyls of the acyl chains show a change in the powder pattern of the C¹ carbonyl consistent with a new orientation of the carbonyl similar to that exhibited by the C² carbonyl. Together these data suggest an alteration in the conformation of the glycerophosphorylcholine portion of PC due to the binding of the fusion inhibitor, ZffG. ¹³C NMR data from ¹³C-labeled ZffG (the terminal carbonyl) show that the pKa of this peptide in the membrane governs the ability of this peptide to alter phospholipid packing. This work was supported by grants from NIH (AI26800; DE05608).

¹ J. Biol. Chem. 265, 12178-12183 (1990); Virology, 182, 690-702 (1991); Biochemistry, 31, 3177-3183 (1992)

W-PM-F6

CALCIUM IONS AND HUMAN CELL COMPONENTS ARE REQUIRED FOR CELL FUSION MEDIATED BY THE CD4-HIV-1-ENVELOPE GLYCOPROTEIN INTERACTION. ((D.S. Dimitrov¹, C.C. Broder², E.A. Berger², and R. Blumenthal¹)) ¹NCI, ²NIH, Bethesda, MD 20892. (Spon. by I. Ambudkar)

To examine the role of calcium ions and human cell components for cell fusion mediated by interactions between CD4 and the HIV-1 envelope glycoprotein (gp120-gp41), we used cells, expressing gp120-gp41 and its receptor CD4, each encoded by recombinant vaccinia viruses. Fusion was measured by counting the number of syncytia and by monitoring the redistribution of fluorescence dyes utilizing video microscopy. Syncytia did not form in solutions without calcium ions. EDTA and EGTA blocked syncytia formation in culture mediums containing calcium ions. Cell fusion was not affected by magnesium ions in the concentration range from 0 to 30 mM. Membrane fusion as monitored by fluorescence dye redistribution also required calcium ions. HIV-1 envelope-expressing cells fused with CD4-expressing human/animal giant hybrid cells but not with giant cells derived from animal cells alone. We conclude that calcium ions and human cell components are essential for cell fusion mediated by the CD4-HIV-1 envelope glycoprotein interaction.

W-PM-F8

HYDROPHOBIC IONS AMPLIFY THE CAPACITATIVE CURRENTS USED TO MEASURE EXOCYTOSIS WITH THE PATCH-CLAMP TECHNIQUE. ((A.F. Oberhauser and J.M. Fernandez)) Mayo Clinic, Rochester, MN 55905

The detection of exocytotic fusion in patch-clamped secretory cells depends on measuring an increase in the cell membrane capacitance as new membrane is added to the plasma membrane or in the measurement of a small capacitative current that charges the fusing vesicle to the same potential as that of the plasma membrane. However, in the majority of secretory cells, secretory vesicles are too small (< 100 nm) to cause a detectable signal. We have sought to amplify these capacitative signals by increasing the specific capacitance of the membrane of a secretory cell. Since the specific capacitance of a membrane depends on the polarizability of the dielectric material, the addition of charged or dipolar groups to the membrane core should increase the membrane capacitance. We have found that short incubations (< 2 min) of mouse peritoneal mast cells with the hydrophobic anion dipyridylamine (DPA, 10 μM), increases the cell membrane capacitance by more than 2.5 times. More importantly, the DPA treatment produces a 7-fold increase in the size of the capacitance steps observed upon the exocytotic fusion of single secretory granules (195±33 fF in DPA treated cells compared to 24±3 fF in untreated cells). The increased granule membrane capacitance dramatically enlarges the transient capacitative discharge measured upon formation of a fusion pore (18±2 fC in DPA treated cells compared to 4.3±0.4 fC in untreated cells; holding at +50 mV). The method presented here should prove useful in the study of exocytotic fusion in neuronal and neuroendocrine cells where the single fusion event has been below our current resolution.

W-PM-F9

RESONANCE ENERGY TRANSFER MICROSCOPY APPLIED TO MEMBRANE FUSION ((W. Niles, ²J. Silvius & ¹F. Cohen)) ¹Dept. Physiology, Rush University, Chicago, IL 60612, & ²Dept. Biochemistry, McGill University, Montreal, Que.

The coalescence of liquids that defines the fusion of two lipid bilayers occurs on relatively fast time and short distance scales. In order to study the stages of fusion on these scales, we are developing a resonance energy transfer microscope. With video microscopy, we observe the interaction of 10- μ m dia. lipid vesicles containing the fluorescent donor probe coumarin-PE with planar lipid membranes containing the acceptor probe rhodamine-PE. Energy transfer has been characterized by the following measurements: intrinsic transfer properties of the dye pair (spectral overlap and polarization anisotropy-determined molecular orientations during transfer), the spectral transfer function of the video microscope, and the photometric behavior of the dye pair in the planar membrane. To obtain the characteristic distance of energy transfer, we have fluorimetrically measured acceptor emission sensitization at varying probe densities in liposomes. This allows us to scale the video brightnesses of the same densities of probes in the planar membrane. Energy transfer is detected when vesicles adhere to the planar membrane. We have determined the area of the vesicle in contact with the planar membrane and found it to be non-contiguous. We will use the calibrated microscope to determine the energy transfer rate and calculate the intermembrane separation. Supported by GM27367.

INTERCELLULAR COMMUNICATION

W-PM-G1

FAST V_j -DEPENDENT GATING IN GAP JUNCTIONS. ((J.B. Rubin, T.A. Bargiello, M.V.L. Bennett and V.K. Verselis)) AECOM, NY, 10461.

Transjunctional voltage (V_j) dependence of homotypic junctions is generally characterized by a slow, symmetric reduction in junctional conductance, g_j , about $V_j=0$, which has been explained as the combined actions of the two opposed hemichannels, each with the same intrinsic sensitivity to V_j . However, in some heterotypic junctions, such as those formed by the pairing of Cx32 with Cx26, the g_j - V_j relations appear not to be explicable in this manner. Cx32/Cx26 heterotypic junctions lack the slow reduction in g_j for one polarity of V_j and possess a novel fast V_j dependent rectification ($t_{1/2} < 5$ ms, Barrio *et al.*, *PNAS* 88: 8410, '91). We now infer, through mutational analysis, that the fast rectification is a component of Cx32 gating that is revealed unopposed by a series gate when Cx32 is paired with Cx26. Also, the slow gating process is of opposite polarity in Cx26 and Cx32, so that when they are paired, their series gates are both closed by one polarity of V_j and left open by the other (Verselis *et al.*, *Soc Neurosci Abstr* 18: 644, '92). Unreported previously, homotypic Cx32 junctions display fast V_j -dependent reductions in g_j symmetric about $V_j=0$ that at large V_j 's constitute 25-30% of the total g_j . Cx26 has no detectable fast V_j -dependence over the same voltage range. Homotypic Cx32*26E1 junctions, which are Cx32 junctions with their first extracellular loop, E1, replaced with E1 of Cx26, show a modified fast V_j -dependence which in Cx32/Cx32*26E1 heterotypic junctions creates a modest asymmetry in fast V_j -dependence. The fast gating properties of Cx32 and Cx32*E1 hemichannels, as inferred from the homotypic junctions, could completely account for the fast rectification observed in Cx32/Cx26 and Cx32*E1/Cx26 heterotypic junctions. The newly described fast gating in Cx32 is less voltage sensitive than the slow gating and is of opposite polarity. These results explain the major features of gap junction gating as a function of hemichannel properties.

W-PM-G3

DIFFERENTIAL PERMEABILITY OF CONNEXIN-SPECIFIC GAP JUNCTIONS TO FLUORESCENT TRACERS ((R. D. Veenstra¹, H.-Z. Wang¹, E. C. Beyer², and P. R. Brink³)) ¹SUNY/Health Science Center, Syracuse, NY 13210, ²Washington Univ., St. Louis, MO 63110, and ³SUNY/Health Sci. Cntr., Stony Brook, NY 11794.

Gap junctions are a specialized form of intercellular junction which permit the diffusion of ions and hydrophilic molecules of $M_r < 1$ kD through an aqueous pore of 1.0 to 1.5 nm in diameter. The connexin family of proteins share a common membrane topology, are expressed in a tissue-specific manner, and form gap junction channels with distinct conductance and regulatory properties. To determine if connexin-specific gap junction channels with dramatic differences in channel conductance exhibit different permeabilities to low molecular weight hydrophilic molecules, we injected the fluorescent dye, 6-carboxyfluorescein (6-CF, $M_r = 376$ D) into one cell of a small cluster (2-8 cells) of connexin37 (Cx37)- or connexin45 (Cx45)-transfected N2A cells. Dye coupling to one or more Cx37 N2A cells was evident in 36% of the injections ($n = 86$) within 1-5 minutes. Dye injections performed under identical conditions in Cx45-transfected N2A cells revealed dye coupling to one cell in only 3 of 43 injections (7%). Control injections in untransfected N2A cells or N2A cells transfected with the pSFFV-neo expression vector lacking any connexin cDNA insert, exhibited dye-coupling ratios of 2-6% ($n = 50, 52$). Electrical coupling was evident in 53% of Cx45 and 67% of Cx37 N2A cell pairs with similar junctional conductances of 3.5 ± 1.0 nS ($n = 16$) and 4.5 ± 1.0 nS ($n = 7$), respectively. However, single channel current measurements revealed unitary conductances of 30 pS for Cx45 and 220 pS for Cx37 gap junction channels. These observations provide the first evidence for distinct molecular permeability limits for gap junctions which depend on the channel size and type of connexin expressed. Supported by HL-42220, HL-31299, and HL-45466.

W-PM-G2

GAP JUNCTION CHANNEL IN DISPERSED VENTRICULAR MYOCYTE: A COMPOSITE ELECTROPHYSIOLOGICAL, DYE DIFFUSIONAL AND MORPHOLOGICAL STUDY S.F. Fan, R. Cameron and P.R. Brink. Department of Physiology and Biophysics, Health Sciences Center, SUNY at Stony Brook, NY 11794.

In freshly dispersed guinea pig ventricular myocytes, single channel activity (50-60 pS) as well as whole cell current were recorded. Both the bath and the pipette solutions contained (in mM) 135 CsCl, 30 TEACl, 2 ZnCl₂, 1 CoCl₂, 1 NaCl₂, 0.1 CaCl₂, 0.6 EGTA and 10 HEPES, pH 7.2, pCa 8.0. Under such circumstances, no current will pass through K⁺, Na⁺, Ca²⁺ and anion-channels. The single channel activity was weakly voltage-dependent. The electrical events were suppressed completely and reversibly by increasing the bath Ca²⁺-concentration to 5 mM. The whole cell current was partially suppressed by 1 mM octanol. Incubation of freshly dissociated cells in CsCl media plus 1 mM carboxyfluorescein resulted in cell filling with dye. If Ca²⁺ in the bath was raised to 2 mM, no dye loading occurred. Fluorescein labeled albumin was not loaded whether the Ca²⁺ level was 100 nM or 2 mM. Electronmicrograph of the cell membranes showed typical gap junction structure while immunocytochemical studies showed that connexin 43 was present. Work supported by NIH Grant HL 31299.

W-PM-G4

DO GAP JUNCTION CHANNELS CONTAIN AN EQUIVALENT TO THE P-ELEMENT OF OTHER ION CHANNELS? ((G. Dahl, W. Nonner and R. Werner)) University of Miami, Miami, FL 33101)

In experiments designed to map binding sites with a peptide inhibition assay of cell-cell channel formation in paired oocytes, a peptide was found that kills oocytes. This peptide (2a) has the amino acid sequence 155-167 of connexin32, a sequence generally thought to be part of the 2nd extracellular loop of the gap junction protein connexin32. Peptide 2a does not interfere with junction formation but leads to depolarization and an increase of nonjunctional membrane conductance irrespective of whether oocytes are expressing connexin32 or not, ruling out opening of connexin32 hemichannels by the peptide. In oocytes the peptide appears to form channels that open upon depolarization. In artificial bilayers it forms voltage dependent channels with unit conductances ranging from 20-160 pS. This heterogeneity may reflect various assembly states of the peptides. These observations, together with other arguments including structure prediction with the Chou-Fasman paradigm, indicate the possibility that the peptide sequence is part of a β -barrel lining the channel similar to the P-element of other ion channels. Early x-ray diffraction data already had suggested the presence of β -barrel structure in gap junctions (Makowski *et al* 1982).

W-PM-G5

THE MULTIPLE CONDUCTANCE STATES OF MAMMALIAN CONNEXIN43. (Moreno A.P., Rook M.B., Spray D.C.) Albert Einstein College of Medicine, Bronx NY 10461 (Spon. J. Brown).

Gap junction channels are constituted by membrane proteins (connexins) which comprise a large related family. Depending on the connexin type, all gap junctions studied to date appear to be more or less sensitive to transjunctional voltage (V_j); gap junctions formed by Connexin43 (Cx43) are moderately voltage sensitive. In rat heart and in SKHep1 tumoral cells transfected with cDNA encoding for human (h) or rat (r) Cx43, macroscopic junctional conductance (g_j) is reduced with V_j of both polarities ($V_0 = 60$ mV, gating charge ≈ 2). However, even at large V_j , there is always a residual conductance (g_{min}) that is a constant proportion (30-40%) of the initial g_j . In hCx43- and rCx43- transfected cells, unitary junctional channel conductance (γ_j) were of three sizes: 60 pS (the major γ_j found between heart cells), 90 pS, and ≤ 30 pS (also found in mammalian heart cells).

The 90 and 60 pS γ_j values show V_j dependent gating. In addition, treatments that induce phosphorylation favor the 60 pS transitions while dephosphorylating agents shift γ_j to the size. The 30 pS γ_j value is conspicuous even at high V_j 's (> 50 mV). Opening and closing transitions of 30 pS are not clearly associated with either of the larger γ_j values, suggesting independent behavior. Although insensitive to voltage, g_{min} can be completely abolished by halothane treatment. Prior to complete uncoupling, high resolution recordings show transitions which represent a series of closures of 30 pS or less and which are virtually the only conductance transitions present, indicating that channels of this size comprise g_{min} . Thus, the connexin43 channel expressed endogenously or exogenously, exhibits at least three γ_j values which are differentially gated by phosphorylation or voltage.

W-PM-G7

PARATHYROID HORMONE STIMULATES BOTH cAMP AND IP_3 SIGNALING PATHWAYS IN GROWTH PLATE CHONDROCYTES. M.J. Zueck, R.N. Rosier, K.K. Gunter, J.E. Puzas & T.E. Gunter, Departments of Biophysics and Orthopaedics, University of Rochester School of Medicine and Dentistry, Rochester, NY 14642.

The effects of Parathyroid hormone (PTH) on growth plate chondrocytes (GPCs) have been extensively documented. The two most notable are a stimulation of mitogenesis (20 - 30 fold increase in DNA synthesis) and an inhibition of alkaline phosphatase activity (to levels 25% of normal). Previously, it was believed that upon binding to its receptor, PTH mediated these ultimate cellular effects (in various cell types) primarily through a stimulation of the cAMP signaling pathway. More recently, the observation that PTH can stimulate intracellular Ca^{2+} transients has indicated that IP_3 metabolism may also be involved with the transduction of PTH initiated signals. Our laboratory has specifically shown that treatment of GPCs with physiologically relevant doses of PTH (1 - 50 nM) stimulates single Ca^{2+} transients as well as Ca^{2+} oscillations (2% - 5% of responding cells) cytosolically. Based on these observations, our hypothesis is that these Ca^{2+} movements are IP_3 mediated, suggesting that PTH transduces its biochemical signals in GPCs through stimulation of both cAMP and IP_3 metabolism.

To verify PTH stimulation of cAMP pool size in GPCs, cells were treated with PTH in the presence of IBMX (an inhibitor of cAMP breakdown). Following stimulation, endogenous cAMP was extracted from the cells with ethanol and was quantitated by RIA. It was shown that PTH stimulated cAMP pool size by 2 - 4 fold over normal, suggesting cAMP pathway involvement in signaling. To study the effects of PTH on IP_3 metabolism, Ca^{2+} movement in the cytosol of individual GPCs was observed with a fluorescence microscope. Cells were loaded with the Ca^{2+} -sensitive indicator fura-2 and the ratio technique was used to determine changes in cytosolic $[Ca^{2+}]_i$ under various conditions. It was initially shown that GPCs resting in Ca^{2+} -free medium regularly exhibited PTH induced Ca^{2+} transients, suggesting that the observed transients were not dependent on external $[Ca^{2+}]_o$ and were likely due to the release of the ion from intracellular stores. Further, pretreatment of the cells with thapsigargin, a Ca^{2+} sequestrator that irreversibly depletes IP_3 -sensitive Ca^{2+} stores, led to the complete suppression of PTH transients. This result further implies that PTH stimulates release of Ca^{2+} from IP_3 -sensitive stores and therefore must stimulate IP_3 metabolism directly.

As a final direct proof of PTH stimulation of both signaling pathways, our laboratory is currently attempting to measure, by RIA, IP_3 pool size changes in response to PTH.

Supported by AR40325

W-PM-G9

STRONTIUM AFTERDISCHARGES AND QUANTAL ANALYSIS OF SYNAPTIC TRANSMISSION BETWEEN PAIRS OF CULTURED MOUSE HIPPOCAMPAL NEURONS. (M. Abdul-Ghani and P. Pennefather) MRC Nerve Cell and Synapse Group, Faculty of Pharmacy, University of Toronto, Toronto, M5S 2S2.

Hippocampal neuron in culture receive a large number of excitatory synaptic contacts from adjacent cells. Quantal analysis of synaptic transmission has proven difficult because of the high variability of quantal size and probability of release between and within synapses. To overcome this problem, we have taken advantage of the ability of Strontium (Sr) to induce after discharges of quantal event following evoked responses. These arise because of a reduced rate of clearance of Sr from the presynaptic terminal and its ability to act as a partial agonist in transmitter release (Bain and Quastel, *J. Physiol.* 450, 1992). We have used the whole cell configuration to record from pairs of hippocampal neuron in low density cultures. In Ringer solutions containing (in mM): 10 Mg, 2 Sr, 1 Ca, spontaneous miniature excitatory post synaptic currents (mEPSC's) are very infrequent, however following evoked responses, a well defined and transient increase in mEPSC frequency is apparent. There is good agreement between quantal content estimated from the mean evoked and spontaneous responses and that calculated by the methods of coefficient of variation (c.v.) or of failures.

Table 1. Release Statistics Estimated from Samples of 100 EPSCs (.25Hz at -80 mV).

Cell	Mean EPSC (c.v.)	Mean mEPSC (c.v.)	Quantal Content		
	p A	p A	EPSC/mEPSC	c.v.	failures
1	263.38 (0.19)	8.76 (0.49)	30.1	34.4	-
2	16.70 (0.12)	10.21 (0.36)	1.6	1.7	1.6
3	844.73 (0.13)	10.57 (0.44)	79.9	74.6	-
4	8.03 (1.32)	12.58 (0.66)	0.6	0.8	0.7

Supported by MRC Canada. M.A-G is an MRC Fellow, P.P. is an OMH Career Scientist

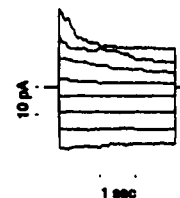
W-PM-G6

KINETICS OF NUCLEAR IONIC CHANNEL.

((M. Mazzanti, B. Innocenti, and M. Rigatelli)) Fisiologia e Biochimica, Università Statale, Via Celoria 26, I-20133 Milano, Italy.

Nucleo-cytoplasmic communication is probably involved in many cell functions, from hormone stimulation to cell-cycle control. Part of the exchange is energy dependent, while part consists of small solutes that diffuse across the nuclear envelope. Recently, experiments on isolated nuclei showed the presence of ionic pathways on nuclear membranes from different tissues. Whether or not these channels are part of the nuclear pore complexes, speculations exist on their physiological functions. In this work we explore the kinetic properties of nuclear ionic channels in relation to the density and the direction of the current.

Average of single-channel records shows a marked inactivation when the current flows from the nucleoplasm to the cytosol. Time-dependent decrease of the current is absent if ions enter into the nucleus (see figure). The control over passive diffusion could play an important role in the duration of the stimulus from external agents.



W-PM-G8

CHARACTERIZATION OF AN ECTO-NUCLEOTIDE DIPHOSPHATE KINASE ON THE CARDIAC ENDOTHELIAL CELL. (I.L.O. Buxton, D.J. Cheek, D.P. Westfall and S. Yang), Department of Pharmacology, University of Nevada School of Medicine, Reno, NV 89557.

We have previously demonstrated that guinea pig cardiac endothelial cells (CEC) maintained in primary culture are repeatedly capable of releasing intracellular ATP when stimulated by numerous agonists (*J. Cell Biol.* 115: 365; *Ann. N.Y. Acad. Sci.* 603: 503). The ability of these same cells to respond to the exogenous application of ATP by releasing vasoactive mediators such as nitric oxide and PGI₂, along with the well known ability of ATP to relax coronary arteries and contract other blood vessels suggests both an origin and a role for ATP in the moment-to-moment regulation of blood flow. In attempts to measure purine nucleotide-induced nucleotide release from CEC we have found that large amounts of ATP are very rapidly (3 sec) generated outside the cells when ADP alone is added to the cultures. In studies in both intact cells and membranes prepared from them, we find evidence for the presence of a nucleoside diphosphate kinase (NDP kinase, EC 2.7.4.6) that we propose exists in an extracellularly directed form in the CEC membrane and can behave in both a myokinase- (2-ADP → ATP + AMP) and an NDP-like (NTP + NDP → NTP + NDP) fashion. In the absence of a phosphoryl donor, the K_m of this enzyme for ADP is 57.4 μ M with a V_{max} of 121.5 pmol/10⁶ cells/sec. The enzyme demonstrated an absolute requirement for Mg²⁺ which produced maximal stimulation between 1 and 2 mM and was inhibitory thereafter. Activity was inhibited in a dose dependent fashion by addition of either of the putative ATP-P₂ receptor antagonists suramin (IC₅₀ = 3 μ M) and reactive blue 2 (IC₅₀ = 0.2 μ M). The existence of an ecto-NDP-kinase capable of converting ADP to ATP on the luminal surface of endothelial cells, along with the ability of cells to release ATP as well as respond to ATP by releasing other vascular mediators suggest that the ecto-NDP kinase is part of a purinergic axis in blood vessels. (This work was supported by HD26227 to ILOB and a grant from the Aortic Heart Association)

W-PM-H1

THE ZN RIBBON: A NOVEL MOTIF OF PROTEIN-NUCLEIC ACID INTERACTION IN THE HUMAN TRANSCRIPTIONAL MACHINERY

X. Qian, H. Yoon, C. Jeon, K. Agarwal, and M. Weiss
Harvard Medical School, Boston, MA; and the University of Chicago, Chicago, IL.

We have determined the solution structure of a novel Zn-binding domain from the human transcriptional elongation factor TFIIS. This Cys4 "Zn finger" binds to a variety of nucleic acids as found in transcriptional pause sites for RNA polymerase II. The structure, determined by homonuclear and heteronuclear 3D-NMR and distance-geometry, is unrelated to previously observed Zn modules (such as the classical Zn finger, glucocorticoid receptor, or GAL4). The structure contains a three-stranded antiparallel beta sheet and is hence designated the "Zn Ribbon." The functional surfaces of the Zn ribbon have been mapped by saturation mutagenesis; these include the third beta strand and a central loop. Observation of a beta-sheet "Zn finger" motif emphasizes the complementary importance of beta-strand/nucleic acid interactions in addition to the well-characterized use of an alpha helix. Sequences analogous to the TFIIS Zn Ribbon are observed in a variety of prokaryotic and eukaryotic genes involved in DNA or RNA transactions.

W-PM-H3

THE STRUCTURE OF NUCLEOSOMAL DNA IS UNAFFECTED BY HIGH SALT CONCENTRATION. ((H.L. Puhl and M.J. Behe))
Department of Chemistry, Lehigh University, Bethlehem, PA 18015

The structure of a 146 base pair nucleosomal DNA has been probed using hydroxyl radical cleavage in buffers containing NaCl concentrations ranging from 80 mM to 800 mM. The highest salt concentrations used here are close to those required to dissociate core histone H2A and H2B from nucleosomal DNA. Nonetheless, the cleavage pattern of the DNA is unchanged over the ten-fold salt concentration range, retaining the ~10.0 bp/turn helical periodicity in the flanking regions and ~10.7 bp/turn periodicity in the central dyad region that is characteristic of nucleosomal DNA. The rotational frame of the DNA is similarly unaffected by salt. These results support the contention that the differential free energy of bending of DNA around the nucleosome is independent of salt concentration.

W-PM-H5

DIRECTION OF BACTERIOPHAGE T7 DNA PACKAGING. ((Saeed A. Khan, Marjatta Son, Robert H. Watson, Shirley J. Hayes, and Philip Serwer)) Department of Biochemistry, The University of Texas Health Science Center, San Antonio, TX 78284-7760.

To determine the direction in which bacteriophage T7 DNA (39.936 Kb) enters a T7 capsid during morphogenesis, incompletely packaged DNA (ipDNA) has been fractionated by agarose gel electrophoresis and probed in-gel by use of oligonucleotide probes specific for either the right or left T7 DNA end. Analysis of ipDNA obtained either *in vivo* or *in vitro* revealed that most (>80%) of the DNA was packaged right-end-first; however, the remainder was packaged left-end-first. Other data indicate that formation of the right end is the usual way to initiate packaging (Son, M. and Serwer, P. [1992] *Virology* 190, 824-833). Some *in vivo* ipDNA was packaged in a previously-demonstrated (Serwer, P. [1980] *J. Mol. Biol.* 138, 65-91), metrizamide-impermeable capsid. These latter particles have been purified in milligram quantities and found to be unusually stable; temperatures above 80°C were needed to expel DNA. The distribution of ipDNA lengths had broad peaks. These peaks are explained by the assumption that the speed of packaging varied as a function of the length of DNA packaged. Supported by NIH (GM-24365).

W-PM-H2

KINETICS DESCRIBING THE SEARCH FOR HOMOLOGY CARRIED OUT BY RECA PROTEIN.

((J.E. Yancey-Wrona and R.D. Camerini-Otero)) NIDDK, NIH, Bethesda, MD 20892. (Spon. by R.D. Camerini-Otero)

RecA protein can pair an oligonucleotide with a homologous target on duplex DNA to generate synaptic complexes. These structures, consisting of three DNA strands and RecA protein, are intermediates in the strand exchange reaction catalyzed by RecA protein. It is likely that the formation of synaptic complexes involves multiple steps including: RecA protein-ssDNA filament formation, the search for homology carried out by protein-DNA filaments on duplex DNA and formation of stable synaptic complexes at the homologous sites on the target duplexes. The kinetics of synaptic complex formation were investigated using a variety of DNA substrates. Synaptic complexes form in a relatively slow reaction which follows apparent second-order kinetics. The reaction rate derived from these experiments is proportional to both the concentration of the RecA protein-ssDNA filaments and the concentration of duplex DNA target sites. The reaction rate is not limited by the amount of nonhomologous DNA in the reaction. That is, the complexity of heterologous DNA in a given system does not affect the rate of the homology search carried out by the RecA protein-DNA filaments. Finally, although the formation of stable synaptic complexes is slow compared to the rates of diffusion-controlled reactions, the reaction is fast enough to account for genetic recombination in the cell.

W-PM-H4

PROMOTER RECOGNITION BY T7 RNA POLYMERASE. ((C. T. Martin & M. Maslak)) Dept. of Chemistry, University of Massachusetts, Amherst, MA 01003. (Sponsored by C. Martin)

The DNA dependent RNA polymerase from bacteriophage T7 is highly specific for the initiation of transcription from a small (~17 bp) promoter sequence. Previous studies have suggested that the enzyme binds to one face a mostly closed duplex form of the promoter. Interactions between the enzyme and DNA can be assayed *in vitro* by a steady state kinetic assay, and the use of synthetic oligonucleotide-based promoters allows well-controlled changes in the promoter. The replacement of thymine by deoxyuridine at individual sites in the DNA provides a probe of proposed major groove contacts, with minimal perturbation of the overall DNA structure. Indeed, few of these substitutions result in any significant decrease in binding. However, the substitution T→dU at position -6 significantly increases K_m , indicating its role in recognition in the proposed central major groove of the promoter. T→dU substitutions in the template strand at positions -1 and -3 also disrupt binding, in apparent contradiction to the simple model. Studies with promoter constructs lacking the non-template strand throughout the message region of the DNA and in the non-transcribed region of the promoter demonstrate that DNA melting is not a barrier to binding or to the kinetics of initiation. A revised model is presented in which the RNA polymerase recognizes duplex DNA upstream of about position -6 and interacts only with the template strand in a melted region downstream of about position -6.

W-PM-H6

RECOMBINATION PROTEIN MEDIATED TRIPLEX DNA: R-FORM DNA. ((M.K. Kim, V.B. Zhurkin, R.L. Jemigan and R.D. Camerini-Otero)) NIDDK, NIH, Bethesda, MD 20892. (Spon. by G. Felsenfeld)

R-form DNA is a putative intermediate in the homologous recombination process. By deproteinizing the strand exchange reaction performed with RecA or other recombinases, R-form DNA can be trapped as a joint molecule composed of single stranded DNA attached to a linear duplex DNA. R-form DNA is a novel form of triplex in which the third (R) strand includes both purines and pyrimidines. It is also distinguished from previously described triplexes by the parallel orientation of the R strand with respect to the identical strand in the duplex. We have proposed that RecA facilitates R-form DNA formation by unwinding and unstacking the DNAs in order to lower the activation energy required for this three-stranded hybridization. To test our previously proposed models, dimethyl sulfate (DMS) protection was carried out on deproteinized joint molecules. The guanines (Gs) in the Watson strand of the duplex are protected from DMS attack over the region of pairing. This result indicates that there are close contacts between the N7 of the Gs in the major groove of the duplex and the R strand in the (GC):G triplets. In contrast, the Gs in the Crick strand are not protected. This probably reflects a lack of stable contacts at the N7 positions of these Gs in the (CG):C triplets. Substitutions of 7-deaza guanine or 7-deaza adenine in a strand specific manner have allowed us to examine the specific contacts in the 4 possible triplets, (GC):G, (CG):C, (AT):A, & (TA):T. All the N7-position substitutions except those on the (CG):C triplets significantly destabilized R-form DNA. In summary, the footprinting and isosteric substitution results indicate that the R-strand is in contact with the major groove of the duplex.

W-PM-H7

Compensating Effects of Osmotically-Induced Changes in Cytoplasmic Macromolecular Crowding and Electrolyte Concentration on Protein-DNA Interactions in *E. coli*

Harry J. Gutman, Scott Cayley, Charles F. Anderson and M. Thomas Record, Jr., Departments of Chemistry and Biochemistry, University of Wisconsin, Madison, WI 53706

Extents and rates of interaction of proteins with nucleic acids typically are strong functions of salt concentrations *in vitro*. However, when the potassium glutamate concentration in the *E. coli* cytoplasm is increased by increasing the osmolarity of a minimal growth medium, expression assays indicate that the interactions of *lac* repressor and of RNA polymerase with their specific sites are relatively unaffected.¹ We have experimentally quantified this *in vivo-in vitro* paradox by measuring amounts and concentrations of cytoplasmic ions, and estimating *in vivo* ionic activities by polyelectrolyte theory. We have quantified the reduction in steady-state water-accessible cytoplasmic volume that accompanies an increase in osmolarity, and have proposed that the resulting increase in macromolecular crowding compensates at a thermodynamic level for the increase in ion concentrations, so that the effect of salt concentration on protein-DNA interactions is masked.² A comprehensive set of calculations has been carried out to quantify these effects of osmotically-induced changes in ion concentration and in macromolecule concentration on the extent of binding of the above gene control proteins to DNA *in vivo*. (Supported by NSF and NIH.)

¹ B. Ritchey, S. Cayley, M. Moseley, C. Koltka, C. F. Anderson, T. C. Farrar and M. T. Record, Jr., *J. Biol. Chem.*, **267**, 7157-7164 (1992).

² S. Cayley, B. A. Lewis, H. J. Gutman, and M. T. Record, Jr., *J. Mol. Biol.* **222**, 281-300 (1991).

W-PM-H8

STABILITY AND BINDING PROPERTIES OF THE EIAV NUCLEOCAPSID PROTEIN. ((C. A. Gelfand, R. Montelaro, B. Woodson and J. E. Jentoft)) Department of Biochemistry, CWRU, Cleveland, OH 44106 and Department of Molecular Genetics & Biochemistry, University of Pittsburgh, Pittsburgh, PA 15213.

Nucleocapsid proteins (NCs), essential and integral parts of the retroviral ribonucleoprotein complex, are unique, basic molecules whose fundamental structural and functional properties are still under discussion. EIAV NC, which has not been previously characterized, is a member of the lentivirus family (as is HIV-1). Analysis of the CD spectrum of EIAV NC shows predominantly antiparallel beta sheet, turn and random secondary structure. It undergoes cooperative denaturation in urea, as monitored by CD, demonstrating that NC has a stable folded structure. EIAV NC forms a complex with the extrinsic fluorophore bis-ANS, and the resulting enhancement of bis-ANS fluorescence was used to monitor binding to NC by both poly(rA) and AMP, using a displacement assay. The similarity between these results and comparable data for avian myeloblastosis virus NC will be presented to support the conclusion that lentivirus and avian NCs have similar structural and functional properties.

W-PM-H9

STUDY OF THE BACTERIOPHAGE T4 HELICASE BY BIOPHYSICAL AND MOLECULAR BIOLOGICAL APPROACHES

(Feng Dong, Edward P. Gogol, and Peter H. von Hippel) Institute of Molecular Biology, University of Oregon, Eugene, OR 97403-1229. (Spon. by F. Dong)

The bacteriophage T4 helicase (gene 41 protein, g41p) catalyzes strand separation of the double-stranded DNA template during DNA replication. In this study, our research effort has focused on a biochemical and biophysical characterization of the structures and stoichiometries of the association states of this protein, as well as of the complexes that it forms with the T4-coded primase (gene 61 protein) and various DNA template constructs.

Determination of the association states and the stoichiometries of the protein components involved in forming the activated helicase and assembling it into a functional complex with the primase and DNA template constructs is crucial to permit us to approach a mechanistic understanding of this important sub-assembly of the T4 DNA replication complex. To this end we have applied a variety of biochemical and biophysical approaches to the problem, including protein-protein chemical crosslinking, native and semi-denaturing gel electrophoreses, analytical ultracentrifugation, dynamic laser light scattering, cryoelectron microscopy, as well as fluorescence and other spectroscopic techniques.

Our results clearly (and unexpectedly) indicate that the g41p helicase functions as a **hexamer**, and that this active association state of the helicase must bind to the g61p primase to interact with appropriate DNA constructs and form a working subassembly of the T4 DNA replication complex.

CARDIAC ELECTROPHYSIOLOGY

W-PM-11

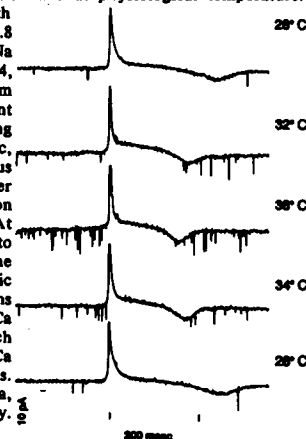
MEMBRANE CURRENTS IN NEONATAL MOUSE CARDIAC MYOCYTES IN PRIMARY CULTURE ((H. Bradley Nuss and Eduardo Marban)) Division of Cardiology, The Johns Hopkins University, Baltimore, MD.

Murine heart is an infrequently used model to study ion channels. The increasing use of transgenic mice in molecular studies of the cardiovascular system has motivated us to characterize the ionic currents in murine ventricular myocytes. Hearts were excised from mouse pups, born from an outbred strain of white albino mice (CD-1, Charles Rivers, NY), at postnatal days 1 to 3. Dissociation of cells by repeated collagenase digestions in serum-free media yielded a high proportion of cardiac myocytes with few supporting cells. Cells were plated at a low density for whole-cell voltage clamp experiments. Cell capacitance measurements (33.3 ± 2.5 pF, $n=19$) confirmed visual estimates that these cells are considerably smaller than freshly isolated adult ventricular myocytes. Robust inward currents were recorded in spontaneously beating myocytes studied from 16h after dissociation to 3 days in primary culture. Na^+ current (I_{Na}) (-234 ± 33.6 pA/pF, $n=11$) was elicited by 60ms depolarizations from -90 mV in 40 mM $[\text{Na}^+]_o$. Block of I_{Na} by TTX suggests that these Na^+ channels bind TTX with low affinity ($\text{IC}_{50} = 1.32 \pm 0.35$ μM , $n=4$). T-type and L-type Ca^{2+} current ($I_{\text{Ca,T}}$, $I_{\text{Ca,L}}$) were recorded in Na^+ -free solutions with Ca^{2+} or Ba^{2+} as the charge carrier. Peak $I_{\text{Ca,L}}$ densities measured -11.5 ± 2.1 pA/pF ($n=7$) in 2 mM $[\text{Ca}^{2+}]_o$ and -57.9 ± 7.8 pA/pF ($n=9$) in 30 mM $[\text{Ba}^{2+}]_o$. Nitrendipine ($10 \mu\text{M}$) completely abolished $I_{\text{Ca,L}}$ during depolarizations (180ms) from -40 mV. $I_{\text{Ca,T}}$ activated by depolarization from -90 mV to -30 mV in the presence of nitrendipine ($10 \mu\text{M}$) measured -25.6 ± 5.4 pA/pF ($n=6$) in 30 mM $[\text{Ba}^{2+}]_o$. Thus neonatal mouse heart cells exhibit large TTX-insensitive I_{Na} as well as sizable $I_{\text{Ca,T}}$ and $I_{\text{Ca,L}}$. Neonatal mouse cardiac myocytes in primary culture is an attractive preparation for comparative studies of whole-cell currents in transgenic mice because of their small cell capacitance and robust inward currents.

W-PM-12

Ion channel activity in the cardiac pacemaker. L.J. DeFelice and M. Mazzanti Anatomy and Cell Biology, Emory University, Atlanta, GA 30322

We used single cells from 7-day chick ventricle to study channel activity during spontaneous diastolic depolarization and at physiological temperature. The patch electrode contained the bath solution (mM: 133 Na, 1.3 K, 0.5 Mg, 1.8 Ca) plus $50 \mu\text{M}$ TTX to eliminate Na currents (Liu et al., *Biophys. J.* **63**:654, 1992). As we changed temperature from 28 to 38°C , two types of inward current became more active. One had long openings and small currents (≈ 100 msec, 0.1 pA). The other, more ubiquitous channel had brief openings and larger currents (≈ 1 msec, 1 pA). Its activation depends on temperature (see figure). At 38°C , openings occur too frequently to estimate the number of channels in the patch. Possible carriers for the diastolic fast inward current include Na ions through TTX-insensitive channels or Ca ions through Ca channels, in which temperature-sensitive removal of Ca inactivation promotes late openings. M.M.'s address: Fisiologia e Biochimica, Universita' Statale, 20133 Milano, Italy. $\frac{1}{2}$ NIH-HL-27385 supports this work.



W-PM-13

EXTERNAL CATION INHIBITION OF ATP-REGULATED K CURRENT (I_{KATP}) IN HEART CELLS DEPENDS ON INTRACELLULAR ATP (ATP_i): EVIDENCE FOR CHANNEL PROTEIN CONFORMATIONAL CHANGES. (W.M. Kwok and R. S. Kass). Dept. of Physiology, University of Rochester Medical Center, Rochester, NY 14642

We have investigated the ATP_i -dependence of external cation-induced inhibition of I_{KATP} in guinea-pig ventricular cells. Whole cell pinacidil-induced I_{KATP} is inhibited by extracellular Cd^{2+} and Zn^{2+} in a concentration-dependent manner when cells are dialyzed with ATP_i concentrations ≥ 0.5 mM. Excised patch experiments indicate that this inhibition, consistent with divalent ion binding to external sites, is not pinacidil-dependent. We find this inhibition of I_{KATP} is dependent on $[ATP_i]$: dialysis with 0 mM ATP_i markedly reduces external divalent cation block of I_{KATP} . For cells dialyzed with $[ATP_i] \geq 0.5$ mM, Cd^{2+} (100 μ M) and Zn^{2+} (100/200 μ M) block I_{KATP} by $83 \pm 5\%$ ($n=5$) and $103 \pm 2\%$ ($n=4$), respectively. However, when $[ATP_i]$ is nominally 0 mM, block of I_{KATP} by Cd^{2+} and Zn^{2+} is reduced to $8 \pm 5\%$ ($n=4$) and $36 \pm 2\%$ ($n=6$), respectively. This allosteric interaction between extracellular cation binding and intracellular ATP_i suggests a conformational change in the channel protein. Though I_{KATP} is a nucleotide-regulated channel, the change in channel protein conformation may be similar to the model proposed by Gilly and Armstrong (JGP.1982.79) for voltage-gated channels. Binding to these or related external sites by other ions may have important physiological (or pathophysiological consequences) because we find that external hydrogen ions also inhibit pinacidil-induced current in these cells. In whole-cell experiments, pinacidil-activated I_{KATP} is blocked by at least 30% when external pH is reduced from 7.4 to 6.0. The rapid time course of onset of and recovery from block resembles that for block by Cd^{2+} and Zn^{2+} , and suggests similarly accessible external sites. Experiments are currently being carried out to determine the pK_a of these sites and to test whether H^+ ions compete with divalent cations for them.

W-PM-15

ROLE OF THE CALCIUM-ACTIVATED CHLORIDE CURRENT, $I_{Cl(Ca)}$, IN THE RABBIT ATRIAL ACTION POTENTIAL. (Andrew C. Zygmunt and W.R. Gibbons) Masonic Medical Research Lab., Utica, NY 13501 and University of Vermont, Burlington, VT 05405.

We have demonstrated a calcium-activated chloride current, $I_{Cl(Ca)}$, in rabbit ventricular and atrial myocytes. $I_{Cl(Ca)}$ is activated by the calcium transient that causes the twitch. We have recorded putative $I_{Cl(Ca)}$ channel activity in on-cell patches after contracture was induced by ionophore A23187. Open channel conductance was 43 pS for outward current and 18 pS for inward current. Steady-state open channel probability was low at negative potentials and high at positive potentials. These observations are consistent with the outward rectification of the whole cell current we previously reported. $I_{Cl(Ca)}$ is large in the atrium and may therefore make an important contraction-related contribution to repolarization of the atrial action potential (AP). In normal chloride, mechanical staircases were associated with AP repolarization changes; $I_{Cl(Ca)}$ may be responsible in part for the correlation of AP and tension. We have used low chloride solutions or anion transport blockers to investigate the contribution of $I_{Cl(Ca)}$ to AP repolarization in atrial tissue and myocytes. Supported by USPHS grant HL14614 and AHA grant 92011690. ACZ was supported by a fellowship from the AHA/Vermont Affiliate.

W-PM-17

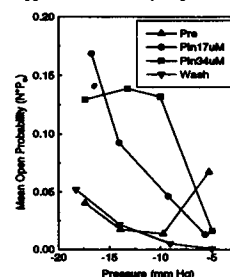
A NEW ROLE FOR Mg^{2+} IN THE INWARD RECTIFICATION OF I_{K1} . (R. L. Martin and R. E. Ten Eick) Northwestern University, Chicago, IL 60611.

When intracellular free Mg^{2+} concentration ($[Mg^{2+}]_i$) is reduced to $< 15 \mu$ M, the single channel current through inwardly rectifying K^+ channels found in guinea pig (GP) ventricular myocytes (VM) loses the property of inward rectification (IR) and its current-voltage (I-V) curve becomes linear. We were able to duplicate this finding with whole-cell-patch recordings of I_{K1} when experimental temperature (T) was cold (10 - 15°C). However, when T was physiologically more relevant (35 - 37°C), reducing $[Mg^{2+}]_i$ to < 1 nM did not remove IR from the whole-cell I_{K1} of GP. In contrast, in cat VM, reducing $[Mg^{2+}]_i$ to < 1 nM does not change the inwardly rectifying nature of its I_{K1} , even at T as low as 5°C. This difference between cat and GP in the effect of Mg^{2+} was investigated because its basis may provide new insight into the role of Mg^{2+} in producing IR of I_{K1} . The hypothesis that Mg^{2+} shifts the voltage dependence of the I_{K1} steady-state activation (SS Act) curve was investigated. When $[Mg^{2+}]_i$ of cat VM was < 1 nM in the cold, the $V_{1/2}$ of the curve defining the SS Act voltage dependence was unchanged from the value for the curve found when $[Mg^{2+}]_i$ was 1 mM. In contrast, when a similar experiment was done using GP VM in the cold and the same parameters were assessed for the GP I_{K1} , there was an $\sim +80$ mV shift in the SS Act curve which was associated with an I-V curve that was linear even to voltages 60 mV positive to E_K . This shift occurring for GP but not for cat means that both GP and cat I_{K1} channels will inactivate positive to -60 mV when $[Mg^{2+}]_i$ is normal, but when $[Mg^{2+}]_i$ is reduced to < 1 nM, cat I_{K1} will inactivate but GP I_{K1} will not, thereby allowing the GP I_{K1} to be linear rather than inwardly rectifying. These findings provide the basis for an alternative idea concerning the involvement of Mg^{2+} in the IR of I_{K1} .

W-PM-14

PINACIDIL POTENTIATES MECHANOSENSITIVE MODULATION OF THE RAT ATRIAL ATP-SENSITIVE POTASSIUM CHANNEL ((David R. Van Wagoner and Michelle Lamorgese)) Cardiovascular Biology, The Cleveland Clinic Foundation, Cleveland, OH 44195-5069.

Using cell-attached or inside-out excised patches from isolated adult rat atrial myocytes, we have previously demonstrated that application of negative pressures to the patch increases both the frequency and duration of openings of the ATP-sensitive potassium channel, K_{ATP} . Potassium channel openers (PCOs) are a structurally diverse class of compounds which also increase K_{ATP} channel open probability. We have examined the effects of pinacidil, a PCO, on the mechanosensitive modulation of K_{ATP} channel activity. In the presence of 1 mM ATP on the cytoplasmic side of an excised patch (30°C), application of 1-40 μ M pinacidil had little effect on spontaneous K_{ATP} channel activity, but caused a dose dependent and reversible increase in the mean open probability in response to negative pressure steps (-5 to -25 mm Hg, 20 second duration). Results of a representative experiment in which two doses of pinacidil were applied to a patch are illustrated to the right. Similar results have been obtained in 4/7 patches surviving the protocol. Several lines of data suggest that pinacidil may modify the phosphorylation state of the K_{ATP} channel. Studies in progress are examining the effects of PCOs, protein kinase activators and inhibitors on mechanosensitive channel activation, and should help to clarify the molecular mechanism(s) whereby deformation of the cell membrane and PCOs modulate the activity of the K_{ATP} channel.



W-PM-16

A SINGLE TYPE OF CHLORIDE CURRENT (I_{Cl}) INDUCED BY ACTIVATION OF PROTEIN KINASE A AND C IN FELINE VENTRICULAR MYOCYTES ((Ke Zhang and R. E. Ten Eick)) Northwestern University, Chicago, IL 60611

Activation of protein kinase A (PK-A) induces a non-inactivating, outwardly rectifying I_{Cl} in guinea pig (GP) ventricular myocytes (VM) (Harvey and Hume, 1989). Activation of protein kinase C (PK-C) also can induce an I_{Cl} . One report shows that phorbol 12-myristate 13-acetate (PMA)-induced I_{Cl} displays an essentially linear current-voltage relationship (Walsh, 1991), implying that PK-C activation induces an I_{Cl} different from that induced by PK-A activation. However, we reported that PMA in feline VM induced a non-inactivating, outwardly rectifying I_{Cl} via a PK-C dependent pathway and which closely resembles the PK-A dependent I_{Cl} in GP VM (Zhang et al., 1991). This lack of agreement in findings led us to test the notion that activation of PK-A and PK-C induce I_{Cl} via the same set of Cl^- channels in feline VM. Using whole-cell-patch-clamp techniques, we found that PMA could induce a non-inactivating, outwardly rectifying I_{Cl} which was sensitive to the chloride channel blocker, 9-anthracene carboxylic acid, and reversed polarity at $-E_{Cl}$. The kinetic properties of PMA- and forskolin (FSK)-induced I_{Cl} were similar irrespective of whether $[Cl^-]_o$ was 22 or 150 mM. Maximal activation of I_{Cl} with PMA prevented FSK from activating any additional I_{Cl} , yet the effects of submaximally activating concentrations of PMA and FSK were roughly additive. These findings are consistent with the notion that both PMA- and FSK-induced I_{Cl} flow through the same set of Cl^- channels and are inconsistent with the notion that different sets of channels are involved.

W-PM-18

TWO COMPONENTS OF DELAYED RECTIFIER CURRENT IN CANINE VENTRICULAR MYOCYTES. ((Gary A. Giantant)) Masonic Medical Research Laboratory, Utica, NY 13501

Delayed rectifier current (I_K) was characterized in canine ventricular myocytes using whole cell and perforated patch techniques. Myocytes were isolated from the mid-left ventricular free wall using low Ca^{2+} and collagenase exposure. Experiments were conducted using high K^+ aspartate/KCl pipette solutions with iK isolated from Na^+ and Ca^{2+} currents by holding potential and nisoldipine (37°C). Tail currents (measured at -40 mV) following conditioning depolarizing pulses were well described kinetically as the sum of a rapid (iKe1, tau range 70-160 msec) and slower (iKe2, tau range 1.5-3.0 sec) exponential components. Using 3 second conditioning pulses, the peak amplitude of iKe2 was maximal following pulses positive to 0 mV. In contrast, the peak amplitude of iKe1 continued to increase following pulses to potentials as positive as +60 mV. The amplitudes of iKe1 and iKe2 are equal following 300 msec pulses to near 0 mV. Reducing $[K^+]_o$ to 0 mM abolished the slower tail component (iKe2) while enhancing iKe1; the kinetics and voltage dependence of iKe1 were not appreciably affected. Time constants for iKe1 deactivation decreased from 500 to 50 msec for potentials ranging from 0 to -80 mV. iK activation and deactivation was compared using the "envelope" test (conditioning potential +40 mV, holding potential -40 mV). With $[K^+]_o = 4$ mM, iK activation lagged that of the envelope of peak tail currents upon repolarization. In contrast, the envelope test was satisfied in the presence of 0 mM $[K^+]_o$, consistent with one iK component under these conditions. In conclusion, two iK components (conductances?) are present in canine ventricular myocytes.

W-PM-19

INTERNAL ANIONS MEDIATE RECTIFICATION OF THE CYCLIC AMP-DEPENDENT CHLORIDE CURRENT IN CARDIAC MYOCYTES

(J.L. Overholt and R.D Harvey)) Department of Physiology and Biophysics
Case Western Reserve University, Cleveland, OH 44016

It has previously been suggested that internal Cl^- modulates rectification of the cAMP-dependent Cl^- current in guinea-pig ventricular myocytes (*Biophys. J.* 61: A442, 1992). Decreasing internal Cl^- increases outward rectification independent of the Cl^- concentration gradient across the membrane. The possibility that other anions might also modulate rectification was investigated using the whole-cell configuration of the patch clamp technique. Rectification was not significantly affected by reducing internal HEPES from control (5 mM) to 1 mM, replacing HEPES with TRIS, or increasing internal HEPES from 5 to 75 mM. Rectification was also not affected by increasing internal ATP from control (5 mM) to 35 mM. However, rectification did depend on the permeability of the anion used to replace internal Cl^- . Rectification was clearly observed when internal Cl^- was replaced with glutamate, a relatively impermeant anion. However, when internal Cl^- was replaced with more permeant anions (NO_3^- and Br^-) rectification was not observed. Furthermore, when Cl^- was replaced with sucrose rather than glutamate, rectification was significantly decreased, although changing internal Cl^- , in the absence of other replacement anions, still modulated rectification in a concentration dependent manner. The Cl^- dependence of rectification could be fit by a single binding site model, and the effect of Cl^- in the presence of glutamate could be described by competitive inhibition of Cl^- by this less permeant anion. Therefore, rectification of this current appears to be a function of the permeability of the intracellular anion(s).

W-PM-110

CESIUM ABOLISHES Ba -INDUCED PACEMAKER POTENTIAL AND PACEMAKER CURRENT IN GUINEA PIG VENTRICULAR TISSUE. ((J.-B. Shen and M. Vassalle)) Dept. Physiol., SUNY, HSC, Brooklyn, N.Y. 11203. (Spon. by D. Eriij)

The aim of the experiments was to determine whether cesium (Cs) blocks the pacemaker potential and pacemaker current induced by barium (Ba) in guinea pig ventricular myocardium. In papillary muscle perfused in vitro, Ba (0.1-0.5 mM) decreased the resting potential, prolonged the action potential and induced diastolic depolarization (DD). Cs (4 mM) reduced or abolished the Ba-induced DD by reducing or abolishing the undershoot of the action potential. In isolated myocytes in Tyrode solution, during hyperpolarizing voltage clamp steps the inward current increased as a function of voltage but did not change as a function of time (no I_f and no K depletion). Adding Cs (4 mM) reduced the amplitude of the steady state current flowing during the clamp steps. In the presence of Ba (0.05-0.1 mM), the resting potential became smaller and the action potential longer. At the end of phase 3 repolarization, the potential undershot the value prior to the action potential and then slowly decreased again, thereby inducing diastolic depolarization. Depolarizing voltage clamp steps were followed by an outward tail current at the resting or less negative potentials. The outward tail current reversed at -92.0 ± 1.3 mV and at more negative potentials it decayed more rapidly to a larger extent. Adding Cs (4 mM) in the presence of Ba abolished the undershoot and the associated DD as well as the tail current at the resting potential, and markedly decreased the inward tail at more negative voltages. It is concluded that in ventricular myocytes Cs abolishes the Ba-induced pacemaker potential and current by blocking the temporary increase in potassium conductance (consequent to the Ba unblock occurring during depolarization) and not by blocking I_f . (Supported by NIH grant HL 27038)

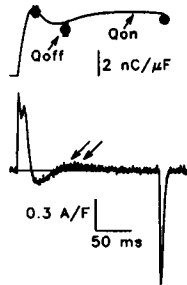
EXCITATION-CONTRACTION COUPLING: SKELETAL MUSCLE

W-PM-J1

THREE PHASES IN I_T , THE HUMP COMPONENT OF CHARGE MOVEMENT IN FROG SKELETAL MUSCLE.

(N.Shirokova, A.González & E.Ríos) Rush Univ., Chicago, IL, 60612. (Spon. by B.R.Russell).

The asymmetric current measured in frog skeletal muscle fibers in the presence of solutions that prevent ionic currents shows a prominent inward phase, especially when the intracellular medium contains high EGTA. We demonstrate that this inward phase is capacitive (charge movement) by showing: conservation of ON and OFF charge at all durations, conservation of OFF charge at various negative voltages, ON-OFF equality at various prepulse voltages and conservation of waveform when substituting Cl^- for glutamate intracellularly. Thus the hump of I_T is followed by an inward phase of charge movement. This in turn is followed by a third (outward) phase (arrows), visible in those cases in which the first two phases are highly developed. The third phase is also capacitive. A negative (inward) phase in charge movement is one of the most characteristic predictions of the model by which I_T is due to a voltage shift associated with Ca release. Supported by NIH.

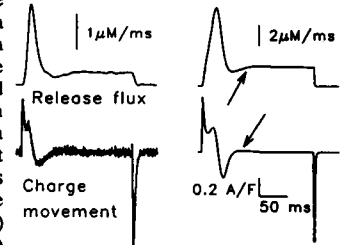


W-PM-J2

THREE PHASES OF I_T AS AN OSCILLATION DUE TO FEEDBACK IN EC COUPLING.

(E.Ríos, N.Shirokova & A.González) Rush Univ., Chicago, IL, 60612.

We measured Ca transients in skeletal muscle fibers exhibiting three phases in I_T (described above). We observed three phases in the waveform of Ca release flux (top, left). The inward phase in I_T is associated with a dip in release flux and the third (outward) phase with a second rise in release. We explored the significance of the outward phase with a mathematical model (Pizarro et al., *Biophys. J.* 59, 1991). It assumes that Ca binds near the internal face of the voltage sensor to increase the local potential and cause the hump of I_T . It predicts: 1) the inward phase of I_T as a consequence of inactivation of Ca release, 2) a second rise in release (arrow, right, top) and 3) third (outward) phase in I_T upon recovery from inactivation of Ca release (arrow, right, bottom). It seems that the three phases constitute a damped oscillation due to the coexistence of positive (I_T) and negative (inactivation) feedbacks. Supported by NIH.

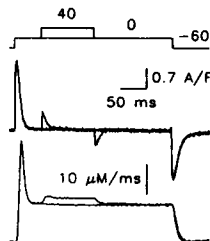


W-PM-J3

CHARGE MOVEMENT AT POSITIVE MEMBRANE POTENTIAL IN SKELETAL MUSCLE.

(A.González, N.Shirokova & E.Ríos) Rush Univ., Chicago, IL, 60612. (Spon. by J.M.Tang).

Improved salines made possible the measurement of intramembrane charge movement in frog skeletal muscle fibers at voltages above 0 mV, with a minimum of ionic currents. This revealed the presence of between 2 and 6 nC/μF of charge, moving at potentials beyond 0 mV. This charge was measurable at ON and OFF, showed signs of saturation at or above +60 mV and was not clearly separable as a distinct Boltzman component. Its kinetics were fast (3-10 ms at 12°C). Simultaneous measurement of Ca release flux showed that even the charge moving above +30 mV causes additional activation of Ca release. High concentrations of intracellular BAPTA and repetitive pulsing (a depletion-causing procedure) reduced the slow current I_{Ca} by between 30 and 70% (confirming Feldmeyer et al., *J. Physiol.* 438, 1991) and reduced the charge above 0 mV by between 30 and 90% with minimal changes on C_m . It appears that the charge above 0 mV is involved both in EC coupling and in I_{Ca} gating. Supported by NIH.



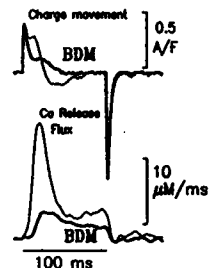
W-PM-J4

BDM SUPPRESSES CALCIUM RELEASE AND Q_T IN SKELETAL MUSCLE FIBERS.

(De Armas, R., Gonzalez, S., Pizarro, G. and Brum, G.)) Depto. de Biofísica, Fac. de Medicina, Montevideo, Uruguay.

The effect of butanedione monoxime (BDM) on EC-coupling was studied in cut skeletal muscle fibers of the frog voltage clamped in a double vaseline gap chamber. 10 mM BDM applied extracellularly reduced the amplitude of the Ca transient monitored with antipyrilazo III. The peak of the release flux was reduced by $48\% \pm 5$ (SEM) whereas the steady level at the end of the pulse was significantly less affected ($21\% \pm 10.3$). The Q_T component of charge movement was reduced and its complex kinetics slowed. Q_0 remained unaltered. Based on the work of Pizarro et al. (*J.G.P.* 97, 1991) these results suggest that BDM acts directly on the release channel or the coupling mechanism.

Partially funded by grants of PEDECIBA and the CSIC.



W-PM-J5

Ca²⁺ TRANSIENTS, Ca²⁺ CURRENT AND CHARGE MOVEMENT IN CULTURED SKELETAL MUSCLE. (K. G. Beam and J. García) Dept. of Physiology, Colorado State University, Fort Collins, CO 80523.

The skeletal muscle DHP receptor functions both as the voltage sensor regulating SR Ca²⁺ release and as a t-tubular Ca²⁺ channel. We have investigated the relationship between electrical signals (measured with the whole-cell patch clamp) and calcium release (measured with indicator dyes) in cultured skeletal muscle of newborn mice. The bath contained 10 mM Ca²⁺; 0.5 mM Cd and 0.1 mM La were added for measurements of charge movement. The pipette contained 0.1 mM Cs₂-EGTA and 200 μM K_v-Fluo-3. Cells were held at -80 mV and 15-20 ms test depolarizations were preceded by a prepulse protocol (Adams et al., *Nature* 346:569-572, 1990) to isolate the slow Ca²⁺ current (I_{slow}) and the charge movement involved in e-c coupling. The Ca²⁺ transient was first detectable at -20 to -10 mV and became maximal at about +40 mV. For depolarizations >10 mV the Ca²⁺ transient continued to increase for several ms after repolarization. This behavior was not detected when the pipette contained 5 mM BAPTA. In the majority of cells, the decay of the transient was slow (100's of ms) and was accelerated by the addition of Cd + La or 1 μM +PN 200-110. Boltzmann fits yielded a steepness factor (k) of 7 mV for both I_{slow} conductance and Ca²⁺ transient and of 13 mV for charge movement. The V_{1/2} values were: I_{slow}, 17 mV; charge movement, 1.4 mV; Ca²⁺ transient, 4 mV in Ca²⁺ alone and 13 mV in Cd + La. Supported by NIH grants NS24444 and NS28323.

W-PM-J7

TETRADES ARE RESTORED IN DYSGENIC MYOTUBES TRANSFECTED WITH cDNA FOR SKELETAL DHPR (H. Takekura*, L. Benner*, T. Tanabe*, K. Beam* and C. Franzini-Armstrong*) *Univ. Pa, *Yale Univ., @Colo. State Univ. (Intr. by S.M. Baylor)

Junctional tetrads are groups of four proteins located in the junctional regions of T tubules and plasmalemma of skeletal muscle fibers, where these membranes face the sarcoplasmic reticulum (SR). The disposition of the four components of the tetrads in freeze-fracture images of T tubules indicates that they are located in correspondence of the four subunits of the ryanodine receptor (foot protein) of the SR. It has been proposed that each of the four elements of the tetrads represents a dihydropyridine receptor (DHPR) complex. In muscle fibers from dysgenic mouse, e-c coupling, slow calcium currents, charge movement and tetrads are missing as a result of a defect in the DHPR. This establishes an initial link between tetrads and DHPRs. We have further explored this question by comparing the structure of the plasmalemma in cultured normal and dysgenic myotubes and in myotubes in which e-c coupling was restored by transfection with a cDNA encoding the skeletal DHPR. 20-40% of the transfected myotubes recovered ability to contract on electrical stimulation. The cultures were fixed in glutaraldehyde, cryoprotected and freeze-fractured by the double replica technique. Electron microscopic examination of replicas of the interior leaflet of the plasmalemma revealed the presence of numerous large groups of tetrads in normal myotubes. The groups of tetrads displayed a non-uniform distribution. In dysgenic myotubes tetrads were not found. Non-uniformly distributed groups of tetrads reappeared following transfection, but they were smaller and less numerous than in normal fibers. This supports identification of tetrads with DHPRs and it has strong implications for the mechanism of e-c coupling.

Supported by NIH HL 15835 to PMI and 24444 and 28323 to KB.

W-PM-J9

RESTING MYOPLASMIC FREE [Ca²⁺] ([Ca²⁺]_i) MEASURED WITH FURA RED AND FLUO-3 IN INTACT SINGLE TWITCH FIBERS FROM FROG SKELETAL MUSCLE. (A. B. Harkins, Nagomi Kurebayashi and S. M. Baylor) Department of Physiology, University of Pennsylvania, Philadelphia, PA 19104.

Fibers were studied at long sarcomere length (3.5-4.0 μm) while bathed in 11.8 mM-Ca²⁺ Ringer's (16°C). The anionic form of fura red or fluo-3 (Molecular Probes, Inc.) was introduced by pressure injection and indicator-related absorbance and fluorescence signals were measured both at rest (A and F) and after an action potential (ΔA and ΔF). To estimate f_r, the fraction of indicator in the Ca²⁺-bound form at rest, the A(λ) signal from fura red (wavelengths λ between 440 and 600 nm) was least-squares fitted with a linear combination of calibration spectra measured in zero and saturating Ca²⁺. With fluo-3, estimation of f_r could not be made from A(λ) alone, since A(λ) varies little with Ca²⁺ complexation; rather, f_r was estimated from combined measurements of A, F, ΔA and ΔF. The mean values (±SEM) of f_r were 0.151±0.005 (N=3; [fura red]=0.5-0.8 mM) and 0.078±0.005 (N=8; [fluo-3]=0.03-0.13 mM). From our best estimate of each indicator's dissociation constant for Ca²⁺ in the myoplasmic environment (1.05 μM for fura red, 2.73 μM for fluo-3), average [Ca²⁺]_i is estimated to be 0.19 μM (fura red) and 0.23 μM (fluo-3). In fibers in normal Ringer's ([Ca²⁺]=1.8 mM), at shorter sarcomere length (2.5-2.9 μm), and with non-perturbing concentrations of indicator (<0.2 mM), the estimates of [Ca²⁺]_i are 0.18 μM (fura red) and 0.28 μM (fluo-3). These values are higher than the 0.02-0.12 μM range estimated in frog fibers with other techniques. Supported by NIH 17620.

W-PM-J6

COMPARISON OF Ca²⁺ TRANSIENTS IN DYSGENIC MYOTUBES EXPRESSING SKELETAL AND CARDIAC DHP RECEPTORS. (J. García, T. Tanabe* and K. G. Beam) Dept. of Physiology, Colorado State University, Fort Collins, CO; *HHMI, Yale University, New Haven, CT.

It has been previously demonstrated that injection of dysgenic myotubes with cDNA (pCAC6) encoding the skeletal muscle DHP receptor restores the slow Ca²⁺ current and skeletal type e-c coupling that does not require entry of external Ca²⁺ (Tanabe et al., *Nature* 336:134-139, 1988); in contrast, injection of cDNA (pCARD1) encoding the cardiac DHP receptor produces rapidly activating Ca²⁺ current and cardiac type e-c coupling that does require Ca²⁺ entry (Tanabe et al., *Nature* 344:451-453, 1990). We report here on Ca²⁺ transients in dysgenic myotubes expressing pCAC6 or pCARD1. Methods were as described in the preceding Abstract. The kinetics and voltage dependence of the Ca²⁺ transients in dysgenic myotubes expressing pCAC6 were qualitatively and quantitatively similar to the transients elicited in normal myotubes. Thus, the Ca²⁺ transient displayed a sigmoidal dependence on voltage and was still present after the addition of 0.5 mM Cd + 0.1 mM La. The transient in dysgenic myotubes expressing pCARD1 showed a bell shaped dependence on voltage, had a slower rate of rise than in pCAC6-injected myotubes and was abolished completely by the addition of Cd + La. Surprisingly, some myotubes expressing pCARD1 displayed a negligible Ca²⁺ transient despite the presence of a large Ca²⁺ current. Supported by NIH grants NS24444 and NS28323.

W-PM-J8

CONFOCAL SPOT DETECTION OF Ca²⁺ TRANSIENTS IN A SINGLE SARCOMERE OF SKELETAL MUSCLE FIBERS

((A. Escobar and J. Vergara) Dept. of Physiology, UCLA School of Medicine.

An inverted double vaseline gap technique was developed for simultaneous recording of high magnification images and electrical activity of skeletal muscle fibers (SMF). Briefly, the fiber was mounted on an ultra-thin coverslip with two vaseline preseals which forms the bottom of a vaseline gap chamber together with a Teflon piece to separate three electrically isolated pools. This set-up allows for the use of a short working distance objective (100x, 1.3 NA) required for high resolution imaging. An Argon laser beam was focused to form a 0.5 μm illumination spot that could be micropositioned with respect to muscle structures visualized with differential interference contrast illumination by a cooled CCD camera. The SMF were internally perfused with a relaxing solution containing 150 μM of the fluorescent Ca²⁺ indicators Fluo-3 or Calcium-Green-5N. The epifluorescent light emitted by the dyes at the illuminating spot was detected by a pin photodiode (micropositioned on the spot) connected to an ultra low-noise high bandwidth amplifier. The area of detection of the photodiode was chosen to assure confocality within an image area of 0.4 μm² and 1.2 μm depth-of-field. Ca²⁺ transients recorded at several intrasarcomere locations from SMF stimulated to elicit action potentials showed significant differences in their kinetic behavior. Transients recorded at spots separated by half-sarcomere showed maximal differences of about 1 ms (17 °C) in their rising phases. In addition, large differences in delays and amplitudes could be observed from transients detected at various locations within the SMF. In particular, detection from spots located inside and outside of nuclei reported transients with remarkable kinetic differences. (Supported by USPHS AR-25201 and MDA)

W-PM-K1

THEORY OF TWO-PHOTON INDUCED FLUORESCENCE ANISOTROPY FOR INDOLES IN WATER. ((Patrik R. Callis)) Dept. of Chemistry, Montana State University, Bozeman, MT 59717.

Drawing on the work of McClain [J. Chem. Phys. 57, 2264(1972)], useful relationships are derived connecting the traditional two-photon polarization ratio, $\Omega = \delta_{\text{circ}}/\delta_{\text{lin}}$ (the ratio of two-photon absorption using circularly and linearly polarized excitation light in fluid solvent) and the expected range of anisotropy (r) of fluorescence from two-photon excitation using linear excitation when the molecules do not rotate. The "ideal" limit of $r=0.5714$ can only be attained if $\Omega=2/3$ but is not expected since the two-photon absorption tensor usually has little relationship to the one-photon transition dipole. Surprisingly, it is found that the maximum possible r is actually 0.597, possible only if $\Omega=7/8$. From experiments on indole we have previously found $\Omega=1.4$ and 0.5 for the 1L_b and 1L_a states respectively, leading to ranges of $r=-0.1$ to $+0.39$ for 1L_b and $r=-0.22$ to $+0.51$ for 1L_a , depending on the direction of the emitting transition dipole. Lakowicz et al. [Chem. Phys. Lett. 194, 282(1992)] have reported $r=0.3$ for indole and $r=0.2$ for two-photon excitation of the 1L_a states of indole and NATA respectively. Their data also suggests $r \approx -0.1$ for 1L_b . This means that the emitting transition dipole makes an angle of about 30° with the major axis of the indole 1L_a tensor and about 40° in the case of NATA. We find INDO/S-CI molecular orbital calculations on indole and 3-methylindole to be in fair agreement with experiment, except for the 1L_b tensor of indole.

W-PM-K3

A MODEL OF MULTIEXPONENTIAL FLUORESCENCE INTENSITY DECAY IN PROTEINS NOT BASED ON CONFORMATIONAL SUBSTATES. ((Ž. Bajzer and F.G. Prendergast)) Mayo Clinic and Foundation, Rochester, MN 55905. (Spon. by Ž. Bajzer)

The fluorescence intensity decay is commonly modeled by multiexponential functions characterized by lifetimes and preexponential factors. A few distinct exponential components are most often recovered for fluorescence decay in proteins, even by the methods of analysis which allow recovery of continuous distribution of lifetimes (e.g. maximum entropy method). Common interpretation of few-exponential decay is based on conformational heterogeneity. We present another possible multiexponential model based on the assumption that an energetically excited donor surrounded by N acceptor molecules decay by radiative or radiationless relaxation processes, and by transferring its energy to acceptors. If the interactions between acceptors and back energy transfer are neglected we show that the intensity decay function contains 2^N components. One component is characterized by donor-associated lifetime τ , N components by energy transfer rates w_i and other components by sums of all combinations of rates. Thus for two acceptors the decay law is: $\exp(-t/\tau)\{p_0 + p_1 \exp(-w_1 t) + p_2 \exp(-w_2 t) + p_3 \exp[-(w_1 + w_2)t]\}$ where p_0, \dots, p_3 are interaction probabilities. We apply the model to azurin from *Ps. aeruginosa* and ribonuclease T_1 . Supported by GM 34847.

W-PM-K5

TIME-RESOLVED FLUORESCENCE OF INDOLE DERIVATIVES AND PROTEINS WITH TWO-PHOTON EXCITATION. ((I. Gryczynski and J.R. Lakowicz)) University of Maryland, School of Medicine, Center for Fluorescence Spectroscopy, Department of Biological Chemistry, 108 N. Greene Street, Baltimore, MD 21201. (Spon. by I. Gryczynski)

Fluorescence of indole, tryptophan and NATA, as well as the proteins HSA and LADH, have been studied using two-photon excitation. The fluorescence spectra and lifetimes are essentially identical as those obtained with one-photon excitation, suggesting that the same excited state is responsible for the emission, irrespective of excitation mode. Also, the rotational correlation times obtained from the time-resolved anisotropy measurements were similar for one- and two-photon excitation. However, the limiting anisotropies obtained with two-photon excitation do not correspond to those expected from one-photon excitation (e.g. $r_2 \neq r_1/10/7$). In the case of indole derivatives the excitation anisotropy spectra may reflect the two-photon absorption spectra of the 1L_b and 1L_a states. The two-photon anisotropy spectra were decomposed with the assumption that only 1L_b and 1L_a states are populated during two-photon excitation. In the case of LADH the intensity and anisotropy decays for one- and two-photon excitation may reflect the relative one- and two-photon cross sections of the two tryptophan residues.

W-PM-K2

EMISSION AND ANISOTROPY DECAY OF THE MOLTEN STATE OF APOMYOGLOBIN DETECTED BY FREQUENCY DOMAIN FLUOROMETRY.

((I. Sirangelo, E. Gratton, G. Irace and E. Bismuto)) Dipartimento di Biochimica e Biofisica, Università di Napoli - ITALY (Spon. by E. Bismuto)

The attention of this communication is devoted to the structural and dynamical aspects of the salt-induced partly folded state of apomyoglobin at acidic pH which is known to correspond to a molten globule state.

Informations on protein structure and dynamics have been obtained from the analysis of the emission and anisotropy decay of intrinsic (tryptophanyl residue) and non-covalently bound extrinsic (1,8-anilino-naphthalenesulfonate, ANS) fluorophores detected by frequency domain fluorometry.

The results are consistent with an asymmetric shape of the molten state of apomyoglobin and with an increased degree of the atomic fluctuations.

W-PM-K4

TIME-RESOLVED FLUORESCENCE ENERGY TRANSFER ((B. Wieb Van Der Meer and Sun-Yung Chen)) Department of Physics and Astronomy, Western Kentucky University, Bowling Green, KY 42101

The effects of the orientation factor, rotational and translational motion of Donors and Acceptors can be taken into account by constructing compartmental models of systems undergoing Fluorescence Energy Transfer (B.W. Van Der Meer, M.A. Raymer, S.L. Wagoner, R.L. Hackney, J.M. Beechem, and E. Gratton. 1992. *Time-Resolved Laser Spectroscopy in Biochemistry III, Proc. Int. Soc. Opt. Engin. (SPIE) 1640: 220-229*). In this method excited Donor and Acceptor "states" are defined in which the Donor or the Acceptor is excited and the molecules have a specific orientation and position. Motion is modeled by transitions from one state to another. Transfer corresponds to transitions from excited Donor states to excited Acceptor states. We will discuss applications to studying dynamics in membranes and proteins. This work is supported by the National Science Foundation EPSCoR program (EHR-9108764).

W-PM-K6

UNIQUE CHARACTERISTICS OF TYROSINE-14 AT THE ACTIVE SITE OF Δ^5 -3-KETOSTEROID ISOMERASE (EC 5.3.3.1)

F.G. Wu, Y-K. Li & L. Brand, Johns Hopkins Univ. Baltimore, MD.

Δ^5 -3-Ketosteroid isomerase of *Pseudomonas testosteronei* converts Δ^5 to Δ^4 -3-ketosteroids by a conservative 4 β - to 6 β -proton transfer. Tyr-14 and Asp-38 are the essential general acid and base, respectively, promoting a concerted, rate-limiting enolization. Tyr-14, -55 and -88 are the only fluorophores in the wild-type isomerase. The wild-type enzyme and all single and double mutants of these tyrosine residues were studied by CD and time-resolved fluorescence. (a) Tyr-14 is isolated in a hydrophobic environment since it has an unusually long fluorescence lifetime (4.6 ns), cf. Tyr-55 (2.0 ns), Tyr-88 (0.8 ns) and to most protein tyrosines (0.2-1 ns). (b) The quantum yields, relative to that of tryptophan, of Tyr-14, -55 and -88 in the double tyrosine mutants are 0.16, 0.06 and 0.03, respectively, whereas those of the wild-type are calculated to be 0.12, 0.01, and 0.03 for each tyrosine, respectively. Thus Tyr-14 and Tyr-55 directly or indirectly mutually quench each other, while Tyr-88 is unperturbed by Tyr-14 or Tyr-55. (c) The rotational motion of Tyr-14 is tightly coupled to the motion of the protein, suggesting that Tyr-14 is buried. Tyr-88 is more mobile, indicating that it is exposed at the surface of the protein. (d) The loss of fluorescence of Tyr-14 in guanidinium parallels the denaturation (by CD) and can serve as a probe for the denaturation of isomerase. Such measurements show that mutants with Tyr-14 substituted are more stable than the wild-type enzyme.

W-PM-K7**DARK-BACKGROUND FLUORESCENCE ENERGY TRANSFER USING LANTHANIDE CHELATES.**

((P.R. Selvin, T. Rana, M.P. Klein and J.E. Hearst)) Calvin Laboratory and Department of Chemistry, University of California, Berkeley and Lawrence Berkeley Laboratory, Berkeley CA, 94720.

Fluorescence Energy Transfer (FET) has become a standard spectroscopic technique for measuring distances in the 10-70Å range. Nevertheless, FET has a number of serious flaws which limit its utility. First, the maximum distance which can be measured is less than desirable for many biological applications. Second, when measuring the sensitized emission of acceptor (which is less sensitive to artifacts than donor quenching and is theoretically a dark-background experiment) the signal to background is poor, typically 0.2:1 at R_0 , the distance of 50% energy transfer. Third, the lifetime of commonly used fluorophores are short (typically a few nanoseconds), making lifetime measurements difficult and of limited accuracy.

We have used FET "dyes" where the donor is based upon a lanthanide chelate with a millisecond lifetime and the acceptor is a standard dye. We find that sensitized emission — both yield and lifetime — can be measured with *no* interfering background, potentially making distance measurements well beyond R_0 feasible (here, R_0 is approximately 38Å). Because of the donor's long lifetime, both donor quenching and sensitized emission measurements can be made with relatively simple instrumentation. Using a series of DNA oligos as rigid tethers separating the dyes, we have generated a calibration curve. Some subtleties of the transfer mechanism will be discussed.

W-PM-K9**EFFECTS OF HYDROSTATIC PRESSURE ON THE STRUCTURE OF PHOSPHOLIPID BILAYERS AS DETECTED BY THE FLUORESCENCE KINETICS OF TRANS-PARINARIC ACID.**

((P.Tauc, C.R.Mateo and J.C.Brachon)) L.U.R.E. CNRS-MEN-CEA Université Paris Sud, F-91405 Orsay, France.

Time-resolved fluorescence of the natural lipid *trans*-parinaric acid (*t*-PnA) has been used to investigate the effects of hydrostatic pressure, up to 3.2kbars, on single and mixed large unilamellar vesicles of different phospholipids in the temperature range of 10°C to 50°C. The samples were excited by a picosecond laser pulse and the measurements were carried out with a modified high pressure cell. The data were analysed by the new quantified maximum entropy method program (MaxEnt). The fluorescence lifetime distributions of *t*-PnA in isotropic solvents at different pressures showed two well-resolved components. Three components were obtained when the probe was introduced in pressurized bilayers. The isotherms of the pressure induced phase transition can be determined with high precision from the changes observed in these lifetime distributions. The effect of pressure on the phase diagram of the DMPC/DPPC lipid mixtures was also studied. A correspondance between temperature and pressure effects on lipid bilayer order was set. In the cases of DMPC bilayer and of equimolar DMPC/DPPC mixtures, the effect of pressure is greater than in the case of unsaturated phospholipids.

W-PM-K8**IN-VIVO MEASUREMENT OF DNA CONTENT AND STRUCTURE USING HOECHST 33258. ((B.K. Stringer and J.T. Blankemeyer)) Oklahoma State University, Stillwater, OK. 74078.**

In this study, we report the use of whole, fertilized, *Xenopus l.* embryos and the fluorescent probe HOECHST 33258 to measure DNA content and structure *in-vivo*. By using excitation spectra of HOECHST 33258 and measuring the emission at 480 nm, we are able to measure the increase in DNA content as the embryo develops from the morula to the gastrula stage. Certain chemicals such as Actinomycin-D, Triethylenemelamine (TEM), and Hydroxyurea alter DNA structure and content via various mechanisms. These compound have been shown to cause malformations in *Xenopus* embryos as well as mammals, although the mechanisms have not been clearly determined. The effects of these chemicals on DNA were studied using HOECHST 33258. An increase in the excitation spectrum of the dye indicates that TEM is acting to "unwind" the DNA from the histones in a dose-response manner, with an EC_{50} value of 0.06 mg/ml. Excitation spectra decreases measured in the presence of Actinomycin-D and Hydroxyurea indicate that these compounds are either inhibiting DNA synthesis during development, cutting the DNA into fragments, or both. These compounds, like the TEM, act in a dose-dependant manner. Control experiments using double stranded calf thymus DNA and calf thymus chromatin verify our conclusions as stated above. These results suggest that it is possible to predict the extent of DNA damage as well as the type of damage in response to a given compound. RESEARCH SUPPORTED IN PART BY THE UNIVERSITY CENTER FOR WATER RESEARCH.

METHODS II**W-PM-L1****STRUCTURAL INVESTIGATION OF PROTEIN BINDING TO THE SURFACE OF SELF-ASSEMBLED MONOLAYERS USING X-RAY INTERFEROMETRY.**

((J.A. Chupa, J.P. McCauley, R.M. Strongin, A.B. Smith III, J.K. Blasie*, L.J. Peticolas and J.C. Bean**)) * Department of Chemistry, University of Pennsylvania, Philadelphia, PA 19104 and ** AT&T Bell Laboratories, Murray Hill, NJ 07974. (Spon. by J.K. Blasie)

X-ray interferometry was applied to meridional x-ray diffraction data to uniquely determine the profile structures of self-assembled monolayers having a bound surface layer of protein. The self-assembled monolayers (SAM) were formed on the surface of Ge/Si multilayer substrates, fabricated by molecular beam epitaxy. The following protein/self-assembled systems were studied: yeast cytochrome *c* tethered to the 11-siloxylundecylthiol SAM, horse heart cytochrome *c* bound to an analogous carboxyl-terminating SAM, and photosynthetic reaction centers on an amine-terminating SAM. The yeast cytochrome *c* was previously found to covalently bind to the thiol moiety of its SAM, while both the horse heart cytochrome *c* and the photosynthetic reaction centers electrostatically bind to their respective SAMs. Optical absorption measurements performed on these systems are consistent with the protein forming densely packed monolayers at the surface of the SAM. The power of the self-assembly technique lies in its ability to specifically bind both the peripheral membrane protein, cytochrome *c*, and the integral membrane protein, photosynthetic reaction center. The vectorial orientation of the reaction center protein was distinguishable in the profile structure at a spatial resolution of 7 Å.

W-PM-L2**DETECTION OF HIGH RESOLUTION SIGNAL IN ELECTRON MICROGRAPHS OF HELICES ((David Morgan and David Reisler)) Department of Biology, Brandeis University, Waltham, MA 02254**

Structures with helical symmetry diffract weakly so that high resolution structural signal can be hidden by noise. In the case of the bacterial flagellar filament, the 10 Å signal can be extracted, however, by averaging about 100 filaments (300,000 flagellin subunits). Do all 100 images contribute equally to the averaged signal? To find out we developed a method to detect high resolution signal hidden by noise. The algorithm tests the phases of a single image against the corresponding phases of the average. We calculated a weighted sum of the cosines of the phase differences, ($\phi_{avg} - \phi_{single}$). The weights were the amplitudes, $|F_{avg}|$, of the Fourier coefficients of the average:

$$sg = \frac{\sum_{j=1}^m |F_{a,j}| \cos(\phi_{a,j} - \phi_{s,j})}{\sum_{k=1}^m F_{a,k}}$$

The output was a single number between 1.0 (perfect phase agreement) and -1.0 (anticorrelated as might occur if the phases of the image were reversed by the contrast transfer function). If the phases of the image and the average are uncorrelated, the expected value is 0.0. To locate a layer line, we took lines of data centered about the expected position of the layer line and applied the equation to each line of data. The output from the set of lines generated a peak at the position of the true layer line. The width of the peak was inversely proportional to the length of the image. The peak height, which measures the amount of signal in the layer line, varied between .4 and .8 depending on the number of reflections included in the sum, the strength of the layer line in the average, and the quality of the single image being tested. With this algorithm we could detect in the transform of a single particle, 10 Å resolution layer lines which were hidden by noise.

W-PM-L3

NEURAL COMPUTING IN THE DEVELOPMENT OF NEW THERAPIES FOR CANCER AND AIDS

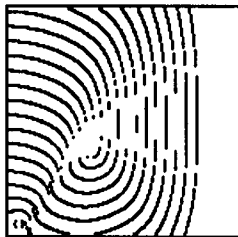
John N. Weinstein, Kurt W. Kohn, Michael R. Grever, Veilarkad N. Viewanadhan, Lawrence V. Rubinstein, Anne Monks, Dominic A. Scudiero, Lester Welch, Antonis D. Koutsoukos, August Chiausua, Jun Yang, Rachel Schiff, Jeffrey Licht, Robert E. Wittes, and Kenneth D. Paull. National Cancer Institute, NIH, Bethesda, MD 20892.

There are literally millions of molecules that ought to be tested for activity against cancer and against HIV. As an approach to that task, the National Cancer Institute has established high-volume drug screening programs. The cancer program tests several hundred compounds a week for activity *in vitro* against a panel of 60 malignant human cell lines representing different types of tumors. Implicit in this strategy is the premise that the agents tested will show reproducible patterns of differential response among the 60 lines. The computer program COMPARE verifies this supposition. It is important to ask, then, whether these patterns of activity can be used to classify new agents by their mechanism of action. If so, the information could be used to guide efforts at rational drug design and to help prioritize agents for the more expensive, lower-volume testing *in vivo*. To this end, we have developed neural networks for prediction of mechanism. Early stages of the work are described in Weinstein, et al., Science, Oct. 16, 1992. Given a set of 6 possible classes of mechanism, the networks miss the correct category for only 12 out of 141 agents (8.5%), whereas linear discriminant analysis misses 20 out of 141 (14.2%) (two-tail McNemar p-value for the difference = 0.02). Current work focuses on the complementary problems of prediction based on molecular structure and prediction of clinical success on the basis of patterns of activity in the screen. Surprisingly, the clinical predictions have yielded Pearson's correlation coefficients > 0.6, despite the many characteristics of *in vivo* pharmacology that are not reflected *in vitro*. Neural computing and other aspects of artificial intelligence, when combined with more classical statistical techniques for pattern recognition and decision-making, can clearly play a number of productive roles in the discovery and development of new agents for treatment of cancer and AIDS. Supported in part by the NIH AIDS Targeted Antiviral Program.

W-PM-L5

COMPUTER SIMULATION OF THE VULNERABLE WINDOW IN THE TWO-DIMENSIONAL HOMOGENEOUS MYOCARDIAL SURFACE. (V.V. Nesterenko) Masonic Medical Research Lab, Utica, NY 13501 (Spon. by Kent L. Thornburg)

Extrastimulus (ES) delivered during the vulnerable window (VW) at the end of a basic propagating wave have been shown to produce unidirectional block in the linear cardiac cable. We simulated the homogeneous myocardial surface (3x3 cm with 0.02 cm steps) described by the Luo-Rudy model to investigate the spread of excitation in two dimensions. If a point ES is delivered during the VW of the basic planar excitation, no abnormal response can be observed in the 2-D surface; the initial non-symmetric excitation wave regains its normal circular shape after first 5-10 msec. However, if additional planar ES is used, it produces slower propagating wave and a higher degree of spatial functional heterogeneity. Subsequent point ES now results in the unique shape of propagating front (Fig). Wave front collides with the tail of the previous wave and penetrates an area of the transient functional block, creating "figure-eight" re-entry. This phenomenon is observed only in the very narrow ranges of the delays between basic stimulus and the 1st ES and the intervals between 1st and 2nd ES. We conclude that only double-pulse protocols can reproduce the VW phenomenon in a 2-D homogeneous surface in a manner similar to experimental and clinical findings.



5-msec isochrones

W-PM-L7

VARIATIONAL FORMULATIONS OF ELECTRO- AND MECHANOCHEMICAL COUPLING. (J.S. Shiner) Department of Physiology, University of Bern, Switzerland.

Chemical reactions play an indisputably central role in biological phenomena, even those which are not primarily thought of as being chemical in nature. Unfortunately it has not been possible to treat the dynamics of chemical reactions with the same formalism as that used for other sorts of processes, mechanical or electrical ones, for example. Chemical kinetics have been used for the reactions, whereas mechanical and electrical aspects have been treated by other formalisms (Newtonian dynamics, network theory, etc.). The coupling between chemical and non-chemical processes has had to be handled on an *ad hoc* basis. Recent advances have shown, however, that the dynamics of chemical reactions can be cast into a formalism common to the other sorts of processes, namely the variational formalism containing Lagrangian and Hamiltonian dynamics. It will be shown how the variational formalism leads to a unified treatment of chemical and nonchemical processes and the coupling between them. A simple electrochemical process will be treated in some detail. It will also be shown that a variational formulation of muscle contraction including both chemical and mechanical aspects leads to an additional dissipative term in both chemical and mechanical equations. This term has been neglected in all previous treatments.

W-PM-L4

DEVELOPMENT AND USE OF A MAC BASED DATA ANALYSIS PACKAGE FOR EQUILIBRIUM SEDIMENTATION DATA FROM THE ANALYTICAL ULTRACENTRIFUGE.

((Ian S Brooks#, K. Karl Sonesson*, and Preston Hensley#))

Department of Macromolecular Sciences, SmithKline Beecham Pharmaceuticals, King of Prussia, PA 19406-0939 * K.K.S. Software, Exton, PA 19341-1730

The recent introduction of Beckman Instruments' second generation analytical ultracentrifuge, the XL-A, has provided researchers with a powerful tool for characterizing macromolecular assembly processes. To complement this technology advance, we have developed a full featured data analysis program. This package runs within the framework of IGOR (Wavemetrics, Lake Oswego OR) a powerful graphical data analysis program for the Mac. The program XLAFIT can import and reduce data from either the XL-A or the Model-E analytical ultracentrifuges. Data is fit to one of the many models encoded by non-linear curve fitting techniques. IGOR's non-linear fitting algorithm has been replaced by NONLIN (Mike Johnson, University of Virginia) to speed computation and give better error analysis. In addition, XLAFIT aids analysis of the model fits by utilizing techniques such as autocorrelation, residual analysis and confidence limit estimation. IGOR's graphical capabilities enable the automatic generation of publication quality page layouts and figures. In routine use, it takes less than 5 minutes from data collection to publication quality output. Recording of the data analysis process is accomplished by the use of log files and IGOR's history window. The latter feature allows the analysis to be continued from the exact point that the previous work ended.

W-PM-L6

THE USE OF LEGENDRE TRANSFORMED THERMODYNAMIC PROPERTIES FOR BIOCHEMICAL REACTIONS AT SPECIFIED pH AND pMg

((R. A. Alberty)) Dept. of Chemistry, MIT, Cambridge, MA 02139

When the equilibrium of a biochemical reaction is studied at a specified pH and pMg, the criterion of equilibrium is the transformed Gibbs energy G' , which is obtained as a Legendre transform of the Gibbs energy. The fundamental equation for G' provides the means for calculating the transformed entropy S' and the transformed enthalpy H' . The standard transformed Gibbs energies of formation of biochemical reactants can be calculated when the standard Gibbs energies of formation of the species are known or from apparent equilibrium constants K' for a number of reactions at the desired pH and pMg. If the effect of temperature is studied, a full set of transformed thermodynamic properties is obtained. This makes it possible to make tables of standard transformed formation properties for use in calculating apparent equilibrium constants and transformed enthalpies of reaction for many more biochemical reactions than it takes to make the tables.

W-PM-L8

REACTION RATE ENHANCEMENT BY SURFACE DIFFUSION OF ADSORBATES.

((D. Wang¹, S. Y. Gou² and D. Azebrod^{1,3}))
¹Biophysics Research Division, ²Dept. of Mechanical Engineering, and ³Dept. of Physics, University of Michigan, Ann Arbor, MI 48109. (Spon. by C. L. Marocco)

Ligands can be captured by a surface target through either direct bulk diffusion or surface diffusion following reversible adsorption to the surface. We have solved a steady state boundary value problem for a perfect sink disk target in the surface, taking into account bulk and surface diffusion coefficients D and D_s and adsorption/desorption kinetic rate constants k_a and k_d at nontarget regions. Solutions have been successfully found by numerical computation on a PC. The results show that the rate of capture from the surface depends nonlinearly on D_s , D , k_a , k_d and geometrical dimensions. In particular, we demonstrate that not only is the nontarget region equilibrium constant K_{eq} ($=k_a/k_d$) important in determining the rate of capture from the surface, but so are the kinetic rate constants k_a and k_d separately. In all cases, the surface adsorption/diffusion combination enhances the total rate of capture. The results should be useful for predicting reaction rates of biological membrane bound receptor clusters and substrate-immobilized enzymes. Supported by NIH NS 14565 and NSF DMB 8805296.

W-PM-M1

STATISTICAL MECHANICS OF PROTEIN FOLDING. ((E. Shakhnovich))
Department of Chemistry, Harvard University, Cambridge, MA 02138

The most important questions for understanding how proteins fold are:

- 1) What interactions between protein fragments give rise to unique structure?
- 2) How does protein find this structure in the process of folding?

Recently an analytical theory based on combination of modern polymer theory with some techniques introduced in Spin-glass theory was suggested. It provided complete thermodynamic description of the formation of unique structure in a polypeptide chain and outlined the features of that transition. It was shown that unique structure is formed below certain temperature via special phase transition involving main free energy barrier but not associated with latent heat. Based on the theory a phase diagram was suggested which exhibited three main regimes with transitions between them: coil, compact globule without unique structure and native state which is compact and with unique structure. To test the theory new lattice models of proteins with full enumeration of conformations were suggested. Monte-Carlo simulation of folding within these models has the advantage that in this case the conformation of the global minimum of energy corresponding to the native state is well known so that one could justify the ability to find such conformation in the process of folding. The results of simulation suggest that the ability to fold rapidly into global minimum is directly related with stability of the native state and does not require any special biases or structural characteristics of the native state.

W-PM-M3

A MODEL SYSTEM FOR EVALUATING KNOWLEDGE-BASED POTENTIALS. ((Scott Le Grand and Kenneth M. Merz Jr.))
Department of Biochemistry and Department of Chemistry,
Pennsylvania State University, University Park PA 16803

Numerous approaches to tertiary structure prediction and the inverse protein folding problem rely on knowledge-based potential functions derived from known protein structures. Unfortunately, the native structures of proteins are frequently not the optimal conformations under such potentials even when supplied with constraints such as the radius of gyration and known disulfide bonds. The specific cause of this problem is unknown but possibilities include error in the protein structure database, the inadequate sample size of known protein structures, the impossibility of specifying an adequate potential function composed of two-body interactions alone, and built-in biases in the derivation of these potentials. To address these questions, we have created a model system composed of two classes of amino acid residues and located the global minimum conformations of the entire range of polymers of specified lengths under a pre-specified potential function. From these global minimum conformations, we have used various protocols to generate knowledge-based potentials. Next, we have located the global minimum conformation of each polymer under these knowledge-based potentials and compared it to the original global minimum conformation to evaluate each potential's performance.

W-PM-M5

SECONDARY STRUCTURAL TYPES IN PEPTIDES AND PROTEINS ASSOCIATED WITH FTIR VIBRATIONAL CIRCULAR DICHROISM TO FREQUENCIES. ((Timothy A. Keiderling¹, Petr Pancoska^{1,2}, Lijiang Wang¹, Rina Dukor¹, Marie Urbanova^{1,2}))¹Department of Chemistry, University of Illinois at Chicago, Box 4348, Chicago, IL 60680 USA and ²Department of Chemical Physics, Faculty of Mathematics and Physics, Charles University, Prague 2, Czechoslovakia.

A number of studies of protein conformation have appeared in recent years that use FTIR determined frequencies to propose an analysis of protein fractional secondary structure. We have reported a series of investigations correlating the band shapes of vibrational circular dichroism (VCD) spectra of both peptides and proteins with secondary structure. VCD has the same frequency base as FTIR but also includes information inherent in the chiroptical sign variation with which one can identify the underlying structure. We will present a summary of FTIR and VCD spectra for model peptides and proteins to demonstrate the effects of deuteration, solvent and side-chain upon the expected IR frequencies. An analysis of protein VCD frequencies yields a consistent pattern that allows better identification of the source of the protein IR frequency through correlation with the sign of its respective VCD band. Here sign patterns sort out the redundancy of peaks assigned to several structural types in the same spectral range which are thus indistinguishable with FTIR. This approach has been applied to some small proteins to reassign the secondary structure from FTIR error.

Supported by the NIH (GM-30147) and NSF (INT91-07588), and samples from Profs. Claudio Toniolo and André Brack and Dr. Stephen Prestrelski.

W-PM-M2

PROTEIN TERTIARY STRUCTURE PREDICTION USING OPTIMIZED HAMILTONIANS

((Richard A. Goldstein, Zaida A. Schulten, and Peter G. Wolynes))
School of Chemical Sciences, University of Illinois, Urbana, Illinois 61801

Protein folding codes constructed using associative memory Hamiltonians based on aligned sequences or energy functions based on local interactions can be optimized using spin-glass theory. Simulated annealing for the optimally-encoded associative memory Hamiltonian generally leads to qualitatively correct structures. A screening method to identify structurally homologous proteins works in the vast majority of instances with either Hamiltonian, even in the "twilight zone" of sequence similarity. The success of this optimization technique with such different functional forms demonstrates its general applicability.

W-PM-M4

A BACKBONE-DEPENDENT ROTAMER LIBRARY FOR PROTEINS: APPLICATION TO SIDECHEIN PREDICTION. ((R. L. Dunbrack, Jr. and M. Karplus.)) Department of Chemistry, Harvard University, 12 Oxford St., Cambridge MA 02138. (Sponsored by G. Petako).

A backbone-dependent rotamer library for amino acid sidechains is developed and used for constructing proteins sidechain conformations from the mainchain coordinates. The rotamer library is obtained from 132 protein chains in the Brookhaven Protein Database. A grid of 20° by 20° blocks for the mainchain angles ϕ, ψ is used in the rotamer library. Significant correlations are found between sidechain dihedral angle probabilities and backbone ϕ, ψ values, which can be rationalized with molecular mechanics calculations. The database probabilities are used to place the sidechains on the known backbone in test applications for six proteins for which high resolution crystal structures are available. A minimization scheme is used to reorient sidechains which conflict with the backbone or other sidechains after the initial placement. The initial placement yields 59% of both χ_1 and χ_2 values in the correct position (to within 40°) for thermolysin to 81% for crambin. After refinement of the values range from 61% (lysozyme) to 89% (crambin). It is evident from the results that a single protein does not adequately test a prediction scheme. The method scales linearly with the number of sidechains. An initial prediction from the library takes only a few seconds of computer time, while the iterative refinement takes on the order of hours. The method is automated and can easily be applied to aid in experimental sidechain determinations and for homology modeling. The high correlation between backbone and sidechain conformations introduces a simplification in the protein folding process by reducing the available conformational space.

W-PM-M6

HELIX FOLDING SIMULATIONS USING A NEW RIGID ELEMENT METHOD ((S.-S. SUNG)) Research Institute, Cleveland Clinic Foundation, Cleveland OH 44195

Because of the large number of degrees of freedom in protein molecules the widely used methods of energy minimization and molecular dynamics are not practical for studying protein folding. One strategy to reduce the degrees of freedom is to use only dihedral angles as variables. However, because independent local motions in the middle of the mainchain are severely restricted by fixed bond lengths and angles, this method becomes inefficient as the number of residues increases. A new rigid element method using non-dihedral variables has been developed and is reported in this presentation. It treats the mainchain amide groups as rigid elements to reduce the degrees of freedom and uses flexible connections between the rigid elements to allow local motion. This new method is physically more realistic and computationally more efficient. It has been applied to Monte Carlo simulations for the alanine-based polypeptides. The results are in excellent agreement with experimental observations (S. Marqusee, V.H. Robbins, R.L. Baldwin, Proc. Natl. Acad. Sci. USA 1989, 86:5286). Starting from the standard extended structure, the alanine based polypeptides with three lysine residues folded gradually into predominantly α -helical conformations during a single simulation at 300°K. Helix folding simulations have not previously been successful at constant room temperature. From these simulations it is found that dipole-dipole interactions between neighboring residues in the sequence favor a β -strand conformation, and those between the non-neighboring residues favor a helical conformation. The enthalpic effect drives the molecule towards forming ordered secondary structures, and the entropic effect drives the molecule towards random structures.

W-PM-M7

INFRARED AND RAMAN STUDIES OF PROTEINS. ((J.R.Powell, R.J. Jakobsen)) Bio-Rad/Digilab, 237 Putnam Ave. Cambridge, MA 02139 (JRP), IR-ACTS, 4842 N. High St., Columbus, OH 43214 (RJJ)

Vibrational spectroscopic studies of proteins have emphasized the analysis of the Amide I and II vibrations. Using Fourier deconvolution, second derivative, and/or band fitting techniques has aided in the interpretation of these bands for the secondary structure of the protein. Some studies have been done on the Amide III region, but there has been little correlation of the Amide III to the Amide I and II. Additionally, previous studies used infrared or Raman spectroscopy, but seldom both techniques. This has resulted in some conflicts in the vibrational assignments, depending on which region was studied by which technique. Here, a series of proteins has been studied by both infrared and Raman spectroscopy. Mathematical techniques described above were applied as needed. Spectral information in multiple regions was used to gain information on the secondary and tertiary structure of the proteins as well as vibrations from key amino acid groups and side chains. This leads to information on folding/unfolding pathways and denaturation mechanisms.

BACTERIORHODOPSIN**W-PM-N1**

HIGH RESOLUTION ELECTRON DIFFRACTION STUDY IN PROJECTION ON BACTERIORHODOPSIN MUTANTS: GROUND STATE STRUCTURE IN D96N IS UNALTERED. ((A.K. Mitra, L.J.W. Miercke, M.C. Betlach, R.F. Shand*, and R.M. Stroud)) UCSF, Dept. of Biochemistry and Biophysics, San Francisco, CA 94143-0448, *Dept. of Biological Sciences, Northern Arizona University, Flagstaff, AZ 86011.

Bacteriorhodopsin (BR), a light-activated proton pump in the purple membrane (PM) of *H. halobium* is arranged *in vivo* in a highly ordered 2-dimensional hexagonal P3 lattice. Upon absorption of a photon of light BR cycles through a series of photointermediates resulting in an outward pumping of a proton. Extensive spectroscopic and functional studies on site-directed mutants have identified which amino acids interact strongly with the all-*trans* retinal chromophore in BR and affect the proton pump. Specifically Asp-85, Asp-212, Arg-82 and Asp-96 are found to be involved in the proton translocation pathway.

To help establish the role of altered residues in the photochemical cycle, it is necessary to characterize any changes in structure in addition to function. Starting with an *E. coli* -expressed β -gal-bacterioopsin fusion analog purified to homogeneity in SDS, we have obtained 2-dimensional crystals of wild type-analog (e-BR) and the D96N variant (e-D96N) after retinalylation and reconstitution into *H. Halobium* lipids. These crystals embedded in glucose diffract to $\sim 3.0\text{\AA}$ resolution at room temperature with a homologous P3 lattice ($a = 63.2\pm 0.4\text{\AA}$) and permit high-resolution structural analyses of the functionally impaired D96N variant. The e-BR crystal is isomorphous to PM with the projection e-BR-PM difference Fourier map at 3.6\AA resolution indicating small conformational changes in e-BR equivalent to movements of <-7 C-atoms distributed within and in the neighborhood of the protein envelope. This result shows that relative to BR there are no global structural rearrangements in e-BR. The e-D96N crystal is isomorphous to the e-BR crystal. The 3.6\AA resolution e-D96N-e-BR difference map showed no statistically significant peaks or valleys within a projected distance of 5\AA from the site of D96 substitution on helix C. Elsewhere in the protein envelope the difference map showed small peaks and valleys whose integrated measure was <-3 C-atom equivalents. Therefore our results show that for the isosteric Asp96 to Asn substitution the surrounding protein structure is essentially unaltered proving that the known effect of D96N on the slowed M-decay is chemical and not structural.

W-PM-N3

THE ACTIVE SITE LYSINE BACKBONE UNDERGOES CONFORMATIONAL CHANGES IN THE BACTERIORHODOPSIN PHOTOCYCLE

H.Takei¹, Y.Gai², Z.Rothman¹, H.Sigrist³, A.Lewis¹ and M.Sheves²

¹The Hadassah laser center, Department of Ophthalmology, Hadassah, Hebrew

University Hospital, Ein Kerem, Israel. ²Department of Organic chemistry, The

Weizmann Institute of Science Rehovot, Israel. ³Institute of Biochemistry, University of Bern, CH-3012 Berne, Switzerland.

Bacteriorhodopsin (bR) is a 26,000 molecular weight pigment in the purple membrane of *Halobacterium halobium*. Changes in the conformational state of the protein component of bR are important in order to understand the constraints available to the retinal chromophore during the photocycle. The present study focuses on vibrational modes connected with the lysine backbone. These modes are investigated with a combination of difference FTIR and isotopically labelled lysine with 2H and 13C. The results demonstrate that the backbone of lysine undergoes a series of structural alterations that are connected with the photochemistry and the functional deprotonation and reprotonation of the Schiff base. In addition the data demonstrate that the lysine amide I band shifts to a frequency associated with highly solvated backbone carbonyls in the deprotonated state of the retinal chromophore (M).

A likely sequence of events following retinal light absorption is, first, a backbone structural alteration causing strain in the active site lysine backbone without a significant change in hydrogen bonding strength of the C=O and subsequently a breaking of the lysine C=O hydrogen bonding to yield a solvated carbonyl.

W-PM-M8

AROMATIC HYDROCARBONS ARE NOT HYDROPHOBIC. ((G.I. Makhatazde and P.L. Privalov)) Department of Biology, The Johns Hopkins University, Baltimore, MD 21218

The thermodynamics of transfer of aliphatic (ethane, propane, butane) and aromatic compounds (benzene, toluene) between different phases (liquid, gaseous, "compact", aqueous) in the temperature range 5-125°C have been analyzed. It is shown that the enthalpies and entropies of hydration of aliphatic and aromatic compounds are negative at room temperature and decrease in magnitude with the increase of temperature. The enthalpic contribution predominates over the entropic contribution to the Gibbs energy of hydration of aromatic compounds. This results in a negative value of the hydration Gibbs energy of aromatic substances, in opposition to the positive Gibbs energy of hydration of aliphatic compounds, indicating that aromatic hydrocarbons are not hydrophobic. The large enthalpic contribution to the Gibbs energy of hydration of aromatic compounds probably comes from the ability of an aromatic ring to accept a hydrogen from water, forming a hydrogen bond. These results are discussed in terms of the contributions of hydration of aromatic and aliphatic groups to the stability of protein structure.

W-PM-N2

STRUCTURE AND DYNAMICS OF BACTERIORHODOPSIN ((G. Büldt¹, N.A. Dencher², J. Fitter¹, M.H.J. Koch³, R.E. Lechner² and G. Rapp³)) ¹ Dept. of Physics/Biophysics, Freie Universität Berlin, Arnimallee 14, W-1000 Berlin 33, FRG; ² HMI, Glienicke Str.100, W-1000 Berlin 39; ³ EMBL/DESY, Notkestr. 85, W-2000 Hamburg 52

Conformational changes as well as the role of water molecules and exchangeable hydrogens involved in the transport mechanism of bacteriorhodopsin (BR) were studied. The photocycle states BR568 and M412 were measured after trapping by neutron diffraction. In the BR568 to M412 transition, which is known to be a key step in transmembrane proton pumping, reversible structural changes of the protein were observed. The time-course of the transition from the M412 intermediate to the BR568 ground state was studied at room temperature with a time resolution of 15 ms using synchrotron radiation X-ray diffraction. These results unequivocally prove that the tertiary structure of BR changes during the photocycle and give a further strong indication that structural changes in the protein are necessary for proton pumping. Water molecules and exchangeable hydrogen ions, the elements of the proton pathway in BR, were localized by neutron diffraction in H₂O/D₂O exchange experiments. Quasi-elastic neutron scattering on oriented films of purple membranes was used to classify different kinds of proton motions in the aqueous channel through BR relative to proton motions parallel to the membrane surface. Spectra were obtained under dark conditions with momentum transfer vector Q from 0.1 to 1.8 Å⁻¹ in the time range from 10⁻¹² to 10⁻⁸ s. Measurements on purple membranes in H₂O and D₂O enabled us to separate motions of protons covalently bound to BR and to the lipids from those of the solvent.

W-PM-N4

FOURIER TRANSFORM INFRARED EVIDENCE FOR TRANSIENT CHANGES IN ANION BINDING TO HALORHODOPSIN ARGININE(S) DURING THE hR→hL PHOTOREACTION.

((T. J. Walter and M. S. Braiman)) Department of Biochemistry, University of Virginia Health Sciences Center, Charlottesville, VA 22908.

Static and time-resolved Fourier transform infrared (FTIR) difference spectroscopy have been used to investigate the mechanism of halorhodopsin (hR), the light-driven chloride pump of *H. halobium*. With the static approach, the hL photointermediate is kinetically trapped at 250 K; with the time-resolved approach, hL is transiently produced by a laser flash and analyzed in spectra acquired between 0.2 and 5 ms after the flash. In both types of hR→hL difference spectra, we assign a portion of a difference band near 1690 cm⁻¹ to arginine. This assignment is supported by a large (~80 cm⁻¹) deuterium-induced downshift of the band, which is observed also in spectra of the model compound phenylguanidinium chloride. Furthermore, in both hR and in phenylguanidinium salts, we observe the following counterion dependence for the ~1690 cm⁻¹ guanidino stretch frequencies: $\nu(\text{Cl}^-) > \nu(\text{Br}^-) > \nu(\text{I}^-)$. This ordering, also observed in the ~1630 cm⁻¹ C=NH⁺ stretch of the Schiff base in the hR state, reflects a decrease in the NH-X hydrogen bond strength as the size of the anion X increases. Our FTIR data are thus in agreement with earlier proposals that arginine residues, as well as the chromophore Schiff base, serve as transient anion binding sites during the hR photocycle.

W-PM-N5

RECEPTOR/TRANSDUCER INTERACTION IN A PHOTOSENSORY SYSTEM. (John L. Spudich and Elena N. Spudich) Department of Microbiology and Molecular Genetics, University of Texas Medical School, Houston, TX 77030.

Sensory rhodopsin I (SR-I) is a 7-transmembrane helix receptor which mediates phototaxis in the archaeobacterium *Halobacterium halobium*. Biochemical studies of mutants defective in signaling have demonstrated a second intrinsic membrane protein transduces SR-I signals to a cytoplasmic signaling pathway. This transducer, designated HtrI, consists of two transmembrane helices near its N-terminal followed by an extensive hydrophilic cytoplasmic domain, which contains a region homologous to the signaling and methylation domains of eubacterial chemotaxis transducers (Yao, V.J. and Spudich, J.L. (1992) Proc. Natl. Acad. Sci. USA *in press*). Physical proximity of HtrI to the chromophore (retinal) binding site of SR-I has been suggested by chromophore chemical linkage measurements. Here we report results from expression of the SR-I gene (*sopl*) in *H. halobium* in the presence and absence of HtrI, which indicate HtrI modulates photochemical reactions of SR-I. Expression of a synthetic *sopl* gene in an *htrI*⁻ *sopl*⁺ strain of *H. halobium* (obtained by targeted deletion of *sopl*) results in complete restoration of phototaxis responses (M.P. Krebs, E.N. Spudich, H.G. Khorana, and J.L. Spudich, *in preparation*). In membranes isolated from these transformants, SR-I photochemistry is normal; i.e., photoexcited SR-I produces in <1 msec a blue-shifted species (S₃₇₃) which decays thermally to the pre-stimulus state with a $t_{1/2}$ = 800 msec. We have used the same expression plasmid to produce SR-I in an *htrI*⁻ *sopl*⁺ deletion strain, Pho81. In the absence of HtrI SR-I photochemistry is altered in a manner indicative of tight coupling between reactions occurring at the SR-I/HtrI interaction site and the proton transfer reactions occurring in the SR-I photoactive site. This coupling may provide a mechanism of signal relay between the photoreceptor and its transducer.

W-PM-N7

ASPARTIC ACID MUTATIONS IN BACTERIORHODOPSIN ALTER TRYPTOPHAN ENVIRONMENT. ((R. Rangel and R. Renthal)), U. of Texas at San Antonio, San Antonio, TX 78249

Two aspartic acid groups involved in the proton release step of the bacteriorhodopsin proton pump cycle, D85 and D212, are located near the protonated Schiff base of all-trans retinal. We have examined the ultraviolet absorbance spectra of bR in which D85 or D212 have been selectively neutralized by site-directed mutagenesis. UV difference spectra were produced by computer subtraction of wild type bR spectra from that of the mutants. Replacement of either D85 by Asn (D85N) or D212 by Asn (D212N) showed UV difference spectra at pH 8 resembling solvent perturbation of tryptophan. In the mutants, one or more tryptophan groups appeared to be in a less polar environment than in the wild type. This result is expected, since both D85 and D212 are known to be ionized at pH 8, and conversion to the neutral amide would make the interior of bR less polar. Surprisingly, the difference spectrum is nearly abolished by titration to pH 5. The pH-dependence is entirely a property of the mutants: pH 8 minus pH 5 difference spectra of both mutants show the tryptophan perturbation, whereas the wild type pH 8 minus pH 5 spectrum is featureless. It seems unlikely that the pH dependence is due to titration of either D85 or D212, since both groups are believed to have much lower pKs. (We thank J.K. Lanyi and R. Needleman for mutant bR. Supported by GM 08194 and GM 25483)

W-PM-N6

BACTERIORHODOPSIN D85N EXISTS AS THREE SPECTROSCOPIC SPECIES IN EQUILIBRIUM.

((George J. Turner, Larry J. W. Mierck, Thorger E. Thorgeirson*, David S. Kliger*, Mary C. Betlach, and Robert M. Stroud)) Department of Biochemistry & Biophysics, University of California, San Francisco, CA 94143 and *Department of Chemistry & Biochemistry University of California, Santa Cruz, CA 95064.

Ground state absorbance measurements show that BR from *H. halobium* containing asparagine at residue 85 (D85N) exists as three distinct chromophoric states in equilibrium. In the pH range 6 to 12 the absorbance spectrum of the three states are demonstrated to be similar to flash-induced spectral intermediates which comprise the latter portion of the wild-type BR photocycle. One of the states absorbs maximally at 405 nanometers, has a deprotonated Schiff base, and contains predominantly the 13-cis form of retinal, identifying it as a close homolog of the M intermediate in the BR photocycle. The other species possess absorbance maxima with correspondence to those of the wild-type N (570 nm) and O (615 nm) photo-intermediates. The retinal composition of the O-like form was found to be dominated by all-trans isomer. The pH dependence of the concentrations of the equilibrium species corresponds closely with the pH dependence of the M, N, and O photo-intermediates. These data support kinetic models which emphasize the role of back-reactions during the photocycle of bacteriorhodopsin. Energetic and spectral characterization of the D85N ground state equilibrium supports its use as a model for elucidating molecular transitions comprising the latter portion of the BR photocycle.

ADVANCES IN BIOLOGICAL FLUORESCENCE

W-PM-WS1-1

USE OF EXCIMERIC FLUORESCENCE TO STUDY LATERAL ORGANIZATION OF LIPIDS IN MEMBRANES

((Parkson Lee-Gau Chong*, Daxin Tang* and Istvan P. Sugar))

*Dept. of Biochemistry, Meharry Medical College, Nashville, TN 37208 and Dept. of Biomath. Sci., Mount Sinai Medical Center, New York, NY 10029.

Pyrene excimeric fluorescence has been used to study lipid lateral distribution in two-component membrane systems. We have observed a series of dips in the plot of E/M (the ratio of excimer fluorescence to monomer fluorescence) vs. the mole fraction of (1-palmitoyl-2-(10-pyrenyl)decanoyl-sn-glycerol-3-phosphatidylcholine (Pyr-PC) in Pyr-PC/dimyristoylphosphatidylcholine (DMPC) binary mixtures. The results can be interpreted in terms of lipid regular distribution into hexagonal super-lattices at critical concentrations. We have also examined the effects of pressure on E/M dips. The pressure data suggest that lipid regular distribution can be maintained at critical concentrations as long as the membrane is in the liquid crystalline state. In addition, we have observed a marked difference in the pressure dependence of E/M between the membranes at dip concentrations and those at nondip concentrations. The pressure data support the idea that E/M dips are related to lipid regular distribution. Monte Carlo simulations and pressure data yield information about lipid packing and lipid lateral distribution at nondip concentrations, which will also be discussed (supported by ARO and NSF-MRCE).

W-PM-WS1-2

THE USE OF FLUORESCENCE DIGITAL IMAGING MICROSCOPY TO VISUALIZE LIPID AND PROTEIN DOMAINS IN MEMBRANES. ((M. GLASER, W. RODGERS, P. LUAN, L. YANG AND F. WANG)) Department of Biochemistry, University of Illinois, Urbana, IL 61801

Methods have been developed to study the lateral organization of lipids and proteins in membranes using fluorescence digital imaging microscopy. In the red blood cell membrane the distribution of phospholipids was heterogeneous with different phospholipids enriched in specific domains. Since domains were not observed in vesicles made from lipids extracted from red blood cell membranes, it appears that the membrane proteins were responsible for creating the lipid domains. Evidence suggests that Band 3 and the spectrin cytoskeleton may play a role in the formation of the lipid domains. The G and M proteins of vesicular stomatitis virus cause the sequestering of phospholipids into domains when these proteins are added to phospholipid vesicles and this resembles the process of domain formation that occurs when the virus buds from the plasma membrane of infected cells. The existence of lipid domains and changes in the domain structure of a membrane may provide a sensitive mechanism to regulate membrane-bound enzymes as illustrated by the effect of domains on the activity of protein kinase C and NADH dehydrogenase.

W-PM-WS1-3

FLUORESCENCE LINE NARROWING (FLN) SPECTROSCOPY TO MONITOR PROTEIN CONFORMATION. ((J. M. Vanderkooi)) Johnson Research Foundation, Dept. of Biochem. & Biophys., School of Medicine, Univ. Pennsylvania, Philadelphia PA 19104

Optical spectra of chromophores in proteins at normal measuring conditions consist of broad bands without vibrational resolution. Since proteins are dynamical structures the broadness may arise because individual chromophores experience a variety of electric fields due to fluctuations of the polypeptide. If so, resolved spectra should be obtained under "energy selection" conditions, i.e., a narrow band laser is used to excite a subpopulation of the sample, which is held at low temperature to ensure that the molecule is at its lowest vibrational level and to prevent conversions between substates. Using energy selection, resolved fluorescence spectra are obtained for metal-free or metal-substituted heme proteins at temperatures < 40 K. The inhomogeneous distribution of the sample, a reflection of the disorder within the heme pocket, is determined by changing laser energy. When the inhomogeneous distribution width exceeds the energy differences of the vibrational levels of the excited state, then the emission spectrum shows a multiplicity of lines which are separated by the energy difference in vibrations of the excited state molecule. FLN spectra therefore reveal the vibrational spectra of both ground and excited state molecules, from which structural and dynamical information can be obtained. Finally, spectral resolution is a function of vibrational and electronic relaxation rates and it is suggested that spectra of some native heme proteins which are usually attributed to resonance Raman may instead be due to FLN. (Supported by NSF)

W-PM-WS1-4

DYNAMIC FLUORESCENCE MEASUREMENTS AND RESONANCE ENERGY TRANSFER: PROTEINS AND CARBOHYDRATES. ((L.Brand and P. Wu)) Department of Biology, The Johns Hopkins University, Baltimore, MD 21218 .

Resonance energy transfer as measured by steady-state and/or dynamic fluorescence techniques has now become a mature approach for investigating spatial relations in biological molecules. Together with our colleague Professor Y.C. Lee and his coworkers K. Rice and M. Quesenberry we have made dynamic fluorescence measurements of energy transfer between two dyes linked at the different ends of a triantennary glycopeptide. These studies indicate that dynamic fluorescence measurements yield narrow distributions of distances in biomolecules when these in fact exist. In contrast rather wide distributions of distances between sites on proteins are usually observed. Our colleague Professor D. Shortle and his coworker W. Stites provided us with a mutant form of s. nuclease containing a single sulfhydryl residue (K78C). Together with our coworker, L. James we conjugated the -SH group with a fluorescent probe, IAEDANS and also with DTNB, a non-fluorescent -SH specific chromophore. Energy transfer between Trp-140 and the acceptor on position 78 was measured to obtain an apparent distance and distance distribution between the two sites. The contributions of the linker arm, orientation and real distance distribution to the results will be discussed.(supported by NIH grant No. GM11632).

EXPLORING STRUCTURE AND FUNCTION RELATIONSHIPS IN THE MYOSIN SUPERFAMILY**W-PM-WS2-1**

EXPLORING STRUCTURE AND FUNCTION RELATIONSHIPS IN THE MYOSIN SUPERFAMILY

Organizers: J. R. Sellers, J. A. Hammer, III

MOLECULAR EVOLUTION OF THE MYOSIN FAMILY: RELATIONSHIPS DERIVED FROM COMPARISONS OF THE AMINO ACID SEQUENCES

Holly V. Goodson, Stanford University

MOLECULAR GENETICS OF UNCONVENTIONAL MYOSINS IN Dictyostelium

Margaret A. Titus, Duke University

MOLECULAR CHARACTERIZATION AND In Vivo STUDIES ON THE Drosophila 95F

Kathy G. Miller

PROPERTIES OF MYOSIN V FROM CHICKEN BRAIN

Richard E. Cheney, Yale University

BIOCHEMICAL, IMMUNOLOGICAL AND MOLECULAR GENETIC CHARACTERIZATION OF VERTEBRATE MYOSIN I

Joseph P. Albanesi, University of Texas Southwestern Medical Center

IDENTIFICATION OF A NOVEL NEURONAL MYOSIN I

Elliot H. Sherr, Columbia University College of Physicians and Surgeons

SINGLE-STRANDED NUCLEIC ACID-BINDING PROTEINS**W-PM-WS3-1**

DOMAINS AND PATTERNS IN T4 GENE 32 PROTEIN: FIRST PRINCIPLES AND LAST MOTIFS (R.L. Karpel, J.R. Casas-Finet and K.R. Fischer) Dept. of Chemistry and Biochemistry, UMBC, Baltimore, MD 21228.

Bacteriophage T4 gene 32 protein is a single-strand specific nucleic acid binding protein that has a well-established role in DNA replication, recombination and repair. It is an excellent model system for structure-function studies. The full-length protein binds single-stranded nucleic acids cooperatively, and this activity is dependent on homotypic protein-protein interactions involving the N-terminal domain of the protein with the central (core) domain of an adjacent nucleic acid-bound protein. We have used synthetic peptides containing portions of the N-terminal domain to establish the essential interactive residues of this region. Peptides corresponding to residues 1-17 and 1-9 bound intact protein, and easily formed a 1:1 complex with core domain. Utilizing a combination of specific enzymatic cleavages and peptide synthesis, we have established the essential interactive sequence to be res. 3-7, Lys-Arg-Lys-Ser-Thr. There is a very similar sequence within the central portion of the protein, res. 110-114, Lys-Arg-Lys-Thr-Ser, which is encoded by virtually the same nucleotide sequence. We call this sequence the *LAST* ((Lys/Arg)₃(Ser/Thr)₂) motif, and, based on these and previous data, have developed a new and testable model for 32 protein binding cooperativity. In accord with a prediction of the model, the presence of interacting peptide reduces the magnitude of binding cooperativity in the interaction with polynucleotide, induces a salt-dependence in protein-oligonucleotide interaction, and increases the susceptibility of residues within the core domain to proteolysis. Removal of the first 4 residues of protein with Arg-C endoprotease apparently eliminates binding cooperativity, but the pattern of further proteolysis is curiously different from that of the core domain generated by trypsin. Peptides with *LAST* sequences are capable of binding nucleic acid. These results are discussed within the context of our model, and the large amount of information available for this interesting system.

W-PM-WS3-2

CHARACTERIZATION OF SINGLE AMINO ACID SUBSTITUTION MUTANTS OF THE N-TERMINAL COOPERATIVITY DOMAIN OF T4 GENE 32 PROTEIN. ((David P. Giedroc and Jana L. Villemain)) Dept. of Biochemistry and Biophysics, Texas A&M University, College Station TX 77843-2128.

Gene 32 protein (g32P) from bacteriophage T4 is a DNA replication accessory protein which binds highly cooperatively to single-stranded (ss) nucleic acids. The current model for the binding of g32P to ssDNA holds that the domains important for cooperativity and ssDNA binding are functionally and physically separate. To further test this model and identify amino acid side chains important for cooperativity, we describe a cassette mutagenesis scheme which allows us to deposit single-amino acid changes in the N-terminal "B" domain (residues 2-8) in a way that readily permits the determination of biological efficacy and physicochemical properties of mutant proteins. Thus far we have focussed on Arg⁴ and have purified and characterized four mutant proteins, R4K, R4Q, R4T, and R4G g32Ps. On model polynucleotides, the hierarchy of binding affinities is wild-type = R4K >> R4Q > R4T > R4G >> g32P-B. The K, Q and T mutants all bind with high cooperativity and exhibit overall binding affinities which appear incompatible with a simple reduction in the magnitude of the cooperativity parameter in any case. The [NaCl]- and temperature-dependence of the binding by the mutant proteins to poly(A) is consistent with the proposal that the roles played by each domain of this multidomain protein are much more interdependent than anticipated. Further, the positive charge at amino acid four seems to be important for g32P to assume an active conformation as R4K g32P displays nearly wild-type binding affinity. This research was supported by NIH Grant GM42569 and American Cancer Society JFRA-270.

W-PM-WS3-3

TRANSLATIONAL REPRESSION BY THE BACTERIOPHAGE T4 GENE 32 PROTEIN INVOLVES THE SPECIFIC RECOGNITION OF AN RNA PSEUDOKNOT. (Y. SHAMOO, A. TAM, W. KONIGSBERG AND K. WILLIAMS) Yale Univ. School of Medicine, New Haven, CT 06510.

An RNA pseudoknot has been shown to form at the 5'-end of bacteriophage T4 gene 32 mRNA that is essential to autoregulation of gene 32 mRNA by gene product 32 (gp32), a single-stranded nucleic acid binding protein. Structure-mapping of the RNA with RNases indicate that two stem regions consisting of nucleotides -67 to -64 base-paired to -52 to -55 (Stem-1) and nucleotides -62 to -56 base-paired to -40 to -46 (Stem-2) can fold into a "pseudoknotted" structure that may be analogous to a semi-continuous A-helical pseudoknot. Our results suggest that the g32 mRNA pseudoknot can form under conditions where specific autoregulation by gp32 is observed. Gel mobility studies carried out with oligonucleotides indicate that gp32 does, bind tightly to the pseudoknot and is in agreement with the proposal of McPheeters *et al.* (*J. Molec. Biol.* 201, 517-535), that the pseudoknot is a nucleation site for gp32 translational regulation. Disruption of tertiary structure interactions in this pseudoknot (with EDTA) significantly reduces the ability of gp32 to specifically recognize its own mRNA, *in vitro* mutagenesis studies suggest the sequence of Stem-2 is also important determinant.

W-PM-WS3-5

THE PHOTOEXCITED TRIPLET STATE IS A SENSITIVE PROBE OF TRYPTOPHAN STACKING INTERACTIONS IN *E. coli* SSB-NUCLEIC ACID COMPLEXES. ((A.H. Maki)) Department of Chemistry, Univ. of California, Davis, CA 95616.

The properties of the photoexcited triplet state of tryptophan have been measured in *E. coli* SSB/single stranded DNA and RNA complexes using optical detection of triplet state magnetic resonance (ODMR) spectroscopy. The substrates poly(5-HgU) and poly(5-BrdU) induce external heavy atom effects (HAE) on stacked trp residues that may be evaluated by ODMR. For poly(5-HgU), when Hg is blocked with a sulfhydryl reagent, a HAE can only result via stacking for steric reasons. The study of W → F mutated SSBs reveals that trp40 and trp54 undergo stacking interactions with heavy atom-derivatized nucleic acids, while trp88 and trp135 do not. SSB binds with particularly high affinity to poly(dT) which produces striking effects on the triplet state of trp54, and to a lesser extent, trp40. Stacking interactions reduce the lifetime of the T_x sublevel of trp54 and trp40 by a factor of 4 and 2, respectively, while a large specific enhancement of intersystem crossing to T₁ of trp54 leads to polarity reversal of the ODMR signals. These effects, along with a large (10%) reduction in the zero-field splitting (zfs) D-parameter of trp54 are consistent with particularly strong interactions between this indole residue and the nucleobases. W → F substitution at position 54 also produces the largest destabilizing effect on the SSB-poly(dT) complex of any such mutation. A linear correlation of zfs reduction with the contribution of aromatic stacking interactions to the binding free energy of protein-nucleic acid complexes is suggested by recent ODMR measurements of bis-intercalating peptide drug-DNA complexes. This result implies that zfs shifts may be used to quantitatively determine trp stacking energies.

W-PM-WS3-7

STUDIES ON THE SOLUTION STRUCTURE OF A UPI/RNA COMPLEX
Marius G. Clore, National Institutes of Health

W-PM-WS3-4

THERMODYNAMICS OF *E. COLI* SSB/SINGLE-STRANDED DNA INTERACTIONS

Timothy H. Lohman, Washington University School of Medicine

W-PM-WS3-6

NMR STUDIES OF RIBO- AND DEOXYRIBONUCLEIC ACID COMPLEXES WITH THE HIV-1 NUCLEOCAPSID PROTEIN. ((Michael F. Summers, Paul R. Blake, Brian Lee, Terri L. South)) Department of Chemistry and Biochemistry, University of Maryland Baltimore County, Baltimore, MD 21228. (Spon. by NIH)

The nucleic acid interactive properties of a synthetic peptide with sequence of the N-terminal CCHC zinc finger (CCHC = Cys-X₂-Cys-X₄-His-X₄-Cys; X = variable amino acid) of the HIV-1 nucleocapsid protein, Zn(HIV1-F1), have been studied by ¹H NMR spectroscopy. Titration of Zn(HIV1-F1) with oligodeoxyribonucleic acids containing different nucleotide sequences reveal, for the first time, sequence-dependent binding that requires the presence of at least one guanosine residue for tight complex formation. An oligodeoxyribonucleotide with sequence corresponding to a portion of the HIV-1 psi-packaging signal, d(ACGCC), forms a tight complex with Zn(HIV1-F1) (K_{dissoc} = 5 x 10⁻⁶ M), and NMR measurements reveal that the bound nucleic acid exists in a single-stranded, A-helical conformation. The nucleic acid binds within a hydrophobic cleft defined by residues Val¹, Phe⁴, Ile¹² and Ala¹³. Backbone amide protons of Phe⁴ and Ala¹³ and the backbone carbonyl oxygen of Lys² that lie within this cleft appear to form hydrogen bonds with the guanosine O6 and N1H atoms, respectively, and the positively charged side chain of Arg¹⁴ interacts electrostatically with the phosphodiester backbone. The structural findings provide a rationalization for the general conservation of these hydrophobic and basic residues in CCHC zinc fingers, and are consistent with site-directed mutagenesis results that implicate these residues as direct participants in viral genome recognition.

W-PM-WS3-8

STRUCTURAL BASIS FOR GENE V PROTEIN COOPERATIVITY. ((T. C. Terwilliger and P. N. Goudreau)) Los Alamos National Laboratory, MS M880, Los Alamos, NM 87544 and Univ. of Chicago, Chicago, IL 60637.

Gene V protein binds to ss-DNA and RNA in a highly cooperative manner thought to involve specific protein-protein contacts. We have studied the cooperativity of the WT gene V protein, of single-amino-acid-substitution mutants of the protein that show altered binding affinity, and of an intragenic suppressor mutant that restores binding affinity to a defective protein. Likely contacts between gene V protein dimers are identified using the results of these experiments and the 3-dimensional structure of the gene V protein determined recently in our laboratory using x-ray multiwavelength anomalous diffraction techniques.

W-Pos1

RAPID DISSOCIATION AND REASSOCIATION OF FORCE GENERATING CROSS-BRIDGES. EFFECTS OF TEMPERATURE AND INORGANIC PHOSPHATE. ((B. Brenner)) University of Ulm, D-7900 Ulm, FRG

Previously we demonstrated that apparent fiber stiffness of Ca^{++} -activated fibers is sensitive to the speed of applied stretch or release. Our data suggested that (a) even during force generation cross-bridges can detach and reattach from and to actin rapidly compared to active cross-bridge turnover, and (b) at our low experimental temperature (5°C), force-generating cross-bridges mainly occupy the first of a series of force-generating states among which cross-bridges are assumed to redistribute during and after length changes (Huxley & Simmons, Nature, 1971).

We studied the response of contracting fibers to stretch and release at higher temperature (T) to see whether (a) rapid detachment/reattachment is still present, and (b) the increase in force with T can be accounted for by a change in distribution among different force-generating states, favoring the second (or subsequent) states which are characterized by higher force per cross-bridge. We find that stiffness-speed relations are only very little affected by T, and plots of force vs. length change imply that redistribution among force-generating states is not a major factor for the increase in force with T. Instead it appears that average strain sustained by cross-bridges in the first of the force-generating states increases with T and kinetics of rapid detachment/reattachment are little affected.

Effects of inorganic phosphate (P_i) was also studied. Both enzymatic reduction and increase of $[P_i]$ up to 5mM do not affect the stiffness-speed relation, except a proportional reduction of stiffness at all speeds when $[P_i]$ was raised. Since reduction of $[P_i]$ inhibits the transition of force-generating cross-bridges back toward the weak-binding states via rebinding of P_i , these observations suggest that rapid detachment/reattachment of force-generating cross-bridges does not involve rapid transfer of cross-bridges back to the weak-binding states but apparently occurs without a change in the state of nucleotide or products.

W-Pos3

THE HIGH-FORCE CURVATURE OF THE FORCE-VELOCITY RELATION STUDIED IN ISOLATED MUSCLE FIBERS OF THE FROG. ((K.A.P. Edman and C. Caputo)) Dept. of Pharmacology, Univ. of Lund, Lund, Sweden.

The force-velocity relation of frog muscle fibers exhibits two distinct curvatures located on either side of a breakpoint near 80% of the isometric force (P_0) where the shortening velocity (V) is approximately 1/10 of V_{max} (Edman, J. Physiol. 1988, 404: 301-321). We here report that the biphasic shape of the force-velocity relation is maintained also after depressing P_0 to 80% of the control value by dantrolene. This finding suggests that the breakpoint of the force-velocity curve is not related to the force level *per se* but rather to the speed of shortening of the contractile system. Thus as the speed of shortening is reduced below 1/10 of V_{max} , the myofibrillar system produces less force and shortens at a lower speed than expected from measurements at low and intermediate loads.

Instantaneous stiffness was recorded as the fiber shortened at different speeds during tetanus by applying a 4 kHz sinusoidal length oscillation (1.5 nm/half sarcomere) to one end of the fiber. The force-stiffness relation is biphasic like the force-velocity curve. At loads exceeding 0.8 P_0 stiffness increases more steeply with force than at lower loads. The results suggest that as the speed of filament sliding is reduced below a critical level, 1/10 of V_{max} , a larger proportion of the myosin crossbridges accumulate in a state where less force is produced.

W-Pos5

THE EFFECT OF ATP ANALOGUES (NTP) ON THIN FILAMENT MOVEMENT IN MOTILITY ASSAYS AND ON THE PHOSPHATE TRANSIENT IN RABBIT GLYCERINATED MUSCLE FIBERS. ((E. Homsher, M. Regnier and S. Tejeda)) Physiol. Dept., Med. School, UCLA, Los Angeles, CA, 90024.

The effects of replacement of ATP by NTP on the sliding velocity (V_s) of rhodamine labeled f-actin filaments in motility assays using HMM were examined to learn to what extent V_s correlated with the unloaded shortening velocity V_{max} in single glycerinated rabbit muscle fibers. The substrates ATP, ITP, GTP, UTP, 2'deoxyATP (dATP) and 2'deoxyUTP (dUTP) altered V_s (with respect to V_s in ATP) in the same direction as V_{max} changed in single muscle fibers. The magnitude of the V_s change differed from that seen for V_{max} : e.g., in 1 mM dUTP V_s was <10% of that in ATP while V_{max} at 5mM dUTP was 65% of that for ATP. This behavior may stem from the NTP concentration differences in the two measurements and the fact that motility assays were performed at 25°C and those for V_{max} at 10°C. Thus V_s in the motility assay parallels changes in V_{max} in the fiber. In other experiments, $[P_i]$ was increased by flash photolysis of caged Pi in isometrically contracting single muscle fibers. The subsequent rate of decline in force is governed by the rate constants for the force generating and Pi release steps of the crossbridge cycle. While preliminary data suggest the rate of this transition is somewhat greater in dATP than ATP, the magnitude of this change is unlikely to account for the increased V_{max} when dATP replaces ATP. (Supported by NIH Grant 30988).

W-Pos2

STIFFNESS-SPEED-RELATIONS FOR ISOMETRIC AND ISOTONIC CONTRACTION. SIGNIFICANCE FOR OCCUPANCY OF STRONG-BINDING STATES DURING HIGH-SPEED SHORTENING. ((R. Stehle, T. Kraft, B. Brenner)) Univ. of Ulm, Germany

Fiber stiffness during isotonic contraction is known to be much lower than under isometric conditions (Julian & Sollins, J. Gen Physiol., 1975; Ford et al., J. Physiol., 1985; Brenner, Biophys. J. 1983). It was usually assumed that for both isometric and isotonic conditions the observed fiber stiffness reflects the fraction of cross-bridges attached to actin in the strong-binding states. We previously demonstrated that fiber stiffness observed during isometric contraction depends on the speed of stretch imposed for the stiffness measurements. If the difference between isometric and isotonic stiffness is due to a decreased fraction of cross-bridges attached in the strong-binding states the isotonic stiffness-speed relation should superimpose with the isometric stiffness-speed relation if properly scaled up. We find, however, that compared to isometric conditions the isotonic stiffness-speed relation is shifted to 20-100 times larger speeds of stretch. This suggests that during high-speed shortening cross-bridges have faster dissociation/reassociation kinetics than under isometric conditions. Thus, comparison of fiber stiffness for isometric and isotonic conditions at only one speed of stretch (or release) does not allow to estimate the relative fraction of cross-bridges in the force-generating states. From position and amplitude of the isotonic stiffness-speed relation, during isotonic shortening at very low load the majority of cross-bridges appear to occupy states with similar actin-binding kinetics as observed in the presence of ATPyS at high $[Ca^{*}]$ (pCa about 4.5); i.e., during unloaded shortening the majority of cross-bridges may occupy weak-binding-type cross-bridge states, or else strong-binding states with much faster dissociation/reassociation kinetics than seen under isometric conditions. Much lower occupancy of force-generating states than previously derived from the stiffness data could provide an explanation for the otherwise unexpectedly low fiber ATPase during high-speed shortening.

W-Pos4

MAXIMUM VELOCITY OF SHORTENING IN RELATION TO MYOSIN HEAVY AND LIGHT CHAIN COMPOSITIONS IN SINGLE FIBERS FROM HUMAN SKELETAL MUSCLES. ((L. Larsson* and R.L. Moss)) Dept of Physiology, Univ of Wisconsin, Madison 53706. *Dept of Clinical Neurophysiology Karolinska Hospital, S-104 01, Stockholm, Sweden.

Maximum velocity of shortening (V_{max}) was measured in skinned single fibers from biopsy samples of vastus lateralis and soleus muscles of human volunteers. The samples were membrane permeabilized in glycerol (CS) or by freeze drying (FD). V_{max} was determined at 15°C using the slack test. Since no differences in V_{max} data from CS or FD fibers were observed, the summary data were pooled. Myosin heavy chain (MHC) compositions were determined by SDS-PAGE and were classified as types I, IIA or IIB. V_{max} varied significantly with MHC type: type I, 0.4 ± 0.3 ML/s (n = 51); type IIA, 1.0 ± 0.4 ML/s (n = 22); type IIB, 3.6 ± 1.4 ML/s (n = 8). Fibers co-expressing types IIA and IIB myosins had V_{max} values intermediate between purely IIA and purely IIB fibers: 1.6 ± 1.3 ML/s (n = 21). Two fibers co-expressing types I and IIA myosins had V_{max} values of 0.3 and 1.0 ML/s. The large variation in V_{max} in fibers co-expressing myosin heavy chains was only partly explained by the variation in MHC. There was also a wide range of V_{max} values in fibers expressing purely I, IIA or IIB MHC. Determination of myosin light chain (MLC) composition of these same fibers by SDS-PAGE suggests that altered expression of MLC may also modulate V_{max} and could account for some of the variation. (Supported by NIH AR31806).

W-Pos6

THE EFFECT OF ATP ANALOGUES (NTP) ON ISOMETRIC FORCE AND UNLOADED SHORTENING VELOCITY (V_{max}) IN RABBIT GLYCERINATED MUSCLE FIBERS. ((M. Regnier, P. Bostani and E. Homsher)) Physiol. Dept., Med. School, UCLA, Los Angeles, CA, 90024.

The effects of replacement of ATP by ATP analogues on isometric force and V_{max} were examined to identify substrates with which to probe specific steps of the crossbridge cycle (cleavage, force generating isomerization, Pi release, NDP release, and actomyosin dissociation). In glycerinated single fibers at 10°C and 6 mM MgNTP, 2'deoxy ATP (dATP), CTP, 2'deoxy UTP (dUTP), UTP, ITP, and GTP produced isometric forces of 100, 92, 49, 37, 18, and 10% of that produced by ATP respectively. In slack tests the V_{max} for the same series of NTP's was 144, 65, 43, 20, 7, and 4% of that observed using ATP. While the apparent Km for NTP binding for V_{max} for ATP was 125 μ M, that for dATP was 790 μ M and that for dUTP was 7.9 mM. Thus V_{max} at saturating concentrations of MgNTP for ATP, dATP, and dUTP were 100, 144, and 64% of that for ATP respectively. The elevated V_{max} produced by dATP suggests that it accelerates the rate limiting step for V_{max} (either the NDP release step or the A.M.NTP \rightarrow A + M.NTP step). The reduction in V_{max} by dUTP suggests it reduces the rate of the rate limiting step. The potentiation of V_{max} by deoxy forms of NTP suggest that these forms accelerate the rate limiting step. Reduced isometric force associated with UTP, GTP, and ITP probably stems from a reduced rate of NTP cleavage. (Supported by NIH Grant 30988).

W-Pos7

SYNTHESES OF NONNUCLEOTIDE NANTP- AND PRNANTP-LIKE ATP ANALOGS AND STUDIES OF THEIR CHEMOMECHANICAL EFFECT ON MUSCLE FIBERS ((Dong Donald Wang*, Ed Pate*, Roger Cooke*, and Ralph Yount*) Depts. of Biochem/Biophys. and Mathematics*, WA. ST. U., Pullman, WA 99164, and Dept. of Biochem/Biophys., UCSF, San Francisco, CA 94143

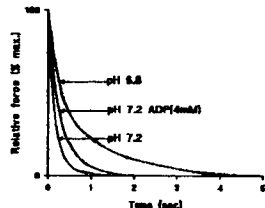
To probe the substrate requirements for actomyosin chemomechanical interaction we have investigated the effects of a series of new non-nucleotide ATP analogs on actomyosin-catalyzed hydrolysis rates and on fiber mechanics. These analogs have substitutions of new functional groups at the 2- and 4- positions of the ATP analog. NANTP, N-[(4- azido-2-nitrophenyl) amino] ethyl triphosphate, and PrNANTP (identical to NANTP except a propyl group replaces ethyl). Previous work (E. Pate et al., *Biophys. J.* 59, 598(1991)) has shown NANTP but not PrNANTP will support active tension and shortening in skinned muscle fibers in a manner almost identical to ATP. Here all 2- and 4- substituted analogs had myosin S1 NTPase hydrolysis rates higher than ATP and the rates were stimulated by addition of actin. In general, the replacement of the 4-azido group of NANTP with -H, -NO₂ or -NH₂ had small effects on fiber mechanics while replacement of the 2-NO₂ group with -H or -NH₂ dramatically lowered the ability of the new analogs to support active tension and shortening. All PrNANTP-based analogs were ineffective in supporting active tension. For all analogs there was a strong correlation between the maximal velocity of shortening (V_{max}) and tension development (P₀) but no obvious correlation with the rate of NTP cleavage. Supported by MDA and NIH; DK05195(R.Y.), AR39643(E.P.) & HL32145(R.C.)

W-Pos9

ACIDOSIS AND ADP SLOW MYOCARDIAL RELAXATION PRODUCED BY PHOTOLYSIS OF DIAZO-2; A CAGED CALCIUM-CHELATOR. ((S.J.Simnett, I.P.Mulligan*, R.E.Palmer and C.C.Ashley)) Univ. Lab. of Physiology, Parks Road, Oxford and *Dept. of Cardiology, John Radcliffe Hospital, Oxford, UK.

During cardiac ischaemia the H⁺ and ADP concentrations within the myocardium rise and relaxation of the heart is slowed. We have investigated the effect of either lowering pH or increasing ADP levels on relaxation, induced by laser-flash photolysis of 2mM diazo-2, in skinned (Triton X100) guinea-pig trabeculae at 12°C. Diazo-2 is a photolabile Ca²⁺ chelator which upon photolysis rapidly (>2000 s⁻¹) increases its Ca²⁺ affinity (from K_d 2.2 μM to K_d 0.073 μM), enabling us to produce a rapid (<2ms) decrease in Ca²⁺ within the trabeculae.

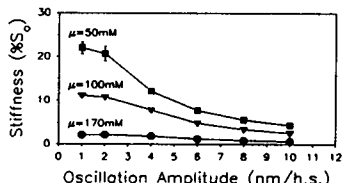
The average tension transients of the relaxations were fitted with two exponentials. At pH 7.2 (n=8) the rate constants of the two phases were 10.70±0.3 s⁻¹ (mean±s.e.m.) and 4.23±0.12 s⁻¹; at pH 6.8 (n=8) the rates were 3.94±0.04 s⁻¹ and 0.64±0.01 s⁻¹. After the addition of 4mM ADP (pH 7.2, n=7) the rates were 6.00±0.16 s⁻¹ and 1.91±0.09 s⁻¹. As the sarcoplasmic reticulum has been rendered inactive by the skinning procedure, we suggest the slowing of the rate of relaxation produced by either acidosis or a rise in ADP levels is probably by a direct effect on crossbridge kinetics.



W-Pos11

RESTING STIFFNESS IN PERMEABILIZED RABBIT PSOAS MUSCLE FIBERS IS SUSCEPTIBLE TO LARGE SINUSOIDAL OSCILLATIONS. ((D.R. Clafflin)) Department of Anesthesia Research Labs., Brigham & Women's Hospital, Boston, MA 02115.

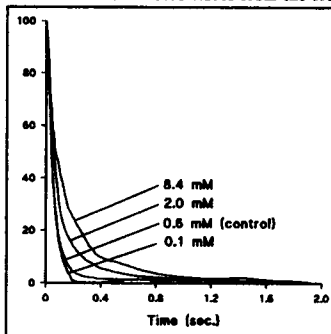
The apparent stiffness of permeabilized skeletal muscle fibers in relaxing solution (pCa=9) increases with decreasing ionic strength. This increase in stiffness has been attributed to the presence of crossbridges attached in the "weak-binding" state. Large, rapid axial movements of the thin filaments relative to the thick filaments would be expected to increase the detachment rate and/or decrease the attachment rate of weak-binding crossbridges. The purpose of the experiments described here was to test this hypothesis. Glycerinated rabbit psoas fibers (length≈2,500 sarcomeres) were attached at one end to a servomotor and at the other end to a force transducer and placed in relaxing solutions with ionic strengths (μ) of 50, 100, and 170mM. Experiments were performed at a sarcomere length of 2.6μm and solution temperature of 5°C. Fiber stiffness was determined by applying sinusoidal length oscillations (2kHz) with peak-peak amplitudes ranging from 1 to 10nm/half-sarcomere (h.s.), and dividing the root-mean-square of the sinusoidal component of the resulting force response by that of the length signal. The resulting stiffness values (mean±SEM, n=3) are reported in the figure below as a percentage of S₀, the maximum stiffness obtained during a fully activated contraction (pCa=4.8, μ=170mM). The results show that the increases in fiber stiffness that appear as ionic strength is decreased can be greatly reduced by large amplitude, high frequency sinusoidal oscillations. These results are consistent with the view that such oscillations shift the equilibrium of weakly-binding crossbridges toward the unbound state.



W-Pos8

PHOSPHATE SLOWS THE RATE OF RELAXATION OF SINGLE SKINNED FROG FIBRES UPON PHOTOLYSIS OF DIAZO-2. ((R.E. Palmer, S.J. Simnett, I.P. Mulligan and C.C. Ashley)) University Laboratory of Physiology, Parks Road, Oxford, OX1 3PT, U.K.

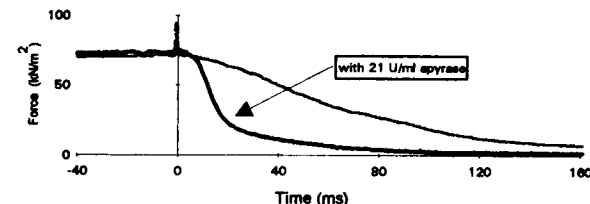
Increased concentrations of inorganic phosphate (P_i) are associated with a decrease in isometric force and a decreased sensitivity to Ca²⁺ of skeletal muscle fibres, presumably due to a reduction in the number of crossbridges in a force-generating state. Photolysis of the caged calcium chelator, diazo-2 within single chemically skinned semitendinosus fibres from the frog, *Rana temporaria*, initiated a rapid relaxation. The figure shows the mean relaxation tension transients from skinned frog fibres upon photolysis of the caged Ca²⁺ chelator diazo-2 (n>12, 12 °C). Photolysis occurred at time zero. Increased concentrations of P_i above the contaminating concentration of 0.6 mM led to a slowing of the rate of relaxation. Decreasing P_i (using sucrose and sucrose phosphorylase) led to an increase in the rate. The P_i concentration was determined using an assay system. Possible mechanisms for this slowing of relaxation are discussed. Support from SERC, BHF, MRC.



W-Pos10

RELAXATION OF RIGOR TENSION BY PHOTOLYSIS OF CAGED-ATP IN PERMEABILISED MUSCLE FIBRES OF THE RABBIT. ((Hilary Thirwell, Frédéric Bancel and Michael A. Ferenczi)) National Institute for Medical Research., Mill Hill, London NW7 1AA, U.K.

The time-course of relaxation following laser-flash photolysis of caged-ATP (Goldman, Hibberd & Trentham, 1984) is shown here to depend on the presence of apyrase (Sleep & Burton, 1990). This enzyme effectively reduces the concentration of ADP and ATP in the rigor muscle, and accelerates the relaxation process, most notably by reducing or accelerating the transient tension rise observed when the initial rigor tension is low (see figure; 20°C). The data suggest that ADP bound to attached cross-bridges slows down the de-activation of thin filaments by allowing the transient re-attachment of rapidly detaching (nucleotide-free) cross-bridges. The presence of inorganic phosphate (10 mM) does not affect the first 70% of the fast apyrase response. The initial delay in relaxation is due in part to the time taken for the appearance of ATP from caged-ATP.

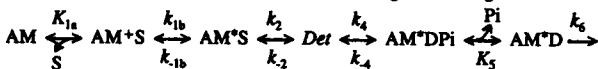


Goldman, Y.E., Hibberd, M.G. & Trentham, D.R. (1984) *J. Physiol.* 354:577-604
Sleep, J. & Burton, K. (1990) *Biophys. J.* 57:542a

W-Pos12

CROSS-BRIDGE SCHEME DEDUCED FROM SINUSOIDAL ANALYSIS IN FERRET MYOCARDIUM. ((M. Kawai*, Y. Zhao* and Y. Saeki*)) *Dept of Anatomy, University of Iowa, Iowa City, IA 52242, and *Dept of Physiology, Tsurumi University, Yokohama, Japan.

Elementary steps of the cross-bridge cycle in chemically skinned ferret papillary muscles were investigated with sinusoidal analysis. The muscle preparations were activated at pCa 4.8, and the effects of MgATP (S) and phosphate (Pi) concentrations on exponential processes B, C, and D were studied. Results are consistent with the following cross-bridge scheme:

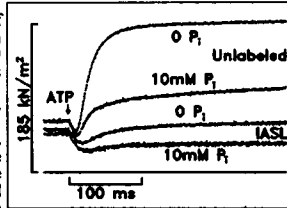


where A=actin, M=myosin, D=MgADP, and Det includes all detached states (MS, MDP) and weakly attached states (AMS, AMDP). From our studies, we obtained K_{1a}=0.76 mM⁻¹ (MgATP association), k_{1b}=230 s⁻¹ (ATP isomerization), k_{1b}=170 s⁻¹ (reversal isomerization), K_{1b}=k_{1b}/k_{1b}=1.4, k₂=48 s⁻¹ (cross-bridge detachment), k₂=10 s⁻¹ (reversal detachment), k₂=k₂/k₂=5.4, k₄=9 s⁻¹ (cross-bridge attachment), k₄=65 s⁻¹ (reversal attachment), K₄=k₄/k₄=0.15, and K₅=0.07 mM⁻¹ (Pi association). k₆ is the rate-limiting step, and it is the slowest forward reaction in the cycle, which results in AMD or AM state. K_{1a} (MgATP binding) is 3X of rabbit psoas, and K₅ (Pi binding) is 0.3X of psoas, indicating that the myocardium is more resistant to ATP depletion and Pi build up. The rate constants of ATP isomerization (k_{1b}, k_{1b}), cross-bridge detachment (k₂, k₂), and cross-bridge attachment (k₄, k₄) steps are generally 10 times slower than rabbit psoas, except that k₄ which is similar to psoas.

W-Pos13

CHANGES IN CROSS-BRIDGE KINETICS INDUCED BY SH-1 MODIFICATION IN RABBIT PSOAS FIBERS ((M.G. Bell*, J. Matta*, D.D. Thomas* and Y.E. Goldman*)) *University of Pennsylvania, Phila, PA 19104 and *Univ. of Minnesota, Minneapolis, MN, 55455

Spectroscopic and kinetic studies with actomyosin and muscle fibers labeled with probes at Cys-707 of the myosin heavy chain (SH-1) can be criticized for the alteration of the system due to labeling. We took advantage of the highly specific labeling (95 % of the probes were on SH-1) possible with iodoacetamide spin label (IASL) in fibers to study the changes in cross-bridge kinetics caused by the probes. Single glycerinated fibers either unlabeled or labeled on >95 % SH-1s were activated from rigor at $[Ca^{2+}] = 30 \mu M$ by photolysis of caged ATP in the presence and absence of 10 mM phosphate (P_i). Steady active tension (T_a) per cross-sectional area of 189 ± 9 kN/m² (s.d., n=4) in unlabeled fibers was reduced to 64 ± 4 kN/m² by IASL labeling. Tension per unit stiffness in IASL fibers was reduced to 54 ± 16 % of control. 10 mM P_i reduced T_a in control and IASL fibers to 70 ± 9 % of the $0 P_i$ value indicating significant population of the force bearing AM·ADP state in both control and IASL fibers. Development of tension following photolysis of caged ATP was slowed by IASL labeling (Fig.). Fitting of a kinetic model to the data suggested that the probes cause ~2-fold slowing of force generation following detachment by ATP, consistent with slowing of the elementary ATP hydrolysis step. Since relative tension and tension per unit stiffness are much greater than the proportion of unlabeled myosin heads in IASL fibers, the results suggest that labeled heads can generate force, albeit less than that of normal heads. Supported by MDA and NIH HL15835 to PMI.



W-Pos15

RADIAL ELASTICITIES OF ATTACHED CROSSBRIDGES IN MUSCLE FIBERS ARE STATE DEPENDENT. ((S. Xu*, B. Brenner*, J.M. Chalovich* and L.C. Yu*)) *NIH, Bethesda, MD; *University of Ulm, FRG; *East Carolina University, Greenville, NC

Radial elasticities of crossbridges strongly attached to actin have been shown to differ, in rigor, during full Ca^{2+} -activation, in the presence of ADP, and with MgPPi (Brenner & Yu, *J. Physiol.*, 1991; Xu et al., *J. Physiol.* 1993). Preliminary results showed that weakly attached crossbridges in relaxed muscle also exhibited radial elasticity (Xu, et al., *BJ abstr.*, 1992) by comparing radial forces generated by relaxed fibers at various lattice spacings (a) with extensive and (b) with little weakly attached cross-bridges. The latter condition was obtained by using the 20 kDa actin binding caldesmon fragment to compete off weakly attached cross-bridges. These results have been reconfirmed. Furthermore, control experiments show that the difference in radial responses is not due to binding per se of the caldesmon fragment to actin, since binding caldesmon to rigor fibers has no effect. A key parameter of radial elasticity (equilibrium spacing where radial force is zero) is 377Å for the weakly attached cross-bridges which differs from that of rigor (386Å) at the same ionic strength (50mM). In addition, estimated radial stiffness per weakly attached cross-bridge appears to be lower than that of rigor. Combined results on strongly and weakly attached cross-bridges indicate that equilibrium spacing and radial stiffness per attached cross-bridge are state dependent. Furthermore, axial stiffness (previously reported) and radial stiffness do not appear to correlate in direct proportion.

W-Pos17

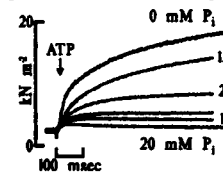
SYNERGISTIC EFFECTS OF TEMPERATURE AND INTRACELLULAR ACIDIFICATION BY CO₂ ON FORCE GENERATION IN FAST-TWITCH MOUSE MUSCLES. ((R.W. Wiseman, T.W. Beck & P.B. Chasse)) Dept. of Radiology, University of Washington, Seattle, WA 98195

Skinned fiber data suggest that metabolic acidosis may be a major cause of the decline in force and shortening velocity observed during muscle fatigue (e.g. Chase & Kushmerick, 1988, *Biophys. J.* 53:935). In contrast, intact muscle experiments in which pH_i was decreased by CO₂ administration show that other significant factors must also be responsible for fatigue (Renand & Mainwood, 1986, *Can. J. Physiol. Pharm.* 64:764; Meyer et al., 1991, *Can. J. Physiol. Pharm.* 69:305). Observations of Rees & Stephenson (1987, *J. Exp. Biol.* 129:309) suggest that differences in experimental temperature may explain the disparity in conclusions. To test the hypothesis that intracellular pH (pH_i) is more effective in depressing contractile function as the temperature is lowered, we studied the effect of altered pCO_2 on tetanic force of mouse extensor digitorum longus muscles between 15°C and 25°C. Isolated muscles were incubated in mouse MOPS ringers equilibrated with either 95% O₂/5% CO₂ or 75% O₂/25% CO₂. Muscles were given supramaximal tetanizing stimuli via Pt electrodes. Maximum force was 29.7 ± 2.5 grams (n=7) at 25°C and was used to normalize subsequent force measurements which were expressed as a percentage of this value at each time point. Force decreased to 0.87 ± 0.03 at 15°C (n=6). In 75% O₂/25% CO₂, force was 0.84 ± 0.04 (n=6) at 25°C and was 0.45 ± 0.02 at 15°C (n=5). Force varied biphasically with temperature between 25°C and 15°C in both 5 and 25% CO₂. Force was maximal at 21°C. At 15°C, force decrease due to CO₂ administration was greater both absolutely and relatively, than at 25°C suggesting that temperature differences are at least partly responsible for different observations on the role of pH_i in muscle fatigue. Provided that there are no effects of CO₂ independent of decreased pH_i , we conclude that intracellular acidification is not the only factor responsible for fatigue at physiological temperature. Supported by NIH: R29 AR41793 and HL31962.

W-Pos14

EFFECTS OF INORGANIC PHOSPHATE ON THE KINETICS OF SKINNED CARDIAC MUSCLE ACTIVATION FROM RIGOR INITIATED BY PHOTOLYSIS OF CAGED-ATP. ((Hunter Martin and R.J. Barott)), Bockus Research Institute, The Graduate Hospital, Philadelphia, PA 19146

Martin et al. (*Biophys. J.* 61:19a, 1992.) reported that the rate of force generation from rigor of Triton-skinned Guinea-pig trabeculae was $21 s^{-1}$, when activated by laser photolysis of caged ATP in the presence of Ca^{2+} (pCa 4.5, I = 200 mM, 23°C). The goal of these experiments was to determine the effects of inorganic phosphate (P_i) on this rate of force production. The level of rigor tension of tissue incubated in solutions containing 10 mM caged ATP remained constant upon addition of up to 20 mM P_i . The level of tension



produced by the tissue following release of 1 mM ATP decreased as the concentration of phosphate was increased, while the rate of tension rise increased. In solutions containing 20 mM P_i , active force was reduced by greater than 60 % and the apparent rate at which force developed, increased over tenfold. These results can be explained by assuming that reversible phosphate release from AM·ADP· P_i

cross-bridges is associated with force generation, and that in the presence of added phosphate, phosphate rebinding shifts the distribution of cross-bridge states toward low force generating states (decreasing active tension), while the reversal of the phosphate binding step is accelerated, thereby increasing the apparent rate of force development as suggested by Hibberd et al. (*Science* 228:1317-1319, 1985) in skeletal muscle. Supported by NIH HL40953 and AHA 88-09960.

W-Pos16

THE ROLE OF TITIN IN LATERAL ORDERING OF MYOSIN FILAMENTS. ((Y. Sasao, E. Kempner, R. J. Podolsky)). NIH Bethesda MD 20892.

The role of titin in the lateral order of thick filaments was investigated by electron microscopy. Chemically skinned fibers were prepared from rabbit psoas muscle. To preferentially degrade titin and/or nebulin, frozen fibers were exposed to ≤ 1.5 Mrads of radiation. After thawing, fibers were placed in pH 7.0 rigor solution or pH 7.0 relaxing solution at 5 C or at 20 C. pH cycling to pH 5.5 and return to pH 7 was repeated 1-3 times before the fibers were fixed and embedded. Longitudinal and transverse sections (40-60 nm) were observed in a Phillips 400 EM. In enlarged photos of transverse sections, several hundred distances were measured between adjacent myosin filaments in myosin filament-based hexagonal lattices. The average distance did not change with radiation dose or pH cycles, but in relaxed fibers the standard deviation (SD) increased significantly with radiation dose or with pH cycles. In rigor fibers, the SD increased slightly with pH cycles, but not with radiation dose. These results reveal progressive lateral disordering of the myosin filament array. In longitudinal sections, the M-line became less intense in irradiated fibers in relaxing solution at 20 C and to a smaller extent at 5 C after pH cycling, in parallel with the progressive longitudinal disorder seen in transverse sections. These observations suggest that titin and actomyosin crossbridges play a role in the lateral order of thick filaments. The order may be due to an influence of titin-modulated M-line material on the thick filaments at the middle of the A-band, or more likely, due to that portion of titin which courses through the entire A-band.

W-Pos18

ACTIVE TENSION GENERATION IN ISOLATED SINGLE MYOFIBRILS. ((Marc L. Bartoo and Gerald H. Pollack.)) Center for Bioengineering, University of Washington, Seattle WA 98195.

Single or double myofibrils from rabbit psoas muscle were suspended between a fine needle and an optical force transducer (Bartoo et al., 1989). The length of every sarcomere along the specimen was measured by employing a photodiode array. Active tension (20-22 °C) was reproducible from contraction to contraction. Specimens could be activated and relaxed 4-5 times before active force levels began to decline; some specimens lasted for 10-15 activation cycles. It was found that pCa 6.0 generated 30% of maximal tension, while pCa 5.5-4.5 fully activated the specimens. At sarcomere lengths of 1.8-2.0 μm , active tension was found to range from 0.25 to 0.49 N/mm² (mean of $0.37 N/mm^2 \pm 0.06$ SD, N=35). This mean value is comparable to that found by Iwazumi (0.40 N/mm², personal communication), and is greater than reported for skinned or intact muscle fibers. Thus, isolated single myofibrils produce more force per cross-sectional area than larger preparations.

When myofibrils were activated at a sarcomere length of 2.5-2.8 μm , one group of sarcomeres usually shortened, while stretching the remainder. We found that stretched sarcomeres exhibited a range of lengths, and held these lengths stably for tens of seconds during activation. We have attributed the measured tension to the shortened sarcomeres (1.8-2.2 μm); however, since the stretched sarcomeres (2.8-4.5 μm) bore the same tension as the contracted ones, one can construct a length-tension relation that includes these longer sarcomeres. For sarcomere lengths of 1.8 to 3.8 μm , this length-tension relation is flat.

W-Pos19

RIGOR BRIDGE FORMATION AT SHORT SARCOMERE LENGTH IN SKINNED CARDIAC AND SKELETAL MUSCLE FIBERS. ((Franklin Fuchs and Yi-Peng Wang)) Department of Physiology, University of Pittsburgh School of Medicine, Pittsburgh, PA 15261. (Spon: G. Romero)

We have suggested that the variation in Ca^{2+} sensitivity and Ca^{2+} binding observed over the ascending limb (sarcomere length 1.7-2.4 μ m) of the cardiac length-force curve is based on variation in the number of cross-bridge attachments as a consequence of double overlap of the actin filaments (Hofman and Fuchs, 1988). However, *in vitro* motility assays show that cross-bridges can form force-generating complexes and rigor complexes with both "correctly" and "incorrectly" polarized actin filaments (Toyoshima et al., 1989). In the intact myofibril at short sarcomere length, where there is intermixing of oppositely polarized actin filaments, force generation is inhibited, while actin-activated myosin ATPase activity is unchanged (Stephenson et al., 1989). We have used two biochemical assays to compare rigor bridge formation in skinned rabbit psoas and bovine ventricular fibers at sarcomere length 1.7-2.4 μ m. These are 1) the effect of rigor bridge attachment on Ca^{2+} binding to troponin C (Bremel and Weber, 1972) and 2) the inhibition of K^{+} -EDTA-activated myosin ATPase by the binding of actin to myosin (Cooke and Franks, 1980). In both types of muscle a reduction in sarcomere length was associated with a reduced binding of Ca^{2+} to troponin C in the rigor state and a marked increase in K^{+} -EDTA-ATPase activity. The data suggest that either 1) double overlap of the actin filaments inhibits rigor bridge attachment, or 2) rigor complexes formed with correctly and incorrectly polarized actin filaments constitute two distinct biochemical species. Supported by NIH grant AR-10551.

W-Pos21

EXTRACTION OF C-PROTEIN ELIMINATES THE DELAYED OVERSHOOT OF ISOMETRIC TENSION DUE TO STRETCH OF MAMMALIAN SKELETAL MUSCLES. ((L. Larsson, M.L. Greaser and R.L. Moss)) Dept of Physiology, Muscle Biology Lab, Univ of Wisconsin, Madison, WI 53706. *Dept of Clinical Neurophysiology, Karolinska Hosp, Stockholm, Sweden.

Release and re-stretch of an actively contracting muscle results in a tension transient subsequent to re-stretch that is characterized by (1) a rapid overshoot beyond the initial isometric tension, P, (2) a rapid decline of tension to a value less than P, and (3) a delayed slow overshoot of tension that gradually returns to P. We investigated the molecular basis for the delayed overshoot in rabbit skinned psoas fibers at various levels of Ca^{2+} activation. In our experiments, the amplitude of delayed overshoot, as a fraction of P, was greatest at low levels of activation, suggesting to us that delayed overshoot may be a transient cooperative response involving thick and thin filament proteins. Up to 70% of endogenous C-protein was extracted by bathing the fibers in solutions of 31 mM Na_2HPO_4 , 124 mM NaH_2PO_4 , pH 5.90, 10 mM EDTA at room temperature. Partial extraction of C-protein almost completely abolished the slow overshoot phase, and the amplitude of residual slow overshoot no longer had activation dependence. Reconstitution of the fiber with C-protein at least partly reversed the effects of its extraction. Functions of C-protein in connection with the delayed overshoot phase of tension recovery will be discussed. (Supported by NIH HL25861).

W-Pos23

THE EFFECT OF SERIES ELASTICITY ON THE DELAY IN DEVELOPMENT OF TENSION RELATIVE TO STIFFNESS DURING MUSCLE ACTIVATION. ((Y. Luo, E. Pate, and R. Cooke)) Dept Math. Washington State Univ., Pullman, WA 99164, Dept. Biochem. Biophys. & CVRI, UCSF, San Francisco, CA 94143.

Using computer simulation, we have investigated the effects of a series elastic element on stiffness and tension development during muscle activation. Mechanical and time-resolved X-ray diffraction studies have provided evidences that in the early phase of muscle activation, the attachment of myosin to actin precedes tension generation by 10 to 30 msec. A number of investigators have offered explanations involving either the existence of intermediate states in the actomyosin interaction or cooperativity among cross-bridges. We used the original model of cross-bridge mechanics by A.F. Huxley. All simulations start from a relaxed state with all cross-bridges detached. Both stiffness, a measure of number of attached heads, and tension increase nearly exponentially with time constants strongly dependent upon series elastic strains. We find that with elastic strain larger than 2.5 nm per half sarcomere, the increase in stiffness always precedes tension increase. The lag between stiffness and tension increases with increasing elastic strain. The experimentally observed 10-30 msec lag can be obtained with about 5 nm elastic strain, which is quite realistic in experiments without sarcomere length servo control. The simulated results generate plots of scaled stiffness versus scaled tension which are very similar to that of experimental measurements. Supported by NIH grants HL32145, AR36943, and AHA.

W-Pos20

CONTRACTION-INDUCED INJURY: INFLUENCE OF THE NUMBER OF CONTRACTIONS ON THE MAGNITUDE OF THE FORCE DEFICIT. ((Susan V. Brooks and John A. Faulkner)) Inst. of Gerontology and Bioengineering Program, University of Michigan, Ann Arbor MI, 48109 (Spon. by J.A. Jacquez).

Contraction-induced injury is focal in nature and appears to occur at the level of single sarcomeres. The magnitude of the force deficit correlates with, but is greater than, the severity of the morphological injury. Consequently, force deficit is the best measure of the totality of the injury. Following a lengthening contraction protocol, the force deficit appears to be related to the magnitude of the displacement, the force developed, and the number of contractions. We tested the hypothesis that when, fatigue is minimized by infrequent contractions, the velocity of lengthening is low, and the displacement is small, the relationship of force deficit with number of contractions is sigmoidal. Anesthetized mice were placed on a temperature controlled platform. The knee was pinned and the foot taped to the platform. An incision was made over the distal tendon of the extensor digitorum longus (EDL) muscle and the lever arm of a servomotor/force transducer was clamped to the tendon. The force deficit was measured one minute after contractions of fully activated EDL muscles during which the muscle contracted isometrically until isometric force plateaued. Lengthening contractions were performed at 150 Hz stimulation, 0.5 fiber lengths (L_p)/s, through a stretch 20% beyond L_p . Contractions occurred every 60 s for 75 min. No force deficit was observed after a single lengthening contraction. Between 10 and 20 contractions the force deficit increased linearly to 30% and then plateaued at 55%. With the same protocol, but contractions every 4 s, by 75 contractions the isometric force had decreased to zero. After recovery from fatigue, the force deficit was 20%. The sigmoidal relationship between force deficit and number of contractions supports the concepts of a threshold for injury and a population of fibers that are not injured by this protocol. Supported by NIH Grant AG-06157.

W-Pos22

SELECTIVE REMOVAL OF ACTIN FILAMENTS WITH A NON-CALCIUM REQUIRING GELSOLIN FRAGMENT (FX45): EFFECTS ON PROTEIN COMPOSITION AND MECHANICAL PROPERTIES OF INSECT FLIGHT AND VERTEBRATE SKELETAL MUSCLES. ((Granzier, H.L.M. & Wang, K.)) Clayton Found. Biochem. Inst., Dept. of Chem. & Biochem., University of Texas, Austin Tx 78712.

A powerful technique for the selective removal of actin filaments from the sarcomere of striated muscle by gelsolin has been recently introduced by Fanatsis et al. (1990), and we have used this technique to reveal the interplay between passive tension and strong and weak bridges in insect asynchronous flight muscle (Granzier & Wang, accompanying abstract). We report here an extension of this technique by substituting intact gelsolin with a N-terminal gelsolin fragment, FX45 (45 kd), which severs actin filaments effectively in the absence of calcium (Yu, Zhou & Yin, 1992. J.Biol.Chem., 266, 19269-75). The use of this small fragment alleviates the need for calcium ions by intact gelsolin and avoids calcium induced proteolysis and structural damage that complicates interpretation. Moreover its smaller size facilitates accessibility to actin filaments.

The effect of gelsolin FX45 on the extent, location and uniformity of actin removal on both insect water bug flight muscle (DLM) and rabbit psoas muscle was studied by incubating short mechanically skinned single fiber segments in relaxing buffer with FX45. The extent of actin removal was monitored by SDS gel electrophoresis and the location and uniformity of actin extraction was investigated with confocal microscopy of rhodamine-phalloidin labeled fibers. Mechanical characteristics (force, stiffness and sarcomere length) were also measured before, during and after actin removal.

Treatment of insect flight muscle fibers with FX45 (~0.3 mg/ml in relaxing solution) at 21-23 °C for 2h extracted a maximal of 80% of total actin and thin filament associated proteins such as arthrin, troponin-T and tropomyosin. The remaining 20% was resistant to further extraction. No proteins known to be thick filament and C-filament components (such as myosin and mini-titin) were either extracted or degraded during this protocol. Confocal fluorescence microscopy revealed a complete removal of actin outside the Z line of every sarcomere in the entire fiber segment. Actin in the Z-lines remained after treatment, accounting for the 20% extraction-resistant actin. Mechanical results were similar to those reported for fibers treated with intact gelsolin (Granzier & Wang, accompanying abstract). For rabbit psoas fibers, maximal actin removal required longer incubation (5-7 h) and the extent of removal was 80-90% of total actin. Mechanical measurements showed that passive force was slightly elevated after actin extraction.

W-Pos24

ELASTIC ENERGY STORAGE IN THE FLIGHT MUSCLES OF A SMALL DIPTERAN. ((J.E. Molloy and D.C.S. White)) Biology, University of York, UK.

Each time an insect beats its wings, work must be done to accelerate the inertial mass of the wings. Many insects are known to use elastic elements to store and return inertial energy during each half wing stroke. This elasticity, plus the wing inertia forms a resonant system. We have used genetic mutants with altered muscle structure but wild-type wing and thorax morphology to investigate elastic storage in the flight system of *Drosophila melanogaster*. We used several lines of heterozygous, flight muscle protein, null mutants. Mechanical kinetics of myofibrillar bundles were essentially the same as wt for all lines tested. However, wingbeat frequency was much lower than wt (only half that of wt in some lines). Wingbeat frequency was proportional (with near zero intercept) to the total number of myofibrils in the flight muscles. We conclude that the flight muscles are the most important elastic element in this animal's flight system and are therefore the major store for inertial energy over the wing stroke cycle. High resting stiffness of asynchronous muscle has probably evolved to permit storage of elastic energy in muscles which have short working distances and very short tendons. Some insects with synchronous muscles (Dragonfly) also have high resting stiffness (Peckham & White, J. exp. Biol., 198, 135-147); the protein Troponin-H (which is glycine & proline rich, like resilin) may be the passive, parallel, elastic element in all these muscles. Supported by SERC.

W-Pos25

HIGH IONIC STRENGTH AND LOW pH DETAIN MUSCLE CROSSBRIDGES IN A LOW FORCE STATE. ((C.Y. Seow and L.E. Ford)) University of CHICAGO, Chicago, IL 60637

To learn more about chemical interactions in the crossbridge cycle, skinned rabbit psoas fibers were studied at 1-2°C. Solutions contained 56 g/l Dextran T-70, 5 mM MgATP, 1 mM Mg²⁺, 20 mM creatine phosphate, 10 mM imidazole, Ca²⁺ buffered to pCa 4.5 with 5 mM EGTA, and varying amounts of K-propionate. Ionic strength was 210 mM in pH studies; pH was 7.0 in ionic strength studies. Raising ionic strength from 125 to 375 mM and lowering pH from 7.35 to 6.35 both decreased force by half and decreased sarcomere stiffness by 1/4, producing a 50% increase in relative stiffness (immediate force change/isometric force per unit length change). The effects were asymmetrical. The larger relative force change seen at high ionic strength persisted for a long time following stretch but relaxed quickly following release, suggesting that the responsible factors imposed very little hindrance to shortening. By contrast, the larger relative force change seen at low pH relaxed quickly following stretch but persisted for a long time following release. Furthermore, the persistent relative force difference seen at pH 6.35 reached a maximum plateau of about 8% isometric force with intermediate releases. An internal load equivalent to this value was exactly sufficient to account for the decreased maximum velocity at pH 6.35. All of the effects of the two interventions can be explained by detention of crossbridges in low force states that differ with regard to their resistance to stretch and release, with very little effect on the remainder of their cycle.

W-Pos27

FORCE REDEVELOPMENT RATE IN FERRET PAPILLARY MUSCLE AS A FUNCTION OF SEGMENT LENGTH AND CALCIUM. ((W.O. Hancock and L.L. Huntsman)) Center for Bioengineering, University of Washington, Seattle, WA, 98195.

Based on results from skinned skeletal muscle in which the tension redevelopment rate constant, k_{tr} , has been found to increase at higher $[Ca^{2+}]_i$, it has often been assumed that in cardiac muscle k_{tr} has a similar Ca^{2+} dependence. In the present study, k_{tr} was measured in intact cardiac muscle and found not to possess the Ca^{2+} dependence observed in skeletal muscle. Using tensioning ferret papillary muscles under segment length (SL) control, rapid shortening steps of 2-3% SL_{max} were imposed at various lengths and extracellular Ca^{2+} concentrations ($[Ca^{2+}]_o$) during the tetanic force plateau. Following a drop in force to zero, force redeveloped to a new steady state level, and the force redevelopment data could be fit by an exponential curve with rate constant k_{tr} . It was found that k_{tr} did not increase at higher $[Ca^{2+}]_o$ or longer SL, and in some cases k_{tr} even decreased at longer lengths and higher $[Ca^{2+}]_o$. The absence of a positive dependence of k_{tr} on SL or $[Ca^{2+}]_o$ suggests that the crossbridge attachment rate constant (f in the Huxley scheme) is not Ca^{2+} or length dependent in intact cardiac muscle despite the strong influence of segment length and $[Ca^{2+}]_o$ on force. An implication of this result for the purpose of modeling myocardial contraction is that it is not valid to employ a Ca^{2+} dependent crossbridge attachment rate since this assumption predicts a Ca^{2+} dependent k_{tr} .

W-Pos29

TIME COURSE OF CHANGE IN Ca^{2+} SENSITIVITY OF MYOCYTES FROM PORCINE STUNNED MYOCARDIUM ((K.S. McDonald, W.P. Miller, P.P.A. Mammen, and R.L. Moss)) Depts of Physiology and Cardiology, Univ of Wisconsin, Madison, WI 53706.

Myocardial stunning is characterized by reversible contractile dysfunction that occurs after brief periods of ischemia. One factor associated with stunning is reduced Ca^{2+} sensitivity of tension (Hofmann *et al.* Biophys. J. 61:A20, 1992). The aim of this study was to determine whether the decrease in cardiac myofilament Ca^{2+} sensitivity occurs during ischemia, reperfusion, or both. The Ca^{2+} sensitivity of isometric tension was measured in skinned single myocytes from endocardial biopsies of myocardium from the left anterior descending (LAD) coronary artery perfusion bed of porcine heart ($n = 5$). Serial biopsies were obtained during control aerobic flow, during low flow ischemia (just prior to reperfusion), and after 30 min of reperfusion. Regional myocardial function in the LAD bed, as assessed by percent systolic wall thickening, was $43 \pm 14\%$ of control in the postischemic stunned state. Control myocytes from the LAD bed had a mean pCa_{50} , i.e. pCa for half maximal tension, of 5.95 ± 0.03 . The pCa_{50} in LAD myocytes was unaltered by the induction of ischemia (5.93 ± 0.03), whereas, following reperfusion the LAD myocytes showed a significantly reduced pCa_{50} (5.80 ± 0.03 , $p < 0.05$). These results indicate that the decrease in Ca^{2+} sensitivity occurs during reperfusion, supporting the idea that reperfusion injury is an independent mechanism for the reduced Ca^{2+} sensitivity of myocardium associated with stunning. Supported by the ARA.

W-Pos26

STRUCTURAL CHANGES IN CARDIAC MUSCLE ASSOCIATED WITH REGULATION: AN X-RAY DIFFRACTION STUDY. ((J.J. Harford, H. Pask and J.M. Squire)) Biophysics Section, Blackett Laboratory, Imperial College, London SW7 2BZ, UK.

At the level of the myofibrillar material, regulation of cardiac muscle is affected by Ca^{2+} binding to troponin-C, but this effect may be modified by the observed reversible phosphorylation of the unusual cardiac isoforms of both troponin-I and C-protein. We have found in our previous studies of vertebrate skeletal muscle (Harford & Squire, in 'Molecular Mechanisms in Muscular Contraction' pp. 287-320, Macmillan Press, 1990) that the meridional X-ray reflection at 44 nm due to C-protein changes in intensity when the muscle is activated, suggesting a possible dynamic role for C-protein even in skeletal muscle. Rat cardiac papillary muscles skinned in saponin have been studied both on a laboratory based single mirror X-ray camera with a linear position-sensitive detector and also using line 2.1 at the Daresbury Synchrotron. Comparison of results from resting and from Ca^{2+} -activated muscles showed: (i) changes of the 10 and 11 reflections previously reported by Matsubara *et al.* (J. Physiol. 417, 555 (1989)), (ii) a general weakening of the 'myosin' layer-lines at 43 and 21.5 nm and the 14.3 nm meridional reflection and (iii) a change to a meridional reflection at about 43.5 nm thought to be due to cardiac C-protein. The difference between this spacing and the 44 nm observed in patterns from vertebrate skeletal muscles is thought to be due to the unusual distribution of C-protein in cardiac muscles (Pask *et al.* in preparation). Further study of this reflection and the rest of the diffraction pattern will show if cardiac muscle regulation is modified by C-protein phosphorylation and associated with C-protein movement.

WORK SUPPORTED BY THE BRITISH HEART FOUNDATION

W-Pos28

TENSION TRANSIENTS IN RAT CARDIAC MYOCYTES INITIATED BY PHOTOLYSIS OF CAGED Ca^{2+} . ((A. Araujo, R.L. Moss, and J.W. Walker)) Department of Physiology, University of Wisconsin, Madison, WI 53706

The rate constant of tension development and its dependence on $[Ca^{2+}]_i$ were measured in mechanically-disrupted Triton-skinned cardiac myocyte fragments which were attached to a force transducer (Cambridge Tech., Model 406, 100 Hz) and a piezoelectric transducer. The attached myocyte fragment was transferred into an 18 μ l photolysis chamber containing 1 mM Nitr-7 loaded to different extents with Ca^{2+} (in 4 mM MgATP, 1 mM Mg²⁺, 14.5 mM creatine phosphate, 88.2 mM KCl, 10 mM glutathione 20 mM imidazole pH 7.0, 15°C). After tension reached a plateau, the chamber was irradiated by a xenon flash (1 msec, 300-350 nm), which caused tension to increase exponentially by 5-22% P_0 . The apparent rate constant was 1.09 ± 0.16 s⁻¹ when the final tension plateau was 13.5 ± 4.5 % P_0 , and 4.35 ± 0.95 s⁻¹ when final tension was 76.9 ± 2.9 % P_0 ($n=8$). Rate constants measured with DM-nitrophen (in 0.1 mM Mg²⁺) were 3.27 ± 0.49 s⁻¹ at 13 ± 1.7 % P_0 and 5.27 ± 0.53 s⁻¹ at 66 ± 3.8 % P_0 . Rates measured with Nitr-7 were also about 2-fold faster in 0.1 mM Mg²⁺. The results indicate that the rate of tension development depends upon $[Ca^{2+}]_i$ and $[Mg^{2+}]_i$, but the Ca^{2+} dependency is less marked than observed in rabbit psoas fibers (2.4 ± 0.8 s⁻¹ at 14 ± 5 % P_0 to 19 ± 4 s⁻¹ at 81 ± 6 % P_0). Ca^{2+} may regulate cross-bridge transitions differently in cardiac muscle than in fast-twitch skeletal muscle.

W-Pos30

1,25 DIHYDROXYVITAMIN D₃ INCREASES MYOCARDIAL TWITCH TENSION. ((G.M. Diffie, S.H. Buck, R.L. Moss)) Depts of Physiology and Pediatrics, Univ of Wisconsin, Madison, WI 53706.

1,25 dihydroxyvitamin D₃ (D₃) stimulates Ca^{2+} uptake into chick ventricular slices and microsomes (Selles and Boland, Mol Cell Endocrinol 77:67, 1991), an effect that was attributed to phosphorylation of sarcolemmal Ca^{2+} channels. The aim of this study was to determine the effects of D₃ on the twitch characteristics of mammalian myocardium. Rat right ventricular papillary muscles were field stimulated at 0.3-0.7 Hz while continuously perfused at 22-24°C with oxygenated modified Tyrode's solution, pH 7, containing 2 mM Ca^{2+} . Muscles attaining stable baseline twitch tension were then perfused with 0.1-6.25 μ M D₃. In nine experiments D₃ increased steady-state twitch tension an average $14 \pm 11\%$ (range of 4-41%). Variability in results between preparations may be due to variable partitioning of the drug into membranes of the outermost cells the papillary muscles. The effects of D₃ were reversed by drug washout. While the β adrenergic agonist isoproterenol (1-10 μ M) increased twitch tension and reduced the duration of the twitch, D₃ had no effects on time to peak twitch or on relaxation time. The twitch-potentiating effects of D₃ were mimicked by altering extracellular $[Ca^{2+}]_o$. We conclude that D₃ induces a positive inotropic response in rat ventricular muscle, most likely by increasing Ca^{2+} entry into the cell during excitation-contraction coupling.

W-Pos31

BETA-ADRENERGIC STIMULATION INCREASES MAXIMUM UNLOADED SHORTENING VELOCITY (V_{max}) OF RAT SKINNED SINGLE VENTRICULAR MYOCYTES. ((K.T. Strang and R.L. Moss)) Dept of Physiology, Univ of Wisconsin, Madison, WI 53706

β -adrenergic stimulation has several effects on contractility in mammalian myocardium, one of which is to alter crossbridge cycling kinetics. While acceleration of overall isometric cycling rate has previously been shown (Hoh *et al.*, *Circ Res* 62:452,1988), it is not known whether β -stimulation accelerates cross-bridge attachment or detachment. To investigate the latter possibility we compared V_{max} in control and isoproterenol (ISO)-treated cells. Single ventricular myocytes were enzymatically isolated, agonist-treated, and rapidly skinned, thus preserving the phosphorylation of myofibrillar proteins (Puceat, *et al.*, *Circ Res* 67:517,1990). Relative tension (P_{rel}) was measured at a submaximal $[Ca^{2+}]_i$ (pCa 5.7), and V_{max} was then determined using the slack test method. P_{rel} was 0.52 ± 0.11 in control and 0.16 ± 0.07 in ISO-treated cells (n=9), demonstrating that the cells responded to β -stimulation with a reduction in Ca^{2+} sensitivity of tension as expected based on earlier results. In same-day paired experiments V_{max} was $40 \pm 29\%$ higher in ISO-treated cells (n=9). We conclude that β -adrenergic stimulation increased the rate of cross-bridge detachment during shortening, an effect that may be mediated by phosphorylation of C-protein. (Supported by HL25861 and the AHA-Wisconsin).

W-Pos33

PHENYLEPHRINE DOES NOT ALTER RELAXATION KINETICS IN RAT MYOCARDIUM ((Michael R. Berman^{1,2} and Lynn E. Dobrunz²), Depts. of Anesthesiology¹ and Biomedical Engineering², Johns Hopkins Univ. Sch. Med., Baltimore MD 21205.

We investigated the effect(s) of an α -agonist, phenylephrine (PhE), on indicators of the time of peak $[Ca^{2+}]_i$ and of crossbridge cycling rate, two (of many) factors which influence relaxation kinetics in mammalian myocardium. Experiments were performed on isolated rat right ventricular papillary muscles superfused with a modified Krebs-Henseleit solution (24° C, 1.5 mM $CaCl_2$). Isometric and load clamped twitches were recorded before and after adding 1 μ M PhE to the superfusate. Isometric twitches were analyzed for time to maximum $+dF/dt$ (T_{max}) and for τ_{100} , the time constant of final force decline. Load clamped twitches were analyzed for load dependence of relaxation (LDoR). PhE did not alter T_{max} (58.2 ± 12.3 to 62.2 ± 13.0 msec, mean \pm SD, n=6) or τ_{100} (100.1 ± 29.8 to 95.7 ± 26.0 msec). T_{max} has been shown (Yue, 1987, *AJP* 252:H760) to be coincident with the peak of the intracellular calcium transient. τ_{100} has been suggested (Peterson *et al.*, 1991, *AJP* 260:H1013) as a measure of crossbridge cycling rate, since at the end of a twitch both free and bound calcium have returned to near baseline values. We interpret these results as demonstrating that neither the timing of the peak of the intracellular free calcium transient nor crossbridge cycling rate are affected by phenylephrine. LDoR was also unchanged; this argues that the complex interplay among the many factors affecting relaxation is also unaltered by PhE. Thus, while PhE is known to affect contraction, our results suggest that it does not affect relaxation. Supported by HL38488 (MRB).

W-Pos35

CARDIAC PACING INCREASES PROTEIN SYNTHESIS IN THE DENERVATED RAT HEART. ((D.L. Geenen, A. Malhotra, D. Liang, R. Cheng, and J. Scheuer)) Montefiore Medical Center and Albert Einstein College of Medicine, Bronx, NY 10467.

The heterotopically transplanted rat heart (TH) which is denervated and exposed to a reduced hemodynamic load exhibits marked atrophy. Our aim was to determine the effect of continuous pacing (CP) on total left ventricular protein synthesis (R_p). Pacing was initiated twenty-four hours after TH, (420 bts/min) and compared with a nonpaced group (CON) for one week. R_p was measured using the continuous infusion of ³H-leucine after one week of pacing.

	CON MAT	CON TH	CP MAT	CP TH
LV WT (mg)	301(16)	239(17)*	290(10)	283(6)**
LV Prot (mg)	37(1)	24(1)	41(4)	32(2)**
K_d (%/day)	11(1.1)	18(3.5)	12(1.9)	18(3.6)
R_p (mg/day)	4.2(0.4)	4.3(0.8)	4.7(0.6)	5.6(0.3)**

Data are \bar{x} (SD;n=4). MAT, Native Heart; LV, Left Ventricle; Prot, Protein Content; K_d , Fractional Synthesis. *P < 0.05 TH vs. MAT; **P < 0.05 CP TH vs. CON TH. Although an increase in protein degradation is primarily responsible for the decrease in LV Prot following TH, the heart rate induced increase in protein synthesis may be partially responsible for the attenuation of atrophy.

W-Pos32

SINGLE ISOLATED CARDIAC MYOFIBRILS: SPONTANEOUS CONTRACTION AND RELAXATION CYCLES OF SARCOMERES AT INTERMEDIATE ACTIVATION LEVELS. (W.A. Linke, M.L. Bartoo, and G.H. Pollack) Bioengineering WD-12, University of Washington, Seattle, WA 98195, USA.

Spontaneous oscillatory contractions observed in various heart muscle preparations are widely thought to be triggered by spontaneous release of Ca^{++} from the SR. Here, we report that such oscillations can occur in the absence of SR. Single, isolated myofibrils were prepared from glycerinated rabbit cardiac tissue and left in 1% Triton X-100-containing buffer for at least 1 hour to ensure SR removal. Myofibrils were mounted between two glass needles and partially activated (pCa 6.0 to 5.5) at 10 °C. The length of each sarcomere was measured to a resolution of 50 nm.

Upon activation, the lengths of all sarcomeres spontaneously fluctuated. In an individual sarcomere, one oscillation cycle usually consisted of a rapid lengthening and a slow shortening phase. Oscillatory contractions persisted from several minutes to one hour. The oscillations generally propagated over a few sarcomeres in a wavelike fashion (mean velocity $15.5 \mu\text{m/s} \pm \text{SD } 9.0$; n=12). The oscillation period of individual sarcomeres was $2.04 \text{ s} \pm \text{SD } 0.40$; n=56. At a SL of 1.8 to 2.4 μm , the average oscillation amplitude was approximately 15 % of mean SL, and decreased with stretch; the period of oscillation was insensitive to stretch. All sarcomere motion ceased beyond a SL of 3.0 to 3.1 μm . In control experiments, we added 10 μM ryanodine (known to interfere with the SR function) to the activating solution, and confirmed no significant alteration of oscillation characteristics. Thus, while spontaneous oscillatory contractions in cardiac cells or tissues involve Ca^{++} release from the SR, comparable oscillations occur in the absence of SR. Thus, the SR is not the ultimate mediator of the oscillations.

W-Pos34

MULTIEXPONENTIAL TRANSVERSE RELAXATION OF WATER PROTONS IN THE MYOCARDIUM INVESTIGATED BY DEUTERIUM EXCHANGE. ((I.C. Balanu, J.R. Lee and E.M. Ozu) University of Illinois at Urbana, AFC-NMR Facility, 580 Bevier Hall, 905 S. Goodwin Avenue, Urbana, IL 61801. (Spon. by H. Pessen).

Nuclear Magnetic Relaxation studies of water protons, as well as muscle protons, were carried out on chicken hearts under physiological conditions. In separate experiments, the transverse relaxation changes were followed as a function of deuterium exchange in order to reduce cross-relaxation effects. Nonlinear regression analysis of such relaxation data for hearts from several animal species revealed the presence of three exponential relaxation components. The longest T_2 component of about 700 ms seems to correspond to both intercellular water protons and blood in the heart chambers and coronary vessels. The intermediate T_2 component of about 80 ms appears to correspond to intracellular water protons. The results obtained by deuterium exchange are consistent with a three-compartment model, with at least one compartment exchanging deuterons slowly. ¹H NMR transverse relaxation changes were observed with the CPMG multipulse sequence up to 40 minutes from the beginning of deuterium exchange. Our NMR results and nonlinear regression analysis are likely to be of interest to MRI investigations of the myocardium and medical diagnosis.

W-Pos36

SPHINGOSINE EFFECTS ON SKINNED CARDIAC MYOCYTE CONTRACTILE BEHAVIOR. R. Webster, R. Sabbadini and P. Paolini, Dept. of Biology, San Diego State University, San Diego CA 92182, and Rees-Stealy Research Foundation, San Diego CA 92101.

The intracellular second messenger sphingosine (SPH) modulates myocyte beating behavior by acting on the sarcoplasmic reticulum (SR) calcium (Ca) release channel, the ryanodine receptor (RyR). Skinned myocytes isolated from adult rabbit ventricles exhibited spontaneous asynchronous contractions in response to micromolar levels of Ca. SPH significantly reduced myocyte beat frequency in a dose-dependent manner with an IC₅₀ of ~0.5 μM . A computerized video-enhancement micrography system was used to determine the effect of SPH on sarcomere contractile parameters and to determine the potential source of the altered beating behavior produced by SPH. Contraction parameters related to myofilament shortening were unaffected by SPH in the submicromolar range, suggesting that SPH had no effect on the contractile machinery itself. However, submicromolar SPH had a significant inhibitory effect on the spread of activation from sarcomere to sarcomere. Activation waves were propagated with an average velocity of 331 and 199 $\mu\text{m/sec}$ in control and SPH (0.58 μM) treated cells, respectively. Permeabilized myocyte Ca uptake was markedly increased by treatment with SPH, consistent with an inhibitory effect of SPH on SR Ca release. The results suggest that the site of SPH action on Ca signalling and beating behavior in the cardiac cell is the SR RyR. By inhibiting channel opening, SPH may increase the Ca threshold necessary to trigger Ca-induced Ca release, thus modulating cardiac excitation-contraction coupling. (Supported in part by the Rees Stealy Research Foundation and the California Metabolic Research Foundation.)

W-Pos37**A HIGH-STIFFNESS, HIGH-SENSITIVITY FORCE TRANSDUCER BASED ON MICHELSON'S INTERFEROMETER.**

((R.G. Dennis and N.M. Cole)) Institute of Gerontology and Bioengineering Program, University of Michigan, Ann Arbor, MI 48109 (Spon. by J.A. Faulkner).

The purpose was to develop a force transducer with high stiffness, resonant frequency, and sensitivity for measuring the mechanics of single muscle fibers. The transducer design is based on a Michelson-type interferometer and uses a laboratory-grade He-Ne laser as a light source (wavelength = 632.8 nm). The principle of operation is that a coherent, monochromatic beam of light enters the transducer and is divided into two perpendicular rays by a beam splitter. Each ray is reflected by a small mirror back to the beam splitter, where they recombine. Because the waves in each ray are coherent, they will interfere and form a circular fringe pattern that is sinusoidally squared in intensity. The interferometer is constructed with one mirror stationary and a second mirror attached to a load beam that can be deflected by an external force, the muscle fiber. Small deflections of the load beam (a few nm) along the axis of the light path cause the path length of the ray to be changed. This results in a shift in the interference pattern that is detected with a photo-diode. The transducer has several characteristics that are important in single fiber mechanics: a full-scale deflection of the load beam less than 100 nm; pre-amplified sensitivities as high as 0.3 V/mN; resonant frequencies above 17 kHz; variability in mechanical response achieved by altering the geometry of the load beam; output signals that span several volts without amplification; and a transducing element that is not capacitively or inductively coupled to its surroundings. Technical difficulties included thermal drift and optical alignment that are inherent in interferometric devices. Thermal drift is virtually eliminated by constructing the device with a low thermal expansion material such as Zerodur (Schott Glass Co.). Optical alignment is achieved by accurate machining and assembly. Supported by AG-06157 to John A. Faulkner.

SMOOTH MUSCLE PHYSIOLOGY I**W-Pos38****REGULATION OF VASCULAR SMOOTH MUSCLE TONE BY CALDESMON** H. Katsuyama, C.-L.A. Wang, & K.G. Morgan Harvard Medical School, Boston, MA 02215 and Boston Biomedical Research Institute, Boston, MA 02114

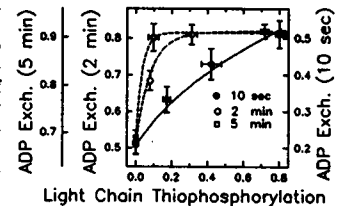
To assess the possible role of caldesmon in the regulation of smooth muscle contraction, we investigated the effects of synthetic peptides on force directly recorded from single hyperpermeable smooth muscle cells of ferret aorta and portal vein. Cells were permeabilized by exposure to 30 μ g/ml saponin for 3-5 min. GS17C, a peptide that contains the residues from Gly⁴⁵¹ to Ser⁴⁶⁷ of the caldesmon sequence plus an added cysteine at the C-terminus, binds calmodulin in a Ca²⁺-dependent manner and also binds to F-actin but does not inhibit actomyosin ATPase activity (Zhan, Q., et al. (1991) *J. Biol. Chem.* 266, 21810-21814). At pCa 7.0, GS17C induced a dose-dependent contraction (EC₅₀ = 0.92 μ M) in aorta cells, whereas it evoked little or no contraction in portal vein cells. The GS17C-induced contraction in aorta cells was inhibited at higher Ca²⁺ concentrations (above pCa 6.6) and by pretreatment with calmodulin. Another peptide, C16AA, which contains the residues from Ala²⁹⁴ to Ala⁶⁰⁹ and does not bind actin or calmodulin, did not induce contraction. Scrambled peptides also did not induce contraction. Our results suggest that GS17C induces contraction by the displacement of the inhibitory region of endogenous caldesmon and, furthermore, that caldesmon present in these smooth muscle cells regulates contraction by providing a basal resting inhibition of vascular tone. Support: NIH HL42293, HL41411 and AHA901345.

W-Pos40**STEADY-STATE ATP METABOLISM IN RESTING AND ACTIVATED α -TOXIN PERMEABILIZED SMOOTH MUSCLE** ((L.A. Trinkle, M.J. Siegman and T.M. Butler)) Department of Physiology, Jefferson Medical College, Philadelphia, PA 19107. (Sponsored by P. Wachsberger)

Rabbit portal veins were permeabilized to low molecular weight compounds (<1000 Da) using *Staphylococcus aureus* α -toxin. ATPase rates were measured as the loss of ³H-ATP in the solution bathing the muscle. The resting ATPase was high (1959 \pm 148 μ M/min, n = 13) compared to about 200 μ M/min in the freeze-glycerinated, triton-treated portal vein. The ATPase measured in the intact muscle was similar to that found after α -toxin permeabilization and was not stimulated by calcium. Therefore, the resting ATPase appears to be mainly a calcium-independent ecto-ATPase. Attempts to decrease this ATPase with sulphhydryl reagents, ecto-ATPase inhibitors and covalently-binding ATP affinity labels met with mixed success. The steady-state [ATP] in the muscle was only 0.31 \pm 0.03 mM (n = 10) following incubation in 1 mM ATP with no ATP regenerating system. The [AMP] was very high (0.37 \pm 0.03 mM), even in the presence of AP5A, a myokinase inhibitor. Sodium azide (10 mM) inhibited an ADPase component of the ecto-ATPase, so that although the overall ATPase rate was not affected to a great extent, the nucleotide accumulated as ADP in the muscle. Use of azide along with creatine kinase and phosphocreatine (PCr) maintained a high level of ATP under both resting and maximally activated conditions. ATPase was then measured as the rate of ³²P-Pi appearance from γ -³²P-ATP and ³²P-PCr which had the same ³²P specific activity. Preliminary results indicate that the ATPase nearly doubles when the muscle is stimulated in high calcium (pCa 4.5) and GTP γ S (10 μ M). (Supported by HL 15835 to the Pennsylvania Muscle Institute and DK 37598).

W-Pos39**KINETICS OF MYOSIN BOUND ADP EXCHANGE IN SMOOTH MUSCLE** ((T.B. Vyas, S.U. Mooers, S.R. Narayan, M.J. Siegman, and T.M. Butler)) Dept. of Physiol., Jefferson Medical College, Philadelphia, PA 19107.

Single turnover experiments on myosin bound ADP were performed on permeabilized rabbit portal vein. After rigor treatment, the muscles were incubated in 1 mM ATP containing ¹⁴C-ATP and caged ³H-ATP, for 3 min. The transition to the doubly labelled ATP was accomplished by photolysis of caged ³H-ATP. At rest, about 40% of the ADP had exchanged at 1 min, but this occurred in only 5 sec when the muscle was maximally activated by thiophosphorylation of the myosin light chain. There are multiple phases in the kinetics of ADP exchange under both resting and activated conditions. The quantitative relationship between myosin light chain phosphorylation and the number of crossbridges that release their ADP at 10 sec is shown in the figure along with previous results at longer times. There is a more linear dependence of ADP exchange on the degree of light chain phosphorylation at shorter times. These data are consistent with the model (lines calculated from AJP 263:C210, 1992) which includes two pools of activated crossbridges: 1) phosphorylated, fast cycling and 2) unphosphorylated, cooperatively activated and slowly cycling. (Supported by HL 15835 to the Pennsylvania Muscle Institute).

**W-Pos41****RATE OF EXCHANGE OF COVALENTLY BOUND PHOSPHATE IN PERMEABILIZED SMOOTH MUSCLE** ((T.M. Butler, S.R. Narayan, S.U. Mooers and M.J. Siegman)) Department of Physiology, Jefferson Medical College, Philadelphia, PA 19107.

Permeabilized rabbit portal veins were transferred from a rigor solution to 1 mM ATP, pCa 4.5 containing γ -³²P-ATP and high specific activity caged γ -³²P-ATP. After 5 min, a UV flash released ³²P-ATP, and the muscles were frozen 0.1-7.5 sec later. The degree of exchange of the phosphate is determined by comparing the ratio ³²P:³¹P in the protein to the ³²P:³¹P in ATP. About one half (25 μ M) of the total phosphorylated protein exchanged phosphate very rapidly with a rate constant of about 7 sec⁻¹. Steady-state ATPase (measured as the rate of ³²P-inorganic phosphate formation) was much less than that required for the rapid incorporation of ³²P from ATP into the phosphorylated protein to result from a kinase-phosphatase futile ATPase cycle. Isoelectric focusing of the proteins from muscles frozen 100 msec after the flash, showed that ³²P was present only in the region containing the phosphorylated myosin light chain, and the phosphate was 54 \pm 7% (n=4) exchanged in this very short time. These preliminary results suggest that a fast exchange of phosphate in the light chain results from a rapid reversal of at least some of the steps of the myosin light chain kinase reaction. This raises the possibility that each myosin light chain could be phosphorylated and dephosphorylated many times during a single crossbridge cycle without the requirement for a futile cycle ATPase. (Supported by HL 15835 to the Pennsylvania Muscle Institute.)

W-Pos42

COOPERATIVE REATTACHMENT OF UNPHOSPHORYLATED CROSSBRIDGES MAY CONTRIBUTE TO MORE EXTENSIVE "LATCH" IN TONIC VS. PHASIC SMOOTH MUSCLE. ((A. Fuglsang, E. Nishiye, A.P. Somlyo, & A.V. Somlyo), Dept. of Physiology, Univ. of Virginia, Box 449, Charlottesville, VA 22908.

Cooperativity (1) and the high affinity of crossbridges (xbs) for ADP (2) may contribute to "latch" in smooth muscle. The force plateau or "hump" following xb detachment from rigor by photolysis of caged ATP is thought to be due to cooperativity: the attachment of unphosphorylated xbs facilitated by attached, rigor xbs (1). MgADP is thought to increase the population of force generating (AM'ADP) states. Inorganic phosphate (P_i) increases the population of weakly bound states, and accelerates the later phases of relaxation that are slowed by cooperative reattachment. We now show that in a tonic smooth muscle (rabbit femoral artery, FA) permeabilized with staphylococcal α -toxin, the rate of relaxation from rigor is significantly slower than the relaxation of the phasic (guinea-pig portal vein, PV) smooth muscle ($t_{1/2}$ 2.5 sec. vs. 0.8 sec.), whereas in the presence of 30mM (P_i), the rates of relaxation are similar ($t_{1/2}$ 0.21 sec. vs. 0.23 sec.). Apyrase, used to eliminate residual fiber ADP, has a much larger accelerating effect on FA than on PV. These results are indicative of muscle-specific rate limiting steps of xb detachment/relaxation that are independent of myosin light chain phosphorylation/dephosphorylation. We suggest that the greater cooperative attachment of xbs and/or their affinity for ADP (or higher [ADP]) contributes to the more extensive "latch" in tonic smooth muscles. Supported by P01 HL19242 and the Danish Medical Research Council.

(1) A.V. Somlyo et al. (1988) *J. Gen. Physiol.*, 91:165-192
(2) Nishiye et al. (1992) *Biophys. J.*, 61(2):P93, A17

W-Pos44

TYROSINE KINASE INHIBITORS ALTER PHARMACOMECHANICAL COUPLING IN INTACT AND α -TOXIN PERMEABILIZED SMOOTH MUSCLE. ((G. Pfitzer, A. Steusloff, K. Kolquist, and J. Di Salvo) II. Physiol. Inst., Univ. of Heidelberg; Dept. Med. Mol. Physiol., Univ. Minnesota-Duluth, Duluth, MN 55812.

Recently, we suggested that tyr-kinase activity (TKA) may be an important regulatory mechanism for contraction-associated signal transduction in smooth muscle (SM). Whether TKA is linked to early events in the signalling pathway between receptor activation and contraction, or to late events such as Ca²⁺ activation of the contractile proteins is unknown. To address this issue we studied the effects of genistein, a potent TKA inhibitor, on (a) carbachol-induced contraction of intact guinea pig ileal longitudinal SM, and (b) direct Ca²⁺ activation of the contractile apparatus in (1) preparations permeabilized with Staphylococcal α -toxin where receptor-coupling is retained, and (2) triton-skinned preparations where receptor coupling is nonfunctional. Genistein markedly reduced carbachol-induced contraction in intact preparations to 56 \pm 3% of control at 4 μ g/ml and to 29 \pm 5% of control at 20 μ g/ml. Inhibition was reversible. Similarly, genistein (4 μ g/ml) reversibly inhibited Ca²⁺-mediated activation of the contractile apparatus in α -toxin permeabilized preparations at either low (pCa 6.57, 34 \pm 8% of cont.) or high [Ca²⁺] (pCa 4.55, 81 \pm 5% of cont.), and markedly suppressed isometric force when it was added to preparations that had already been contracted at pCa 6.57. In contrast, genistein did not inhibit Ca²⁺ activation in triton-skinned preparations. These observations show that TKA can modulate Ca²⁺ sensitivity of the contractile apparatus and that such modulation requires regulatory factors which are retained by α -toxin permeabilized SM but lost from triton-skinned preparations. The results suggest the exciting possibility that Ca²⁺ sensitivity of SM contractility may be regulated by TKA activity.

W-Pos46

SYNTHETIC C-TERMINAL PEPTIDES OF SMOOTH MUSCLE MYOSIN HEAVY CHAINS AND THEIR CORRESPONDING ANTIBODIES MODULATE SHORTENING VELOCITY AND CALCIUM SENSITIVITY IN SKINNED TAENIA COLI. ((Shuang Cai, Anne F. Martin and Richard J. Paul)) Depts. of Physiology & Biophysics, and Pharmacology & Cell Biophysics, University of Cincinnati, College of Medicine, Cincinnati, OH 45267-0576.

Two smooth muscle isoforms, SM1 (204 kDa) and SM2 (200 kDa), possess identical amino acid sequences except for the C-terminal tail region. We investigated the role of the C-terminal region using antibodies and synthetic peptides as probes of function in permeabilized fibers. Two peptides corresponding to the amino acid sequences specific to the C-terminal region of SM1 and SM2 were synthesized and HPLC purified. Antibodies against these two peptides were raised in rabbits, immunoaffinity purified, and shown to be isoform specific. Guinea pig taenia coli fibers were permeabilized by exposure to Triton X-100. The fibers were first contracted in a Ca²⁺-EGTA buffered solution ([Ca²⁺] = 8.0 \times 10⁻⁷ M). When the force reached the steady state, the fibers were transferred to solutions containing either the SM1 or SM2 peptide (SM-p) or the antibody to SM1 or SM2 (Ab-SM) at the same [Ca²⁺]. Isometric force was unchanged but V_{max} was reduced to 20%-30% by the Ab-SM1 (0.9 mg/ml) and SM1-p (100 μ M) and to 50%-70% by the Ab-SM2 and SM2-p. The effect of the SM1-p on Ca²⁺ sensitivity was tested by contracting fibers in 1.9 \times 10⁻⁷ M Ca²⁺ and then transferring into identical solutions containing the SM1-p (70 μ M), which doubled the tension. Photoaffinity labeling of the skinned fibers indicated that the SM1-p binds primarily to myosin. Our results suggest that the myosin C-terminus affects crossbridge detachment and thus may play a novel role in regulation of smooth muscle contractility. Supported by NIH HL 22619.

W-Pos43

CALCIUM DEPENDENT REGULATION OF THE Ca²⁺ SENSITIVITY OF MYOSIN LIGHT CHAIN KINASE IN SWINE CAROTID ARTERY. ((D.A. Van Riper, B. A. Weaver, and C. M. Rembold)) Internal Medicine (Cardiology), University of Virginia, Charlottesville, VA (sponsor M. Barber)

In smooth muscle, the [Ca²⁺]_i sensitivity of myosin light chain (MLC) phosphorylation is dependent on the stimulus. We tested the hypothesis that changes in the [Ca²⁺]_i sensitivity of MLC phosphorylation result from decreases in the Ca²⁺ sensitivity of myosin light chain kinase (MLCK) which is known to result from phosphorylation of MLCK. We measured [Ca²⁺]_i with aequorin, the Ca²⁺ sensitivity of extracted MLCK with the kinase activity ratio assay, MLC phosphorylation, and isometric stress in swine carotid artery. As previously described, histamine stimulation induced a higher [Ca²⁺]_i sensitivity of MLC phosphorylation than was observed with high K⁺ stimulation. We found that increases in [Ca²⁺]_i were associated with decreases in the kinase activity ratio and that this relationship was independent of the stimulus. These data suggest that changes in MLCK phosphorylation are dependent primarily on [Ca²⁺]_i and are not responsible for the differences in the [Ca²⁺]_i sensitivity of MLC phosphorylation. Addition of forskolin (30 μ M) to high K⁺ depolarized tissues decreased myosin phosphorylation and force without significantly changing [Ca²⁺]_i or kinase activity ratio, suggesting that forskolin induced relaxation of 109 mM K⁺ induced contraction is not associated with changes in [Ca²⁺]_i or MLCK phosphorylation. Support: Markey, NIH HL38918, & VA AHA.

W-Pos45

VANADATE INHIBITS CROSSBRIDGE CYCLING BUT ACTIVATES CONTRACTION IN PERMEABILIZED SMOOTH MUSCLE. ((J. Lalli, G. Doerman and R.J. Paul)) Department of Physiology & Biophysics, University of Cincinnati College of Medicine, Cincinnati, OH 45267-0576 (Sponsored by T. Kirley)

We investigated the effects of sodium orthovanadate (VO₄) on contraction and activation of Triton X-100 permeabilized guinea pig taenia coli. Fibers were mounted isometrically and force measured with an AME 801 transducer. Control contractures were elicited with [Ca²⁺]_i = 6.6 μ M in Ca²⁺-EGTA buffered solutions. After attainment of a steady state, concentration-inhibition curves were measured. 10 μ M VO₄ was the apparent threshold level and 50% inhibition of isometric force occurred at approximately 50 μ M. 500 μ M VO₄ elicited a complete relaxation in agreement with previous studies. Although concentration >800 μ M completely inhibited contraction, surprisingly, a return to Ca²⁺-free conditions was associated with a partial contraction. After incubation with [VO₄] in Ca²⁺-free solutions for 10 min, fibers contracted when immersed in VO₄-free, Ca²⁺-free solution. A maximal contracture of approximately 70% of control was elicited by 4 mM VO₄. Pre-incubation with DTT (5 mM) completely blocked the activation by VO₄. Our results indicate that the effects of VO₄ are likely mediated by -SH group oxidation. The mechanism of activation by oxidation is unknown, but may be either a direct activation of smooth muscle myosin or mediated via phosphorylation/dephosphorylation. Supported by NIH HL22619 and TG HL07571.

W-Pos47

EFFECTS OF CALCIUM AND MYOSIN LIGHT CHAIN PHOSPHORYLATION ON THE FORCE-VELOCITY RELATION IN SMOOTH MUSCLE. ((U. Malmqvist and A. Arner)) Dept: Physiol. and Biophys., Lund University, Sweden (Spon. by B.J. Rydqvist)

The maximal shortening velocity (V_{max}) of smooth muscle is dependent on free calcium (Arner 1983. *Pflügers Archiv* 397:6). This is most likely due to variations in myosin light chain phosphorylation but might also involve direct effects of calcium via phosphorylation independent regulatory systems. We have used the phosphatase inhibitor okadaic acid (OA) to dissociate the effects of calcium and phosphorylation on V_{max}. Force-velocity relations were determined in chemically skinned fibres from the guinea pig taenia coli using the isotonic quick release method. Both force and V_{max} were dependent on [Ca²⁺]. At pCa 5.75 force was about 35% and V_{max} about 55% of the corresponding values at pCa 4.5. At pCa 6.0 force was essentially zero. At this [Ca²⁺] level OA (in the range 0.05 to 10 μ M) caused a dose-dependent increase in force. The maximal force at 10 μ M OA (pCa 6.0) was similar to that at pCa 4.5 in the absence of OA. When force (and myosin light chain phosphorylation) was varied with OA the relation between force and V_{max} was identical to that obtained when [Ca²⁺] was varied. OA did not influence force or V_{max} at pCa 4.5 or in thiophosphorylated fibres. In conclusion, the results suggest that the effects of calcium on V_{max} are mediated by myosin light chain phosphorylation and does not involve phosphorylation independent effects of calcium.

W-Pos48

INCREASES IN $[Ca^{2+}]_i$, MYOSIN LIGHT CHAIN (LC) PHOSPHORYLATION, AND FORCE DURING THE INITIATION OF SMOOTH MUSCLE CONTRACTION. ((R.A. Word, D.C. Tang, and K.E. Kamm)) Depts. of Ob-Gyn and Physiology, Univ of TX Southwestern Medical Center, Dallas, TX 75235.

Increases in free intracellular Ca^{2+} concentration ($[Ca^{2+}]_i$) initiate phosphorylation of myosin LC and force development in smooth muscle. We determined the temporal relationships of $[Ca^{2+}]_i$, LC phosphorylation, and force development in neurotransmitter-induced contractions of bovine trachealis and in spontaneously depolarized contractions of human myometrium. In trachealis, stimulus conditions that induced maximal force of contraction (80 V, 0.2 msec, 50 Hz) resulted in immediate and rapid increases in $[Ca^{2+}]_i$ (from 112 ± 5 to 295 ± 15 nM, $t_{1/2} = 2.0 \pm 0.3$ sec). After a 232 ± 34 msec latency period, contractile force increased at a slower rate ($t_{1/2} = 4.9 \pm 1.1$ sec). LC phosphorylation increased from 5 to 65% in 1.0 sec, and maximal levels were obtained prior to maximal increases in $[Ca^{2+}]_i$ (2.0 sec compared with 8.9 ± 1.5 sec). Likewise, during spontaneous depolarization of myometrium, the maximal extent of LC phosphorylation (41%) was obtained prior to maximal increases in $[Ca^{2+}]_i$ (234 nM) (3.0 compared with 17 ± 1.3 sec). In both smooth muscles (though using different sources of activating Ca^{2+}), increases in $[Ca^{2+}]_i$ preceded LC phosphorylation; but, the rate of increase in LC phosphorylation was significantly greater than the rate of increase in $[Ca^{2+}]_i$. We conclude that myosin light chain kinase (MLCK) is very sensitive to small increases in $[Ca^{2+}]_i$ in the first second after excitation and thereafter is less sensitive to activation by Ca^{2+}/CaM . These kinetic data are consistent with our previous findings that MLCK is phosphorylated and thus desensitized to Ca^{2+} after some delay during the initiation of smooth muscle contraction.

W-Pos50

STIFFNESS DOES NOT FOLLOW FORCE DURING SUSTAINED AGONIST STIMULATED CONTRACTIONS OF INTACT SINGLE VASCULAR SMOOTH MUSCLE CELLS.

((M. Yamakawa and F.V. Brozovich)) Bockus Research Institute, The Graduate Hospital, Philadelphia, PA 19146.

To determine the properties of sustained agonist induced contractions, we measured isometric force and relative stiffness during histamine activation of intact single vascular smooth muscle (VSM) cells. Single fully relaxed intact VSM cells were enzymatically isolated from the hog carotid artery and attached to glass electrodes, one of which was connected to a force transducer. The total amplitude of stiffness was measured with a constant amplitude (<0.4% L_0), sinusoidal oscillation (2 - 4 Hz) of cell length (Am. J. Physiol., in press). Activation with 5 μ M histamine increased both force and stiffness. During the 6 - 7 min of the contraction, the force level remained constant (n=4), or in some cases (n=2), decreased slightly. While after activation, stiffness gradually increased by up to 2 times. This indicates that during sustained contractions, force and stiffness transients do not follow the same time course. The decrease in the force per stiffness suggests that the force maintenance phase of agonist activated contractions of single intact VSM cells is accompanied by a modulation of the cross-bridge state(s), formation of a rigor-like state, and/or formation of force bearing structures other than cross-bridges. Support: NIH HL44181 and AHA EI (FVE).

W-Pos52

CONTRACTION OF SMOOTH MUSCLE CELLS IS NOT ASSOCIATED WITH A CHANGE IN INTRACELLULAR pH. (Michael A. Laflamme, David R. Walker, Peter L. Becker) Dept. of Physiology, Emory University, Atlanta, GA.

The calcium affinity of fura-2 is pH-sensitive. Because of the potential for pH-induced artifacts in fura-2 estimates of $[Ca^{2+}]_i$, it is essential to characterize the pH changes that occur under experimental conditions. In this study, we examined pH changes in isolated smooth muscle cells under a variety of experimental conditions normally employed to study Ca^{2+} regulation. Toad gastric smooth muscle cells were loaded with fura-2 and the pH-sensitive dye BCECF. Intracellular pH (pH_i) and $[Ca^{2+}]_i$ was monitored in cells bathed in bicarbonate (BR) and in 5 mM hepes-buffered (HR) Ringers solutions (pH 7.4) at rest and in response to local application of 10^{-6} M acetylcholine (ACh). $[Ca^{2+}]_i$ and pH_i were also monitored in cells bathed in a 20 mM Ca^{2+} , 5 mM TEA, hepes-buffered solution when depolarized under voltage clamp using a single microelectrode (containing 3M CaCl). Resting pH_i was $7.87 \pm .08$ (SEM), n=10 in BR and $7.55 \pm .05$, n=10 in HR solutions. In response to ACh, $[Ca^{2+}]_i$ rose and the cell contracted, but pH_i did not change ($\Delta pH = .00 \pm .02$, n=4, in BR and $-.02 \pm .02$, n=6, in HR). In cells depolarized under voltage clamp, $[Ca^{2+}]_i$ also rose and the cell contracted, but again pH_i did not change ($\Delta pH = -.005 \pm .005$, n=5) either in response to brief (<1 s) command pulses to 0 mV (from a holding V_m of -100 mV) or to an 8 s train of 200 msec depolarizing command pulses given at 2 Hz. These results indicate that cellular pH homeostatic mechanisms are sufficient to handle whatever proton changes occur in response to contractile stimuli regardless of external buffer, stimulus type, external $[Ca^{2+}]_o$, or microelectrode impalement. Further, we conclude that under these experimental conditions it is extremely unlikely that pH_i could cause calcium-independent fluctuations in the fluorescence of calcium dyes in this preparation. (Support: AHA Grant-In-Aid).

W-Pos49

CALCIUM SENSITIVITY OF MYOSIN LIGHT CHAIN PHOSPHORYLATION IN TRACHEAL SMOOTH MUSCLE. ((Tang, D.C., Kamm, K.E., and Stull, J.T.)) Department of Physiology, UT Southwestern, Dallas, TX 75235

Cytosolic Ca^{2+} concentrations required to increase myosin regulatory light chain (RLC) phosphorylation in smooth muscle cells treated with agonists that stimulate signal transduction pathways and release Ca^{2+} from sarcoplasmic reticulum (SR) are lower than those required by agents that simply increase Ca^{2+} influx. This difference in Ca^{2+} sensitivity for RLC phosphorylation is observed in bovine tracheal smooth muscle cells in culture stimulated with histamine (His) vs Bay K 8644 (BK). Pretreatment of intact cells with thapsigargin (Thap) did not alter the steady-state Ca^{2+} response to His but did decrease the extent of RLC phosphorylation to that observed with BK. Thap had no effect on the responses to BK. In smooth muscle cells made permeable with 8-escin, 0.3 μ M Ca^{2+} increased RLC phosphorylation from 8 \pm 4% to 21 \pm 4%. His plus GTP had no effect on RLC phosphorylation under relaxing conditions but increased phosphorylation to 36 \pm 5% in the presence of 0.3 μ M Ca^{2+} . Pretreatment of permeable cells with thapsigargin, menadione, or ryanodine (agents which disrupt SR function) had no significant effect on RLC phosphorylation in the presence of relaxing solution or 0.3 μ M Ca^{2+} alone. However, all 3 agents inhibited the potentiated response to His plus GTP. These results suggest that agonist-induced increases in Ca^{2+} sensitivity of RLC phosphorylation in smooth muscle are dependent upon a functional SR.

W-Pos51

THE EFFECT OF INTRACELLULAR pH AND BUFFER TYPE ON $[Ca^{2+}]_i$ AND CONTRACTION OF SWINE CAROTID ARTERY. ((Xiao-Liang Chen and Christopher M. Rembold)) Department of Internal Medicine (Cardiology), University of Virginia, Charlottesville, VA 22908

We evaluated how contractile agonists and changes in extracellular pH (pH_o) affect intracellular pH (pH_i) and intracellular $[Ca^{2+}]_i$ ($[Ca^{2+}]_i$) in arterial smooth muscle. Swine carotid medial tissues were loaded with BCECF to measure pH_i or sequestrin to measure $[Ca^{2+}]_i$. Resting pH_i was 7.11 ± 0.04 and $[Ca^{2+}]_i$ was 83 ± 9 nM when tissues were bathed in a MOPS buffer (an organic buffer). Resting pH_i was 7.27 ± 0.04 and $[Ca^{2+}]_i$ was 134 ± 46 nM in a KREBS buffer (an bicarbonate buffer). Changes in pH_i induced nearly proportional changes in pH_i , although the pH_i changes were slower in the KREBS buffer than in the MOPS buffer. This may represent a larger buffering capacity when tissues are bathed in the KREBS buffer. Extracellular acidosis induced a small relaxation and extracellular alkalosis induced a small contraction when tissues were bathed in the MOPS but not in the KREBS buffer. Histamine induced a substantial intracellular acidosis in MOPS and a smaller acidosis in KREBS buffer. The time course of the histamine-induced acidosis did not correlate with contraction. Histamine stimulation induced both a transient and sustained increase in $[Ca^{2+}]_i$ in both the MOPS and KREBS buffers. Changes in pH_i appeared not to be responsible for changes in $[Ca^{2+}]_i$ sensitivity. Support: Markey Trust, NIH HL38918, and the Virginia AHA.

W-Pos53

TEMPORAL RELATIONSHIPS AMONG FORCE, Ca^{2+} , ATPase ACTIVITY, AND MYOSIN LIGHT CHAIN PHOSPHORYLATION IN DETERGENT SKINNED SWINE CAROTID ARTERIES.

((Y. Zhang and R.S. Moreland)) Bockus Research Institute, Graduate Hospital, Philadelphia, PA 19146. (Spon. by S. Moreland)

Detergent skinned swine carotid fibers were used to simultaneously measure force and tissue ATPase activity; these measurements were correlated with levels of myosin light chain (MLC) phosphorylation. Tissue ATPase activity measured in the detergent skinned fiber was shown to be due to actin-activated myosin ATPase and not other cellular ATPases because cyclopiazonic acid, thapsigargin, cisapride, quercetin, and ouabain, all inhibitors of cellular ATPases, had no inhibitory effect on basal or Ca^{2+} stimulated tissue ATPase activity. In addition, okadaic acid did not inhibit either basal or Ca^{2+} stimulated ATPase activity which clearly demonstrates that MLC kinase/MLC phosphatase activity does not significantly contribute to total ATPase activity. We then examined whether myosin ATPase activity correlates to the level of Ca^{2+} and/or MLC phosphorylation. Force development in response to 1 or 7 μ M Ca^{2+} was characterized by a monotonic increase in MLC phosphorylation, while myosin ATPase activity increased transiently achieving a stable suprabasal value with time. High levels of force were maintained following a decrease in the $[Ca^{2+}]_o$ from 7 to 1 μ M. Force maintained by 1 μ M Ca^{2+} was characterized by similar levels of MLC phosphorylation as those determined during the development of force in response to 1 μ M Ca^{2+} , however myosin ATPase activity was significantly lower. These results demonstrate that MLC phosphorylation is not the sole regulator of actin-activated myosin ATPase activity. There is a time or Ca^{2+} dependent process that slows myosin ATPase activity at constant levels of MLC phosphorylation. Supported by NIH HL 37956.

W-Poe54

CHELERYTHRINE SPECIFICALLY INHIBITS THE NOREPINEPHRINE AND GTP DEPENDENT INCREASE IN Ca^{2+} SENSITIVITY IN ALPHA-TOXIN PERMEABILIZED RABBIT MESENTERIC ARTERY ((H.Y. Ahn and R.S. Moreland) Bockus Research Institute, Graduate Hospital, Philadelphia, PA 19146. (Spon. by N.J. Lodge)

Smooth muscle myofibrillar Ca^{2+} sensitivity is increased following agonist activation as compared to stimulation by membrane depolarization. Studies using alpha-toxin permeabilized smooth muscle, in which receptor and G-protein mediated pathways are intact, have suggested that the enhanced Ca^{2+} sensitivity may be the result of either G-protein dependent inhibition of a myosin light chain (MLC) phosphatase or activation of protein kinase C (PKC). The goal of this study was to determine the effects of chelerythrine, a specific inhibitor of PKC activity, on force and MLC phosphorylation levels during Ca^{2+} plus norepinephrine (NE) plus GTP induced contractions of alpha-toxin permeabilized rabbit mesenteric arteries. Stimulation of the permeabilized arteries with $1 \mu M Ca^{2+}$ alone elicited a sustained increase in levels of force and MLC phosphorylation. The addition of NE plus GTP significantly enhanced both force and MLC phosphorylation levels consistent with the hypothesis of G-protein dependent MLC phosphatase inhibition. Chelerythrine ($100 \mu M$) had no effect on force or MLC phosphorylation levels in response to $1 \mu M Ca^{2+}$ alone but specifically abolished the NE plus GTP dependent increase in both parameters suggesting the involvement of PKC. These results suggest that MLC phosphatase activity may be down-regulated by G-protein dependent activation of PKC. This regulation may be direct by phosphorylation of the phosphatase or indirect by phosphorylation induced activation of a phosphatase inhibitor. Supported in part by NIH HL 37956 and WW Smith Charitable Trust Grant H9103.

W-Poe56

MUSCLE LENGTH HISTORY IS A DETERMINANT OF ISOTONIC SHORTENING VELOCITY IN CANINE TRACHEAL SMOOTH MUSCLE. ((S.J. Gunst, M.F. Wu, and D. Smith) Dept. of Physiology and Biophysics, Indiana Univ. Sch. of Medicine, Indianapolis, IN 46202

In smooth muscle tissues, the isotonic shortening velocity is a function of the external load and muscle length during shortening, the contractile stimulus, and the duration of isometric contraction prior to the measurement. We investigated whether the isotonic shortening velocity is also affected by the length history of the muscle during contraction. Muscles were first contracted isometrically at L_0 , $0.85L_0$, or $0.70L_0$ using electrical field stimulation. After 20 sec, they were either: (Protocol 1), stepped to $0.70L_0$, and allowed to shorten isotonically under a 5, 10 or 20% afterload; or (Protocol 2), allowed to shorten under the same afterloads with no length step. Instantaneous shortening velocities were plotted with respect to instantaneous muscle length during shortening. In all cases, velocities decreased progressively during isotonic shortening at a nearly constant rate with respect to instantaneous muscle length. Velocities were highest after contraction at $0.70L_0$, and lowest after contraction at L_0 . Identical length-velocity curves were obtained for Protocols 1 and 2 after isometric contraction at the same muscle length. Results demonstrate that the isotonic shortening velocity of tracheal muscle is not unique under conditions which are identical with respect to external load, muscle length during shortening, contractile stimulus and the duration of isometric contraction prior to shortening. The velocity is also modulated by the mechanical conditions present at the time the muscle is activated. Results suggest that the relationship between the contractile filaments and cytoskeletal elements is not fixed but is determined upon activation of the muscle. Supported by PHS HL29289.

W-Poe58

DEPENDENCE OF ATP CONSUMPTION AND THE ECONOMY OF FORCE GENERATION ON CROSS-BRIDGE PHOSPHORYLATION IN THE SWINE CAROTID MEDIA. ((C. J. Wingard¹, R. J. Paul², C. M. Rembold^{1, 3}, and R. A. Murphy¹) Departments of Physiology¹ and Internal Medicine (Cardiology)³, University of Virginia, Charlottesville, VA. 22908 and Department of Physiology and Biophysics², University of Cincinnati, Cincinnati, OH. 45267. (Spon. by B. Gaytann)

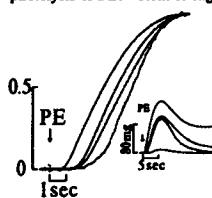
We evaluated the energetics of force generation in arterial smooth muscle. Oxygen consumption (J_{O_2}) and lactate production (J_{lac}) were measured, and ATP consumption (J_{ATP}) was calculated in porcine carotid media ring preparations set at optimal length (L_0) for force generation (See Table, N = 8). J_{O_2} at all levels of phosphorylation did not exceed the metabolically uncoupled J_{O_2} in rings exposed to $100 \mu M$ dinitrophenol. K^+ -depolarization increased steady-state phosphorylation, J_{O_2} , and J_{ATP} while inducing a near maximal contraction. K^+ -depolarization in a Na^+ -free (TRIS) + $100 \mu M$ Histamine solution significantly increased phosphorylation and J_{O_2} , while stress increased modestly. The calculated economy (stress / suprabasal J_{ATP}) in isometric contraction decreased with increasing phosphorylation suggesting that economy is a regulated parameter in smooth muscle. These results will be compared to the predictions of several 4-state models for cross-bridge regulation in vascular smooth muscle, (R. J. Paul, Am. J. Physiol. 258: C369-C375, 1990; C-M. Hai and R.A. Murphy, Physiol. J. 61: 530-541, 1992). Supported by NIH (HL19242; HL223240, HL226119) and AHA-VA-92-F39.

STIMULUS	% PHOS. mol Pi / mol L.C.	J_{O_2} nmol / min · g	STRESS $\times 10^3 N / m^2$	ECONOMY $\times Stress / J_{ATP}$
Resting	5.6 ± 1.6	58.0 ± 5.9	0.007 ± 0.003	—
K^+ (109) mM	20.0 ± 1.9	87.8 ± 8.6	1.753 ± 0.010	0.0143 ± 0.0036
K^+ , TRIS & Hist.	52.0 ± 1.9	114.3 ± 13.0	2.123 ± 0.123	0.0075 ± 0.0011

W-Poe55

KINETICS OF α -ADRENERGIC ACTIVATION IN VASCULAR SMOOTH MUSCLE STUDIED BY LASER PHOTOLYSIS OF CAGED PHENYLEPHRINE. ((Robert J. Barsotti, Hunter Martin, & Jeffery W. Walker^{**}) Bockus Research Institute, The Graduate Hospital, Phila., PA 19146, *Department of Physiology, University of Wisconsin, Madison, WI 53706

The time course of agonist induced contraction of smooth muscle consists of an initial delay before the onset of force (Somlyo et al., *Philos. Trans. R. Soc., London*, 320:399, 1988). The goal of this study was to examine the dose dependence of this delay and the rate of the rise of force and stiffness in an effort to determine the rate limiting step in agonist induced smooth muscle activation. Strips of intact caudal artery of the rat were stimulated by laser pulse photolysis of a new form of caged phenylephrine (PE): O-(α -carboxyl)-2-nitrobenzyl phenylephrine, whose quantum yield and photolysis rate are 3 and 3000 times those of previous forms. The [PE] released was varied between 50 nM and 50 μM by changing the [caged PE] and keeping the laser energy constant. The duration of the delay decreased as [PE] increased, reaching a minimum of 0.93 ± 0.09 sec at $25^\circ C$ (mean \pm sem, n=7). The amplitude of the force response was dose dependent (inset), while the 10-90% rise time of force was relatively constant at 3.4 sec (see Figure, forces are normalized to maximum). The time course of the change in tissue stiffness was similar to that of force. These results suggest that the reactions in the



activation pathway of smooth muscle from agonist-receptor interaction up to and including the activation of myosin light chain approach equilibrium before the onset of force, as suggested by Barr & Gu (*Biophys. J.*, 51:895, 1987) and that the apparent rate of at least one process, occurring during the delay, increases at higher [PE].

W-Poe57

EFFECT OF TEMPERATURE ON $[Ca^{2+}]_i$, PHOSPHORYLATION, AND STRESS IN RABBIT BLADDER SMOOTH MUSCLE. ((S.-C. Kwon, C.M. Rembold^{*}, and R.A. Murphy[†]) Departments of Physiology and Internal Medicine (Cardiology^{*}), University of Virginia, Charlottesville, VA 22908.

We investigated K^+ -induced desensitization and carbachol-induced sensitization in rabbit urinary bladder preparations at 22 and $37^\circ C$. Tissues were either loaded with aequorin to measure $[Ca^{2+}]_i$ or frozen for determination of myosin light chain phosphorylation. K^+ -depolarization induced phasic contractions and carbachol induced tonic contractions. Carbachol, but not K^+ contractions were significantly slowed at $22^\circ C$. The $[Ca^{2+}]_i$ -sensitivity of phosphorylation was higher with carbachol than with K^+ depolarization at both 22 and $37^\circ C$. In K^+ -depolarized tissues, addition of carbachol increased phosphorylation and stress without increasing $[Ca^{2+}]_i$ at both 22 and $37^\circ C$. This suggests that carbachol can resensitize rabbit bladder that has been previously desensitized by high K^+ as previously shown for other smooth muscles (Himpens, Matthijs and Somlyo, *J. Physiol. (Lond.)* 413: 489-503, 1989). The relationship between phosphorylation and contractile stress was almost linear at $22^\circ C$ and was independent of stimulus. At $37^\circ C$, the dependence of stress on phosphorylation was steeper and non-linear. Surprisingly, maximally activated stress was much higher at $22^\circ C$ ($1.33 \pm 0.32 \times 10^9 N/m^2$) than at $37^\circ C$ (0.74 ± 0.07) while phosphorylation was modestly increased (44.4 ± 7.1 vs. $35.8 \pm 3.4\%$). These data suggest that temperature can substantially alter the dependence of stress on myosin phosphorylation. Supported by NIH grants HL19242 and HL38918.

W-Poe59

INTERRUPTED SHORTENING IN SMOOTH MUSCLE: IMPLICATIONS FOR THE MECHANISM OF CONTRACTION. ((R.A. Meiss), Indiana University School of Medicine, Indianapolis, IN 46202.

During isotonic shortening in smooth muscle the velocity steadily decreases. This has been variously attributed to an internal load, to shortening-induced inactivation, or to a length- or time-dependent decrease in the number of active crossbridges. To determine whether external factors could modify this behavior, two methods were used to cause brief interruptions of afterloaded shortening in rabbit ovarian ligament muscle. At similar times during isotonic contraction, either a 1-second episode of sinusoidal length vibration (SLV; 50 Hz, approx. 5% of L_0) or a 1-second step-increase in force (FS) was applied. Both were chosen to be sufficient to arrest shortening. Plots of unmodified length vs. velocity were approximately linear; SLV interrupted (but did not substantially alter) this relationship, and velocity was appropriate to muscle length and contraction time before and after SLV. During FS the velocity fell to zero; after FS, the velocity increased to about 110% of the pre-FS value. This may be due to the effects of crossbridge recruitment during the FS. SLV produced interruptions of shortening proportional to frequency, duration, amplitude, and to the afterload. Recovery from isotonic SLV and FS episodes was very rapid, but SLV applied during isometric contraction produced a large fall in force with a slow recovery. SLV and FS (for the same final afterload) applied together were more effective than either alone. These results imply a forced detachment of crossbridges (by FS) and a transient contractile element displacement (by SLV).

W-Pos60

DIFFERENT LEVELS OF INTRACELLULAR CALCIUM ($[Ca^{2+}]_i$) BETWEEN SMOOTH MUSCLE ISOMETRIC AND ISOTONIC CONTRACTIONS. ((H. Jiang, J. Wang, K. Rao, and N. L. Stephens)) Dept. of Physiol., Univ. of Manitoba, Winnipeg, Manitoba R3E 0W3 Canada.

The major regulatory role of the Ca^{2+} -calmodulin-myosin light chain kinase (MLCK) pathway in smooth muscle contraction has been generally accepted except that most of the studies were conducted under isometric conditions, with the physiological importance of isotonic shortening being overlooked. Different time courses of the 20 kDa myosin light chain (MLC₂₀) phosphorylation between these two kinds of contraction had been reported by us. Muscle shortening resulted in the partial inhibition of MLC₂₀ phosphorylation. In order to elucidate the mechanisms for such inhibition, $[Ca^{2+}]_i$ levels (*Fura-2*) were monitored during isotonic and isometric contractions of canine tracheal smooth muscle. The results obtained were consistent with our biochemical findings. Although $[Ca^{2+}]_i$ showed initial transient increases and later plateaus both in isometric and isotonic contractions elicited by KCl, histamine and acetylcholine, quantitative difference in $[Ca^{2+}]_i$ existed between isometric and isotonic contractions. A much smaller calcium transient was found in isotonic shortening. Our results suggest that: 1) length change may play a role in regulating $[Ca^{2+}]_i$, MLC₂₀ phosphorylation, and crossbridge cycling of smooth muscle; 2) the inhibitory effect of shortening on $[Ca^{2+}]_i$ may serve as part of the "internal resistor", preventing the muscle from excessive shortening. mechanism(s) of length on $[Ca^{2+}]_i$ is unclear. (Supported by the Natl. Ctr. of Excellence, Res. Health, Canada; H. Jiang is a M.R.C. fellowship recipient, K. Rao is supported by a fellowship from Manitoba Lung Assoc. and J. Wang is supported by a Man. Health Res. Coun. Studentship).

W-Pos62

SHORTENING-INDUCED INACTIVATION OF FLUOROALUMINATE- AND GTP- γ -S-MEDIATED CONTRACTION AND MYOSIN PHOSPHORYLATION IN SMOOTH MUSCLE.

((Chun Bong Benjamin Ma and Chi-Ming Hai)) Div. Biol. & Med., Brown University, Providence, RI 02912. (Spon. by K. Chapman)

GTP-binding proteins in bovine tracheal smooth muscle strips were activated by fluoroaluminate and GTP- γ -S, and the sensitivities of fluoroaluminate- and GTP- γ -S-induced active stress and myosin phosphorylation to muscle shortening were compared. In comparison with the value of myosin phosphorylation at L_0 , unloaded shortening induced a 63% decrease in fluoroaluminate-activated steady-state myosin phosphorylation, but had no significant effect on GTP- γ -S-activated myosin phosphorylation. These results were consistent with the hypothesis that shortening-sensitive and shortening-insensitive signal transduction pathways coexist in airway smooth muscle. However, unlike myosin phosphorylation, active stress induced by fluoroaluminate was actually less sensitive to shortening. The amount of shortening necessary to reduce active stress to half of that at L_0 was 65% in fluoroaluminate-activated tissues, but was only 34% in GTP- γ -S-activated tissues. The observation of different sensitivities of fluoroaluminate-activated myosin phosphorylation and active stress suggests that GTP-binding proteins modulate the dependence of active stress on muscle length in smooth muscle, via mechanisms independent of myosin phosphorylation.

W-Pos64

THE PROTEIN PHOSPHATASE INHIBITOR, OKADAIC ACID, INHIBITS INCREASES IN STRESS, CALCIUM AND MYOSIN PHOSPHORYLATION PRODUCED BY K^+ -DEPOLARIZATION IN ARTERIAL MUSCLE. ((J.J. Sadighian, F.A. Lattanzio, and P.H. Ratz)) Eastern Virginia Medical School, Norfolk, VA 23501.

Smooth muscle contractile agents increase the level of isometric stress by elevating cytosolic free calcium levels ($[Ca^{2+}]_i$) and the extent of myosin phosphorylation. The ser/thr protein phosphatase inhibitor, okadaic acid (OA), increases stress by directly increasing the extent of myosin phosphorylation. However, recent studies have shown that OA can also reduce stress produced by contractile agents. How relaxation occurs is not clear because OA has been reported to decrease stress without reducing $[Ca^{2+}]_i$ (artery) and the extent of myosin phosphorylation (trachea). In this study we found that OA inhibited stress and concomitantly reduced $[Ca^{2+}]_i$ and the extent of myosin phosphorylation produced by K-depolarization (KCl). In addition, OA inhibited steady-state stress but only slightly reduced initial stress produced by the receptor agonists, histamine and phenylephrine. Because initial and steady-state stress are largely dependent on the mobilization of, respectively, intracellular and extracellular calcium, these data suggest that OA relaxed rabbit femoral arteries by selectively reducing calcium influx, presumably by elevating the level of calcium channel phosphorylation.

W-Pos61

SHORTENING-INDUCED INACTIVATION OF PHOSPHATIDYLINOSITOL (PI) TURNOVER AND MYOSIN PHOSPHORYLATION IN SMOOTH MUSCLE. ((R.E. Ellis and C.-H. Hai)) Div. Biol. & Med., Brown University, Providence, RI 02912.

Muscarinic activation of airway smooth muscle induces PI turnover, increase in cytosolic $[Ca^{2+}]_i$, and myosin light chain phosphorylation. We investigated shortening-induced inactivation of PI turnover and myosin light chain phosphorylation in carbachol-activated bovine tracheal smooth muscle. PI turnover was measured using 3H -inositol in 10 mM LiCl. Myosin phosphorylation was measured by two-dimensional polyacrylamide gel electrophoresis. The data are shown as follows:

	3H -IP ₁ 10 ⁴ cpm/g	Myosin Phosphorylation mole P _i /mole LC
Control (Unstimulated)	2.5 ± 0.6	0.17 ± 0.03
Isometric Contraction	6.6 ± 0.7	0.43 ± 0.05
Unloaded Shortening	4.5 ± 0.8	0.26 ± 0.03
Unloaded Shortening with Prior Pre-Shortening	3.2 ± 0.7	0.22 ± 0.04

Linear regression analysis of the paired 3H -IP₁ and myosin phosphorylation data yielded a correlation coefficient of 0.98 and intercepts near origin. The observed proportional inactivation of PI turnover and myosin phosphorylation suggests that shortening-induced inactivation of PI turnover may be sufficient to explain shortening-induced inactivation of myosin phosphorylation in smooth muscle.

W-Pos63

NITROVASODILATORS RELAX ARTERIAL SMOOTH MUSCLE IN PART BY DECREASING THE CALCIUM SENSITIVITY OF PHOSPHORYLATION. ((N.L. McDaniel, P.W. Girling, R.A. Murphy and C.M. Rembold)) University of Virginia, Charlottesville, VA 22908

We have previously shown that sustained relaxation of maximally stimulated swine carotid artery induced by nitroglycerin (NTG) or sodium nitroprusside (SNP) was associated with elevation of $[cGMP]$ and reductions in force for a given level of myosin phosphorylation (Am. J. Physiol. 263: C461-467, 1992). In this project we tested the hypothesis that the acute phase of nitrovasodilator-induced relaxation is associated with decreases in the calcium sensitivity of myosin phosphorylation. Aequorin estimated $[Ca^{2+}]_i$ (nM), myosin light chain phosphorylation (mol P_i/mol MLC by 2D gel electrophoresis), and stress ($\times 10^5$ N/m²) were measured in swine carotid media tissues at 37° C. Ten μ M histamine induced $[Ca^{2+}]_i$ and phosphorylation transients associated with rapid stress development. NTG (100 μ M) or SNP (100 μ M) was added 10 minutes after histamine stimulation, and induced approximately half-maximal relaxation. Small transient reductions in $[Ca^{2+}]_i$ were noted one minute after SNP or NTG addition. At both one and four minutes after NTG or SNP addition, significant decreases in myosin phosphorylation were observed without significant decreases in $[Ca^{2+}]_i$. This data suggests that nitrovasodilators acutely reduce the calcium sensitivity of phosphorylation. (Spons. by AHA #92004100; AHA Virginia Affiliate #92-G-12; NIH #HL19242, HL38918)

W-Pos65

DIFFERENTIAL RESPONSE OF DOG AND PIG TRACHEAL SMOOTH MUSCLE TO ACETYLCHOLINESTERASE INHIBITOR. ((L.C. Gershman, R.R. Kyle, H.J. Bryant, and P.H. Abbrecht)) Stratton D.V.A. Medical Center, Albany, NY 12208 and Departments of Physiology and Medicine, USUHS, Bethesda, MD 20814.

It has been reported that the cholinesterase inhibitor soman (O-(1,2,2-trimethylpropyl)-methyl 1-phosphonofluoridate) causes a marked increase in upper airway resistance in the dog. Preliminary experiments in which tracheal rings from dog and pig were exposed to soman suggested that response to soman was much greater in tracheal rings from the dog than from the pig. The effect of soman on resting tension, response to electrical field stimulation (EFS), and on half-relaxation time of EFS-train induced contractions was measured in isolated tracheal smooth muscle (TSM) preparations from dog and pig. The resting tension of dog TSM preparations is increased much more by soman than is the case for pig TSM. However, the effect of soman on response of TSM to EFS stimulation and on half-relaxation time of EFS-train induced contractions was similar for preparations from both animals. The latter finding suggests that acetylcholinesterase inhibition and diffusion of acetylcholine from the neuroeffector junction are similar in both dog and pig TSM. The results suggest that there is a high basal acetylcholine release within the neuroeffector junction for dog TSM.

W-Pos66

OUABAIN AUGMENTS CAFFEINE CONTRACTIONS IN RAT MESENTERIC ARTERY: EVIDENCE FOR A Na PUMP COMPONENT WITH HIGH SENSITIVITY TO OUABAIN. ((D.N. Weiss, D.J. Podberesky, J. Heidrich and M.P. Blaustein)), Dept of Physiology and ¹Cardiol. Div., Dept of Med, Univ. of Maryland Sch. of Medicine, Baltimore, MD 21201

Ouabain (OU), a hypertensinogenic (*FASEB J.* 6:A945, 1992) adrenal cortical hormone (*PNAS USA* 88:6259, 1991), sensitizes vascular smooth muscle (VSM) to vasoconstrictors and may thereby regulate vascular reactivity and tone. We tested low doses of phenylephrine (PE) and OU on 10 mM caffeine (Caf)-evoked isometric tension (T) in rings of rat small (<400µm) mesenteric artery. Caf response amplitude indicated the relative amount of sarcoplasmic reticulum (SR) Ca²⁺. OU, alone, or PE, alone, increased tonic (resting) T and Caf-evoked T in a dose-dependent manner. Neither 1-3x10⁻⁶ M PE nor 10⁻⁶ M OU, alone, increased baseline tonic T, but the OU dose-Caf response curve was shifted leftward (i.e., to lower OU doses) by 1-3x10⁻⁶ M PE; the PE dose-Caf response curve was shifted leftward by 10⁻⁶ M OU. In 3x10⁻⁶ M PE, the OU dose vs Caf-evoked T curve was biphasic: 10⁻⁶ M OU induced a small but significant increase in Caf-evoked T (123±8% of control; n=10; p<0.01) and >10⁻⁶ M OU greatly increased Caf-evoked T. The data show that low doses of PE and OU are synergistic. Caf selectively mobilizes SR Ca²⁺; thus, Caf response amplification indicates that OU sensitizes VSM to vasoconstrictors, at least in part, by augmenting the SR Ca²⁺ store. The biphasic OU dose vs Caf-evoked T curve suggests that rat VSM cells have Na⁺ pumps with at least two different α subunit isoforms, one of which (probably α3) is very sensitive to OU (EC₅₀ circa 10⁻⁶ M). These findings may help to account for the hypertensinogenic effect of OU.

W-Pos68

AFTER-LOADED ISOTONIC RELAXATION OF CANINE TRACHEAL SMOOTH MUSCLE IS FACILITATED BY TRANSIENT ZERO LOAD SHORTENING ((W. Li, X. MA & N.L. STEPHENS)) Dept. of Physiology, Univ. of Manitoba, Winnipeg, Manitoba, Canada R3E 0W3

This is the first report of the phenomenon of facilitation of after-loaded isotonic relaxation induced by the brief interposition of a zero load shortening. In the course of a supramaximal electrically elicited, 8 s, isotonic contraction of canine tracheal smooth muscle carrying a load equal to 35% of relaxation time was measured by turning off the stimulus at 8 s. The relaxation time developed in a second contraction identical to the first one with a 3 second zero load shortening abruptly imposed just after the 8s point, was 8% less (p<0.05) than that of the first one. Further experiments showed that the stiffness of the relaxing muscle subjected to a zero load shortening was less than that in the absence of zero load shortening, indicating that zero load shortening had reduced the cycling crossbridge number. Experiments using a double quick release and double stimulus technique showed that in addition to the reduction of muscle stiffness, the zero load velocity (V₀) at the time of 2 s after the first zero load shortening being finished was less than that of a release made at the same time point in the absence of the initial zero load shortening. A tentative explanation for our results is that latch bridges made in the later phase of muscle excitation produce internal resistance and reduce the velocity of normally cycling bridges. Zero load shortening results in the breakage of normally cycling bridges and further reduction in shortening velocity. These findings can best be explained on the basis of Murphy's latch bridge hypothesis.

(Supported by an operating grant from the Council for Tobacco Research, W. Li is the recipient of a studentship from the Manitoba Health Research Council)

W-Pos67

INFLUENCE OF A SUPEROXIDE PRODUCING XENOBIOTIC ON CONTRACTION OF RABBIT AORTIC SMOOTH MUSCLE ((John D. Edmondson and George D. Ford)) Medical College of Virginia, Virginia Commonwealth University, Richmond, VA 23298

The role of reactive oxygen intermediates (ROI), such as the superoxide anion (SOA), in the pathophysiology of cardiovascular diseases is a topic of great interest. We have used the xenobiotic nitrazepam (NZ), an agent shown to selectively generate SOA intracellularly, to test the influence of this ROI on the contractility of arterial strips. Phenylephrine (PE) was used to generate pre-exposure (control) and post-exposure contractions. The response to 1.0 µM ACh was used to verify presence or absence of endothelium. Aortic rings were exposed to varying concentrations of NZ (5, 10, and 15 minute exposures) in the presence and absence of endothelium. Aortic strips with intact endothelium showed attenuated response to PE at all NZ exposures, with only 63% force generated after 15-minute exposure to 0.1 mM NZ (n=6). Aortic strips with mechanically denuded endothelium showed enhanced contraction at short term exposure, 112% of control at 5 minutes (n=6), and attenuated contraction with prolonged exposure, 48% of control at 15 minutes (n=6), again with 0.1 mM NZ.

The results on the endothelium-denuded preparations are consistent with previous findings in subcellular preparations which demonstrated SOA effects on both IP₂-induced Ca²⁺-release and Ca²⁺ sequestration of the muscle's sarcoplasmic reticulum. The results with the endothelium intact then argue that NZ also influences the endothelial cells role in the contractile response to PE. (Supported by a grant-in-aid from the American Heart Association/Virginia Affiliate to GDF).

W-Pos69

A RAPID AND TRANSIENT INCREASE IN PHOSPHORYLATION OF THE ACTIN-MEMBRANE ATTACHMENT PROTEIN TALIN OCCURS DURING SMOOTH MUSCLE CONTRACTION. ((F.M. Pavalko, L. Adam, M.H. Al-Hassani and S.J. Gunst)) Department of Physiology and Biophysics, Indiana University School of Medicine, Indianapolis, IN 46202.

Proteins such as talin, vinculin, and α-actinin are thought to participate in linking actin filaments to the plasma membrane. Evidence from non-muscle tissue culture cells suggests that phosphorylation of these and other actin-membrane attachment proteins in focal adhesions may regulate their function with dramatic consequences on the overall organization of the actin cytoskeleton. It has been difficult, however, to correlate phosphorylation of these proteins with any actin-mediated function of cells grown in culture. The membrane-associated dense plaques of smooth muscle contain most of the same actin-membrane attachment proteins as focal adhesions and are thought to be functionally analogous to focal adhesions as sites of actin filament attachment in smooth muscle. We have examined the phosphorylation state of dense plaque-associated cytoskeletal proteins during the contraction of ³²P-labeled canine tracheal smooth muscle strips. By immunoprecipitating talin from muscle extracts, we found that an increase in the phosphorylation of talin occurs within 15 sec. of stimulation with acetylcholine (10⁻³ M) and then rapidly decreases to baseline levels within 3 min. This time course parallels changes in intracellular Ca²⁺, which could indicate a Ca²⁺-dependence of talin phosphorylation. Thus, talin phosphorylation may be involved in receptor-mediated smooth muscle activation, possibly by regulating the attachment of actin filaments to the membrane at dense plaques. Regulation of coupling between dense plaque-associated cytoskeletal proteins and contractile filaments may play an important role in modulating the functional properties of smooth muscle tissues. Supported by PHS HL 29289 and by the American Heart Association, Indiana Affiliate.

TUBULIN AND MICROTUBULES

W-VCR1

TAXOL-INDUCED FLEXIBILITY OF MICROTUBULES AND ITS REVERSAL BY MAP-BINDING. ((R.B. Dye and R.C. Williams, Jr.)) Department of Molecular Biology, Vanderbilt University, Nashville, Tennessee 37235.

Microtubules, observed *in vitro* by video-enhanced DIC microscopy, are quite inflexible (Young's modulus near 10⁹ dynes-cm⁻²). If glass-adherent pieces of sperm-tail axonemes are employed as nuclei, and microtubules are assembled in a flow-chamber, the extent to which they bend in a flow of buffer can be employed as a rough measure of their flexibility. When taxol (50 µM) was introduced into the flow (0.03 cm²/sec), microtubules composed of pure tubulin rapidly (<1 sec) developed a wavy appearance and become strikingly flexible. When MAP-2 (0.1 mg/ml) or tau were subsequently added to these taxol-treated microtubules, their flexibility disappeared within 1-2 minutes, and their appearance became indistinguishable from that of untreated microtubules. That the MAP-induced rigidity was not due to loss of taxol was shown by the fact that flexibility was restored when the MAPs were removed by briefly including 0.4 M NaCl in the flow of buffer. One interpretation of these observations is to suppose that the rigidity of microtubules results from strong circumferential interactions between protofilaments, that binding of taxol greatly reduces the strength of these interactions, and that MAPs increase their strength, perhaps by bridging protofilaments. Supported by NIH GM25638.

W-Pos70

TAXOL INCREASES THE FLEXURAL RIGIDITY OF MICROTUBULES. ((B. Mickey, F. Gittes*, and J. Howard)) Dept. of Physiology & Biophysics and *Center for Bioengineering, Univ. of Washington, Seattle WA 98195.

Microtubules are polymers of the dimeric protein tubulin which perform structural roles in cells. We have previously measured the flexural rigidity of taxol-stabilized microtubules to be 2.15±0.08·10⁻²³Nm² (Gittes *et al.*, *J. Cell Biol.*, in press). Taxol is an antimitotic alkaloid which stabilizes microtubules by decreasing the dissociation rate of dimers from the polymer. We asked the question: does taxol also affect the rigidity of microtubules?

In the absence of taxol it is difficult to measure the rigidity of microtubules because, at 25°C, they depolymerize within minutes. To circumvent this problem, GMP-CPP-tubulin was polymerized onto the ends of freshly-grown microtubules, creating stable cap regions which prevented the microtubules from depolymerizing. Rhodamine-labelled tubulin was polymerized for 50 minutes at 37°C with GTP, MgCl₂, and DMSO. The microtubules were diluted into unlabelled tubulin and 0.5 mM GMP-CPP for 5 minutes; this resulted in stable, slightly fluorescent, distinct caps. Unconstrained microtubules in a solution depth of less than ~3 µm were imaged by fluorescence microscopy at 25°C and recorded on videotape, from which microtubule shapes were digitized.

The flexural rigidity of four microtubules, ranging in length from 30 to 54 µm, was measured. Our method of measurement decomposes the shape of the microtubule into Fourier modes, so several independent estimates could be obtained from a single microtubule. The weighted mean flexural rigidity from 12 measurements was 3.81±0.22·10⁻²⁴Nm², corresponding to a persistence length of 930±50 µm. These microtubules are 5-6 times less stiff than taxol-stabilized rhodamine-labelled microtubules: a remarkable result, considering that taxol (MW=769) adds virtually no mass to the polymer.

W-Pos71

CONFORMATIONAL STUDIES ON TUBULIN HETERODIMERS BY CD, LASER RAMAN AND THIN SECTION. ((J.J. Correia*, B.S. Hennington*, A. Thureson-Klein*, T. Lit, G.J. Thomas, Jr.†) *Dept. of Biochemistry, Univ. of Mississippi Medical Center, Jackson, MS. 39216 and †Division of Cell Biology and Biophysics, University of Missouri-Kansas City, Kansas City, MO. 64110.

Tubulin heterodimers bind GDP or GTP at an exchangeable site on the β -subunit. GDP-tubulin favors the formation of single or double walled rings. GTP-tubulin favors the formation of microtubules. Previous CD studies (5–50 μ M concentrations) done as a function of pH and temperature demonstrated that the nucleotide content does not alter the near- or far-UV CD spectra of tubulin (J.J. Correia, J. Cell Biol. 107, 669a, 1989). Studies by laser Raman spectroscopy (1–2 mM concentrations) reveal significant differences in protein secondary structure and/or side-chain configuration of GDP-tubulin and GTP-tubulin. The exchange of GTP for GDP causes a significant decrease in α -helix and an increase in β -sheet. There are also changes associated with skeletal C-C stretching vibrations that may reflect changes in side-chain orientations. Thin section studies on pellets of GDP- and GTP-tubulin heterodimers reveal a time dependent formation of tubulin rings and ring aggregates with GDP- but not GTP-tubulin. The ring aggregates are laterally associated with occasional stacks of rings. Thus, any conformational differences observed by laser Raman spectroscopy may be due in part to packing forces within the rings and ring aggregates. [Supported by NIH grant GM41117 (J.J.C.) and AI11855 (G.J.T.)]

W-Pos73

AN ELECTRON CRYSTALLOGRAPHIC STUDY OF TUBULIN CRYSTAL FORMS

((Sharon G. Wolf, Gervaise Mosser, and Kenneth H. Downing)) Life Sciences Division, Donner Laboratory, Lawrence Berkeley Lab, Berkeley, CA 94720.

It is known that zinc ions can induce tubulin to polymerize into two-dimensional crystalline sheets suitable for structural studies using electron crystallography. We have refined conditions in order to control crystal growth, and can obtain large, well ordered sheets up to about 2 μ m in width. Adding NaCl to the incubation solution slows down the rate of crystal growth, but significantly retards the degradation of the tubulin crystals. We have obtained electron diffraction and image data to better than 4 Å resolution, using samples embedded in glucose. In projection maps calculated from the data, the α and β monomers can be identified within the protofilament, as well as detailed of internal structure not seen in lower resolution work. Such high quality data encourages us to proceed with a full 3-D reconstruction at high resolution.

In addition, we have studied the structure of so-called "macro tubes" (MACt's): sheets which twist and close into wide cylindrical tubes. We have defined and can control the conditions in which MACt's appear. We also show from 15 Å-resolution projection maps that there are significant differences in protofilament packing between MACt's and sheets.

W-Pos75

CYTOSKELETAL MODELS FOR SIGNAL TRANSMISSION AND INTRACELLULAR PROTEIN INTERACTIONS

((J. E. Dayhoff¹, S. R. Hameroff², R. Lahoz-Beltra³, S. Rasmussen⁴, C. E. Swenberg⁵)) ¹Univ. of Maryland, College Park, MD; ²Univ. of Arizona, Tucson, AZ; ³Universidad Complutense, Madrid, Spain; ⁴Los Alamos National Laboratory, Los Alamos, NM 87545; ⁵AFRRI, Bethesda, MD.

The cell cytoskeleton, a lattice of protein polymer strands including microtubules (MTs), actin filaments, cross-bridge proteins (MAPs) and anchoring proteins, plays multiple key roles in cellular organization and is particularly complex in neurons. In either MTs or actin filaments, protein conformational changes are possible and conformational changes of proteins may even influence adjacent proteins and thus provide a sort of communication among neighboring molecules. We present here models of protein conformational interactions that serve to identify the nature and implications of the proposed molecular communications mechanisms. We explore the possibility that cell cytoskeleton may be utilizing such signaling mechanisms, or that the cytoskeleton may utilize material transport or other mechanisms to provide intracellular signaling. We examine the potential implications of cytoskeletal signaling at the cellular level, especially for neurons, in which the cytoskeleton plays a role in synaptic adaptation and neural learning. Cytoskeletal signaling could influence or mediate neural learning paradigms, and the cytoskeleton may in fact be necessary to certain learning models that involve networks of neurons.

W-Pos72

IMAGING TUBULIN MICROTUBULES WITH THE ATOMIC FORCE MICROSCOPE. ((D.C. Turner, S.L. Brandow, D.B. Murphy* and B.P. Gaber†) Code 6900, Naval Research Laboratory, Washington, DC 20375-5000 and *Department of Cell Biology and Anatomy, Johns Hopkins University Medical School, 725 N. Wolfe St., Baltimore, MD 21205-2105.

Microtubules (MTs) are of interest due to their role in both structure and transport within the cell. We have chosen to use atomic force microscopy (AFM) as a tool for investigating the structure of the MTs *in vitro*. Tubulin was extracted from chicken brain, phosphocellulose-purified and then dispersed in a standard PMG assembly buffer (PIPES, GTP, and MgCl₂) for polymerization into MTs. Taxol was added to the broth to stabilize the MTs for work at room temperature. Substrates used for this experiment were polished silicon wafers silanized with an amino silane (N-(2-aminoethyl)-3-aminopropyltrimethoxysilane; Huls America, Piscataway, NJ) for improved adhesion of the MTs to the substrate. Images were collected from dry samples with a Nanoscope III AFM in constant force mode (Digital Instruments, Santa Barbara, CA). It was observed that whenever the MTs were dried onto the substrate directly from the PMG buffer they would fall apart. However, when uranyl acetate was added to the solution, the structural integrity of the MTs remained after drying and AFM images could readily be obtained. In fact, even after the dried sample was thoroughly washed with a stream of deionized water, the AFM obtained images of intact MTs that remained adhered to the surface. It is apparent that the uranyl acetate salt is preserving the structure of the MTs through the drying process. Investigations are underway to determine if other acetate salts have the same effect and if the dried MTs show activity upon rehydration. Supported by the Office of Naval Research.

W-Pos74

DYNAMIC INSTABILITY OF ANTARCTIC FISH MICROTUBULES. ((R.C. Williams, Jr.*, R. Mynatt* and H.W. Detrich, III†)) *Dept. of Molecular Biology, Vanderbilt University, Nashville, TN and †Dept. of Biology, Northeastern University, Boston, MA.

The cytoplasmic microtubules (MTs) of Antarctic fishes (Af) assemble and function at body temperatures (T) as low as -1.8°C. To evaluate the physiological significance of dynamic instability in cold-adapted organisms, we have measured *in vitro* the rates of growth and shortening of individual Af MTs, and frequencies of interconversion between these states, by video-DIC microscopy at 5°C. MAP-free tubulins (Tbs) were purified from brains and eggs of *Notothenia coriiceps neglecta* and from brains of *N. gibberifrons* by DEAE ion-exchange chromatography and cycles of MT assembly/disassembly. At [Tb_{brain}] = 0.6–1.1 mg/ml, rates of MT elongation from axonemal nuclei were slow and heterogeneous (ca. 0.01–0.5 μ m/min), shortening rates were also slow and variable (-0.1 to -3.7 μ m/min), and catastrophes and rescues were rare ($f < 0.007$ /min and 0.0004/min, respectively). These values may be compared to typical values for bovine MTs at 37°C: rates of 1–3 μ m/min for elongation and -10 to -100 μ m/min for shortening ([Tb] = 1.3 mg/ml), and catastrophes and rescues occurring at intervals of a few min. Elongation and shortening rates for egg MTs were smaller than those for Af brain MTs, yet egg-MT catastrophes occurred more frequently ($f \approx 0.014$ /min). We conclude that Af MTs at low, physiological T are dynamic polymers, but less so than are MTs of homeotherms at higher T. Furthermore, Af brain MTs appear to differ from Af egg MTs in their intrinsic dynamic instability. Supported by NSF DPP-8919004 and DPP-9120311 (HWD) and by NIH GM 25638 (RCW).

W-VCR2**FORCES OF SINGLE KINESIN MOLECULES MEASURED WITH OPTICAL TWEEZERS.**

((Scott C. Kuo and Michael P. Sheetz)) Dept. of Cell Biology, Box 3709, Duke University Medical Center, Durham, NC 27710

Biological forces are usually studied as the sum of contributions from many force-generating units. Using laser-induced optical forces, we have measured the isometric force of single molecules of the microtubule-dependent mechanochemical enzyme, kinesin. For such measurements, we had to characterize the force-displacement profile of our optical tweezers with nanometer-level resolution. At the center of the optical trap, the displacement is proportional to force (spring constant $1.8 \text{ pN}/\mu\text{m-MW}$) for approximately 100 nm, and the maximum optical force is at approximately 140 nm radius. Using biotinylated microtubules and special streptavidin-coated latex microspheres, we reversibly stalled microtubule translocation by single squid kinesin molecules (densities were $< 2 \text{ molecules}/\mu\text{m}^2$). The minimum optical force required to stall kinesin is $1.89 \pm 0.09 \text{ pN}$ (SEM, $n=18$) and higher order forces that corresponded to multiple kinesin molecules were also detected. Under certain conditions, the resulting velocity with submaximal loads could also be monitored. Our preliminary force-velocity curves are linear, suggesting a very large viscoelastic component in mechanism of kinesin force generation.

W-Pos77**KINESIN STEP SIZE AND FORCE-VELOCITY RELATIONSHIPS: ESTIMATION USING A CENTRIFUGE MICROSCOPE BASED MOTILITY ASSAY.** ((K. Hall, D. Cole, Y. Yeh, J. Scholey and R. Beekun)) University of California, Davis, CA 95616

We have used a centrifuge microscope to obtain a force-velocity curve for kinesin and to estimate the step size, d_k , of the kinesin molecule (where d_k = distance that the tubulin lattice is moved per ATP hydrolysed). Sea urchin egg kinesin was purified (by modifications of Cohn et al. JBC 264, 4290) then adsorbed to the coverlip base of a motility assay cell. In the presence of 10 mM MgATP, this kinesin moved demembrated sea urchin sperm at an "unloaded" speed of $0.7 \mu\text{m/s}$. To apply varying loads to the sperm head, the assay cell was inserted into the well of a centrifuge plate rotated at various speeds. From measurements of sperm velocity under various centrifugal forces (Loads, P) we have constructed a hyperbolic force (P) velocity (V) curve and determined the constants a, b, and P_0 (the force necessary to stop movement) for kinesin molecules. The sliding velocity (V) is equal to V_0 (the maximum sliding speed) times the fraction of time that at least one kinesin molecule is propelling the sperm ($1-(1-F)^n$), where F is the proportion of stroking time to the total cycle time ($F = T_s/T_c$) and n is the average number of interacting kinesin molecules. ($V = V_0(1-(1-F)^n$), where $V_0 = d_k V_{\text{max}}/F$. Substitution into the hyperbolic force-velocity curve gives an equation for kinesin step size:

$$d_k = bF(P_0 - P) / ((P+a) V_{\text{max}} (1-(1-F)^n)) ; \text{ and at zero load } (P = 0), d_k = bFP_0/aV_{\text{max}}$$

In a series of runs we have determined values of $P_0 = 33 \text{ pN}$, $a = 12 \text{ pN}$, and $b = 0.25 \mu\text{m/sec}$. The value of the microtubule activated MgATPase activity (V_{max}) is under investigation. However, d_k appears to be larger than any possible stroke size predicted from geometric considerations of a "swinging" kinesin motor domain. Thus, the hydrolysis of one ATP molecule cannot be tightly coupled to a single molecular stroke.

W-Pos79**MICROTUBULES ACCOMMODATE DIFFERENT NUMBERS OF PROTOFILAMENTS BY ROTATIONS OF THEIR SURFACE LATTICES.**

((E. Meyhöfer*, S. Ray*, R. A. Milligant† and J. Howard*)) *Dept. of Physiology and Biophysics, U. of Washington, Seattle, WA 98195, †Dept. of Cell Biology, The Scripps Research Institute, 10666 N. Torrey Pines Rd., La Jolla, CA 92037.

Microtubules are polymers of the heterodimeric protein tubulin. The head-to-tail association of dimers forms a protofilament whose axis roughly parallels that of the microtubule; the lateral associations of between 10 and 16 protofilaments, depending on the polymerization conditions we used, form a sheet whose closure defines the cylindrical surface of the microtubule. How does a microtubule's surface lattice accommodate different numbers of protofilaments?

In order to produce microtubules with different numbers of protofilaments, purified tubulin was polymerized at 37°C in several different buffer conditions. The surface lattices of these microtubules were characterized by electron cryo-microscopy.

Based on the microtubule diameter and the helical path around the surface of the microtubule taken by the protofilaments (the so-called supertwist), we determined how many protofilaments each microtubule had. The effect of the various growth conditions was to alter the proportion of microtubules in each protofilament class (see Ray et al., accompanying abstract).

The supertwist pitches accorded with the lattice-rotation model (Chrétien and Wade, *Biol. Cell*, 71: 161-174) in which it is hypothesized that the local geometry of the lattice is not altered, but that the entire lattice rotates in order to accommodate different numbers of protofilaments. (This work was supported by the NIH, the AHA, and the PEW Foundation.)

W-Pos76**THE FORCE EXERTED BY A KINESIN MOLECULE AGAINST A VISCOUS LOAD.** ((A. Hunt and J. Howard)) Dept. of Physiology and Biophysics, University of Washington, Seattle, Wa. 98195

Kinesin is a microtubule based motor which uses energy derived from ATP hydrolysis to generate force required for intracellular transport. We have asked: how much force can a kinesin molecule generate?

In order to load the motor reaction, we increased the viscosity of the solution through which microtubules were moved by kinesin molecules adsorbed to glass surfaces. The viscous force was then calculated according to slender body theory to be proportional to the viscosity (measured both with a viscometer and from the analysis of microtubule diffusion), the microtubule length, and a geometric factor dependent on the proximity to the surface.

Low viscosity solutions did not significantly load the motors: the speed of movement was independent of microtubule length at both high and low densities of kinesin on the surface. At a viscosity of ~ 100 times that of water and at high kinesin density, the speed was also independent of microtubule length: this is expected because both the viscous force and the number of motors should increase in proportion to length. However, at kinesin densities of $< 10/\mu\text{m}^2$, at which we expect that the movement is due to single motors, the longer microtubules moved more slowly than the shorter ones, indicating that the reaction was being significantly loaded.

Within the uncertainty of the data, the relationship between speed and viscous force was linear. By extrapolation, the maximum viscous force necessary to stop movement was estimated at $2.2 \pm 0.3 \text{ pN}$ (\pm standard error) with an uncertainty of $\pm 30\%$ in the geometric factor. This work was supported by the NIH and the Pew and Sloan Foundations.

W-Pos78**PRESTEADY STATE KINETIC ANALYSIS OF THE MICROTUBULE-KINESIN ATPASE.** ((S.P. Gilbert and K.A. Johnson)) Department of Molecular & Cell Biology, Pennsylvania State University, University Park, PA 16802. (Spon. by T. Fujimori)

Mechanistic studies of the kinesin ATPase have been pursued to understand the enzyme's ability to couple ATP hydrolysis to organelle translocation along microtubules. For these studies the N-terminal 401 amino acids of the *Drosophila* kinesin heavy chain were expressed in *E. coli* and purified to homogeneity in mg amounts. The protein designated K401 was active and behaved as native kinesin with respect to its steady state kinetic properties: K401 demonstrated a very low ATPase activity ($k_{\text{cat}} = 0.01 \text{ s}^{-1}$) which was stimulated 1000-fold by the addition of microtubules ($k_{\text{cat}} = 10 \text{ s}^{-1}$; $K_{0.5, \text{MT}} = 0.9 \mu\text{M}$ tubulin; $K_{\text{m,ATP}} = 31 \mu\text{M}$). When purified, K401 contained ADP tightly bound at its active site. During the steady state, ADP release at 0.01 s^{-1} is rate limiting in the absence of microtubules. The transient state kinetic analysis of the microtubule-K401 pathway reveals a burst of product formation during the first turnover with full burst amplitude indicating 1 active site per mole K401 protein. The rate of ATP binding is ATP concentration dependent and faster than the rate of ATP hydrolysis. Experiments at high ATP concentration with saturating microtubule concentrations show that the maximal rates of ATP hydrolysis and ADP release are comparable such that the two steps in combination limit the maximal rate of turnover. Supported by NIH GM26726.

W-Pos80**KINESIN FOLLOWS THE MICROTUBULE'S PROTOFILAMENT AXIS.** ((S. Ray, E. Meyhöfer, and J. Howard)) Dept. of Physiology and Biophysics, U. of Washington, Seattle, WA 98195.

We tested the hypothesis that the motor protein kinesin follows a path which runs parallel to the microtubule's protofilament axis.

Polymerized from purified tubulin in three different buffers, microtubules had protofilaments which were observed by electron cryo-microscopy either to run parallel to the microtubule's long axis (paraxial protofilaments) or to run along shallow helical paths around the microtubule's cylindrical surface (supertwisting protofilaments): (a) the majority of microtubules grown in phosphate buffer with taxol had 12 protofilaments with a supertwist pitch of $3.4 \pm 0.2 \mu\text{m}$ (s.d., $n=13$); (b) the majority seeded from axonemal doublets in MES had 13 paraxial protofilaments; and (c) the majority grown in PIPES had 14 protofilaments with a pitch of $6.2 \pm 0.4 \mu\text{m}$ ($n=9$).

From the motion of these microtubules across kinesin-coated glass surfaces in the presence of ATP, we concluded that: (a) 12-protofilament microtubules rotate with a pitch of $+4.8 \pm 0.8 \mu\text{m}$ ($n=3$); (b) 13-protofilament microtubules do not rotate ($n=127$); and (c) 14-protofilament microtubules rotate with a pitch of $-5.9 \pm 1.1 \mu\text{m}$ ($n=13$). The pitch and the sign of the rotations accorded with structure and with the lattice-rotation model (Meyhöfer et al. accompanying abstract). Analysis of the motion in low density assays indicated that the probability, at each step, that an individual kinesin motor switches protofilaments is less than 0.01.

Because kinesin follows the protofilament axis so precisely, it is likely that the motor's single step is either a multiple of 4.1 nm, the tubulin monomer spacing along the protofilament, or 8.2 nm, the interdimer spacing. (This work was supported by the NIH, the AHA, and the PEW Foundation.)

W-Poe81**KINESIN DECORATION OF THE MICROTUBULE SURFACE.**

((B.C. Harrison, S.P. Marchese-Ragona, N. Cheng, A.C. Steven and K.A. Johnson)) Pennsylvania State University, University Park, PA 16802, and NIAMS, NIH, Bethesda, MD 20892. (Spon. by P.D. Ross).

The interaction of the kinesin motor domain with the microtubule surface lattice was examined by electron microscopy of negatively stained and frozen-hydrated specimens. The N-terminal 401 amino acids of the *Drosophila* kinesin heavy chain (K401) which contains both the ATP and microtubule binding domains, were expressed in *E. coli* and purified to homogeneity as soluble, fully active, protein. This truncated monomeric form of kinesin made it possible to decorate individual microtubules heavily without cross-linking them into bundles. Complexes were formed by mixing taxol-stabilized microtubules and K401 at 1 to 3 times the molar concentration of tubulin, pelleted, and analyzed by gel electrophoresis. Saturating binding was found to correspond to one molecule of K401 per tubulin dimer. According to both conventional negative staining and cryo-electron microscopy, the complexes were coated with regular patterns of bound K401 molecules with an axial repeat of 8nm. Optical diffraction of decorated microtubules showed a strong layer-line at this spacing, confirming that one kinesin head binds per tubulin heterodimer. The addition of ATP to the K401-microtubule complex led to complete dissociation of kinesin from the microtubule surface.

W-Poe82

FUNCTIONAL AND STRUCTURAL ASPECTS OF ASSOCIATION OF A REGULATORY LIGHT CHAIN WITH 22S DYNEIN ((K. Barkalow, T. Hamasaki and P. Satir)) Department of Anatomy and Structural Biology, Albert Einstein College of Medicine, Bronx, N.Y. 10461.

A 29kD polypeptide that copurifies with 22S dynein of *Paramecium tetraurelia* is phosphorylated or thiophosphorylated in a cAMP-dependent, Ca^{2+} -sensitive manner. This phosphorylation regulates the speed of microtubule translocation by 22S dynein *in vitro* (PNAS, 88:7918-7922, 1991). The 29kD polypeptide may be considered a dynein regulatory light chain (dLC_r). After thiophosphorylation within the axoneme we isolated the dLC_r away from the heavy chains and partially purified the protein. Isolated 22S dynein not otherwise treated retains substoichiometric amounts of the 29 kD polypeptide. The partially purified 29kD dLC_r specifically rebinds to this 22S dynein but not to 14S dynein (a single headed molecule) nor BSA. The specific association with 22S dynein can be competed away by using either partially purified thiophosphorylated or a corresponding unphosphorylated dLC_r. A standard *in vitro* microtubule motility assay was used to test if this rebinding is functional. When 22S dynein with reassociated dLC_r was used as a substratum microtubule translocation velocity increased significantly over controls. Velocity increased further when the reassociated dLC_r was thiophosphorylated. *Paramecium* 22S dynein can be proteolytically digested with chymotrypsin to yield one headed and two headed structures, as previously shown in *Tetrahymena* by Y. Y. Toyoshima (JCB 105:887-895, 1987). The dLC_r binds preferentially to the one headed fraction. Based on these results the 29 kD dLC_r is probably part of a single unique subunit of the 22S dynein arm that includes one specific heavy chain. Furthermore this association is apparently functional in that it modifies the translocation rate of microtubules by 22S dynein according to the phosphorylation state of the 29kD dLC_r, thereby regulating ciliary beat frequency.

W-Poe83**SINGLE CELL MEASUREMENT OF CILIARY BEAT FREQUENCY AND INTRACELLULAR CALCIUM IN TRACHEAL EPITHELIAL CELLS**

((M. Salathe & R.J. Bookman)) Division of Pulmonary Diseases and Dept. of Mol. & Cell. Pharmacology, Univ. of Miami School of Medicine, Miami, FL 33136

Mucociliary clearance is the primary mechanism by which inhaled foreign particles, including bacteria, are removed from the airways and lung. This clearance depends upon both the mucus secreted by the goblet cells and the microtubule-based ciliary beat frequency (CBF) of airway epithelial cells. To determine changes in CBF and $[Ca^{2+}]_i$ of the same cell, tracheal epithelial cells were obtained from sheep by dissociation with protease and grown in culture for 2-14 days. Cells were imaged with a 100X Fluor DL oil objective, enabling single cilia to be clearly observed. CBF was measured by online FFT analysis of intensity changes of single pixels from digitized phase contrast microscopy images. Using a video camera with RS-170 timing, frequency response is limited to <15Hz since each pixel represents a 1/30s sampling interval. With 128 samples per FFT (=4.26s), the magnitude spectra usually showed a clear single peak. At 20°C, this peak frequency was between 5Hz and 10 Hz and was stable (± 1 Hz) for >30minutes. This measure of CBF increased with increasing temperature, and often surpassed the 15Hz limit at >30°C. Cholinergic stimulation with 10 μ M ACh produced a reversible increase in CBF at 20°C by ~30% above baseline. By switching the light path to an intensified CCD camera, we could measure Fura-2 fluorescence of the same ciliated cell. Using the ratio of emitted light with alternating 340/380nm excitation, we found ACh reversibly increased $[Ca^{2+}]_i$. This $[Ca^{2+}]_i$ increase was likely due to Ca from internal stores, since Ca-free medium did not prevent the rise in $[Ca^{2+}]_i$. This demonstrates that $[Ca^{2+}]_i$ and CBF can be measured in a single cell and that ACh produces temporally correlated increases in CBF and $[Ca^{2+}]_i$, thus setting the stage for an exploration of the role of $[Ca^{2+}]_i$ in the regulation of CBF. (Supported in part by the Swiss National Science Foundation).

NUCLEIC ACID STUDIES**W-Poe84****EQUILIBRIUM ELECTROPHORESIS OF SS PD(A)₂₀, SS PD(T)₂₀, DS PD(AT)₂₀.**

((D. B. Hayes*, J. B. Chaires#, T. M. Laue**))

*University of New Hampshire, Durham NH 03824 and #Dept. of Biochemistry, Univ. of Mississippi Medical Center, 2500 North State ST., Jackson, MS 39216.

Equilibrium electrophoresis is a method to determine the apparent charge on macroions in aqueous solution. A second generation instrument has been used to study DNA oligonucleotides with a length of 20 bases or base pairs. In 20 mM Tris, 20mM KCl, pH 8.00 buffer, either form of ss DNA had an apparent charge from 5.97 to 6.17 electron equivalents, 31% of its titrable charge. In the same buffer, the ds DNA had an apparent charge of 7.57 electron equivalents, 18.9% of its titrable charge. Condensed ion theory predicts 30% of the titrable charge will be expressed for the ss DNA, in excellent agreement with these measurements. However, the agreement between predicted (12%) and measured (18.9%) charge is not as good for the ds DNA. The theory, operation and limitations of this device are discussed. Supported by NSF DIR 8914571.

W-Poe85

RMS AMPLITUDE OF LOCAL ANGULAR MOTION OF PURINES IN DNA ((Bryant S. Fujimoto, Sirkuu Nuutero, and J. Michael Schurr)) Department of Chemistry, BG-10, University of Washington, Seattle WA 98195.

Deuterium NMR and time-resolved fluorescence polarization anisotropy (FPA) measurements were made to determine the rms amplitude of local angular motion of purines in a 12 bp duplex DNA (CGCGAATTCGCG) which is deuterated at the H8 positions of the adenines and guanines. FPA measurements of this sample made in dilute solution yield the hydrodynamic radius of the DNA, $R_H = 9.94 \pm 0.2 \text{ \AA}$. FPA measurements of the sample at the NMR concentration are employed to characterize the collective motions of the DNA in terms of either an enhanced viscosity or end-to-end dimer formation. Expressions we have derived for R_2^0 and the results of the FPA measurements are used to analyze the linewidth of the deuterium NMR spectrum. When the principal-axis frame of the electric field gradient tensor is assumed to undergo overdamped libration around each of its three body-fixed axes in an isotropic deflection potential, then the rms amplitude of local motion around any single axis is found to lie in the range 10 to 11° provided the high DNA concentration acts to enhance the viscosity, and about 9° if it acts to produce end-to-end dimers. The proton NMR data of Eimer *et al.* are reanalyzed and shown to yield an rms amplitude of angular motion of the cytosine H5-H6 internuclear vector of 9 to 10° depending upon its orientation with respect to the helix-axis. Within experimental error these results lie in the same range (8 to 10°) inferred for base motions at low and intermediate hydration levels in the solid state.